

A reaction-diffusion model for inter-species competition and intra-species cooperation

Shaker M. Rasheed, MSc

Thesis submitted to The University of Nottingham
for the degree of Doctor of Philosophy

May 2013

Abstract

This thesis deals with a two component reaction-diffusion system (RDS) for competing and cooperating species. We have analysed in detail the stability and bifurcation structure of equilibrium solutions of this system, a natural extension of the Lotka-Volterra system. We find seven topologically different regions separated by bifurcation boundaries depending on the number and stability of equilibrium solutions, with four regions in which the solutions are similar to those in the Lotka-Volterra system. We study RDS in the small parameter of the range $0 < \lambda \ll 1$ (fast diffusion and slow reaction), and in a few cases we assume $\lambda = O(1)$. We consider three types of initial conditions, and we find three types of travelling wave solutions using numerical and asymptotic methods. However, neither numerical nor asymptotic methods were able to find a particular travelling wave solution which connects a coexistence state say, (u_0, w_0) to an extinction state $(0, 0)$ when $0 < \lambda \ll 1$. This type can be found when the reaction-diffusion system satisfies the symmetry property and $\lambda = 1$.

From asymptotic methods, we find that RDS is a singular perturbation problem (one inner and two outer regions) when one of the equilibrium solutions associated with the travelling wave has $u = 0$, whereas, when $u \neq 0$ we get a regular perturbation problem. We find the numerical and asymptotic solutions for RDS. We have published the above

results [\[RB13\]](#).

We study the stability of travelling wave solutions for RDS in two dimensions using numerical and asymptotic methods. We also used the Evans function as a tool for computing the stability of the three types of wave. We find that all the types of travelling wave solutions are stable for all values of the parameters.

Acknowledgements

I would like to thank my supervisor, Professor John Billingham for his great support and help. Great thanks for his patience and for encouraging me throughout my study. I really want to thank my second supervisor, Professor Stephen Coombes for his help. Thanks are also due to all my friends and colleagues in the school of Mathematical Sciences, The University of Nottingham.

Gratitude is due to the Iraqi government for offering me this scholarship and for their financial and social support during my study.

Finally, yet most importantly, I would like to thank my wife, Sharza. Without her love, help, patience and support, it would have been difficult to finish this work. My love is to my brave son, Ameer and my pretty daughter, Yara. Great thanks are due to my father, mother, my sisters and my brothers for their prayers and to all of my family, friends and colleagues back home.

Contents

1	Introduction	1
1.1	Reaction-diffusion equations	1
1.1.1	Fisher equation	3
1.1.2	Reaction-diffusion equation for generalized Fisher equation	4
1.2	Lotka-Volterra system for interacting populations	7
1.3	Travelling wave solutions of diffusion Lotka-Volterra system	11
1.4	Stability of travelling waves	14
1.5	Reaction-diffusion system	18
2	Equilibrium solutions	23
2.1	Equilibrium solutions and bifurcation	23
2.1.1	Stability of the equilibrium points and the phase portrait in the re- gions $R_1 - R_7$	32
2.2	The effect of the parameters $\alpha_{1,2}$ on the bifurcation boundaries	37
3	Travelling wave solutions for the initial value problem (1.5.3)	41
3.1	Travelling wave solutions	41
3.2	Numerical solutions	43

CONTENTS

3.3	Numerical solutions of the initial value problem	47
3.3.1	Initial Condition A : $u_0(x)$ is a step function and $w_0(x) = 1$	47
3.3.2	Initial Condition B : $u_0(x) = 1$ and $w_0(x)$ is a step function	50
3.3.3	Initial Condition C: $u_0(x)$ and $w_0(x)$ are step functions	53
3.4	Symmetry properties of (1.5.3) when $\lambda = 1$	58
3.5	The impact of the cooperative and competitive coefficients on the wave speed	59
3.6	Founder control case	62
3.7	The effect of the diffusion coefficient D on the travelling wave solutions .	67
3.8	Dynamics of the growth and development of travelling wave solutions with initial condition C	70
3.8.1	Asymptotic solutions	72
3.8.2	Laplace transform method	74
4	Travelling wave solutions for $\lambda \ll 1$ and $\lambda = O(1)$	80
4.1	Asymptotic solutions for $\lambda \ll 1$	80
4.2	Regular perturbation solutions	82
4.2.1	Asymptotic solutions for type (I_b)	82
4.2.2	$\gamma_2 < 1$, R_1 and R_4 : saddle-node connection	85
4.2.3	$\gamma_2 > 1$, R_2 and R_5 : saddle-saddle connection	88
4.3	Singular perturbation solutions	91
4.4	Asymptotic solutions for type (I_a)	92
4.4.1	Inner solution for (I_a)	95
4.5	Solutions for type (II)	98

CONTENTS

4.6	Asymptotic solutions for type (III)	99
4.6.1	Asymptotic solutions for type (III_r)	99
4.6.2	Inner solutions for type (III_r)	100
4.6.3	Asymptotic solutions for type (III_l)	101
4.6.4	Inner solutions for type (III_l)	102
4.7	Computing the wave speed in the range of $0 < \lambda = O(1)$	104
4.8	The reaction-diffusion system (1.5.3) for $\lambda \gg 1$	105
5	Stability of travelling wave solutions in two dimensions	107
5.1	Numerical solutions	107
5.2	Perturbation of the planar wavefront	113
5.2.1	Example test: Gray-Scott	114
5.2.2	Numerical results	116
5.3	Stability analysis of travelling waves of (5.1.1)	121
5.4	Linearisation of (5.1.3)	121
5.5	Asymptotic solutions for (5.4.3)	123
5.5.1	Multiple scale method	125
5.5.2	Calculating M_1	127
5.5.3	Calculating the Evans function for (5.5.11) and the travelling wave of type (I_a)	130
5.5.4	Computing the Evans function for (5.5.11) with type (III_r)	133
5.5.5	Computing the Evans function for (5.5.11) for type (I_b)	134
5.6	Calculating the Evans function for inner problem	136
6	Conclusions and future work	140

CONTENTS

6.1	Conclusions	140
6.2	Future work	145

Introduction

1.1 Reaction-diffusion equations

The theory of reaction-diffusion equations has been studied since 1930, by Fisher, Petrovskii, Kolmogorov and others [VP09]. Fisher and others have defined a travelling wave solution for the reaction-diffusion equations, and they have found the existence, stability and speed of the wave for some types of reaction-diffusion equations, for example the Fisher equation. There are many applications of reaction-diffusion equations in biology, physics, chemistry, epidemiology and ecology; (for more details see [Pas08, Mur02, Kot01, Bri05]).

In population dynamics, reaction describes the rate of some populations reproduction, cooperation or competition (see for example [Owe01, HJW11]), whereas, diffusion models the random motion of individuals. Predator-prey models and two species competition models are examples from population ecology. For population models the analysis of travelling wave solutions is relevant for describing the spread of growth. A travelling wave is a wave that travels with time and with a shape that is the same for all time. Examples of travelling waves, are a chemical wave which arises when reaction and

diffusion occur simultaneously, and wavefront which describes the invasion in ecology (see [BK06, VP09, VG03]).

A system of reaction-diffusion equations for m species can be written in the form,

$$\frac{\partial \bar{u}(x, t)}{\partial t} = D \nabla^2 \bar{u} + \bar{f}, \quad (1.1.1)$$

where ∇^2 is the Laplacian operator, $\bar{u} = (\bar{u}_1, \bar{u}_2, \dots, \bar{u}_m)$ and the entries are the concentrations or the densities of the species. We denote the space by x and the time by t . A diffusion coefficient D can be written as a diagonal matrix, with entries $D_i, i = 1, 2, \dots, m$, in the diagonal column. The interaction among species is defined by the vector source term \bar{f} . A scalar reaction-diffusion equation in one dimension has the form:

$$\frac{\partial u}{\partial t} = D \frac{\partial^2 u}{\partial x^2} + f(u), \quad (1.1.2)$$

where D is a positive diffusion coefficient and u is the population density. From the reaction function $f(u)$ we can deduce that the feature of a travelling wave, for example in a pulse wave, $f(u)$ has one state corresponding to homogeneous equilibrium solutions of (1.1.2). Another example on waves is a wavefront which needs two equilibrium solutions as $x \rightarrow \pm\infty$. The equilibrium solution behind the wave must be stable whilst the second state could be stable or unstable [SM96a]. A travelling wave solution has the form $u(x, t) = U(x - ct)$, where c is the wave speed. If we substitute it in (1.1.2), we get an ordinary differential equation,

$$\frac{d^2 U}{dz^2} + c \frac{dU}{dz} + f(U) = 0, \quad (1.1.3)$$

where $z = x - ct$.

1.1.1 Fisher equation

In 1937, Fisher and Kolmogorov [Fis37, Mur02] studied the reaction-diffusion equation (1.1.2) when $f(u) = ku(1 - u)$, which is called the Fisher equation or the Fisher-Kolmogorov equation. There are two equilibrium solutions for this equation, a stable state ($u = 1$) and an unstable state ($u = 0$) (see for example [Mur02, Wit94, SM96b, LN01]). In order to study the travelling wave solutions of the Fisher equation, first we rescale the Fisher equation [Mur02] with

$$\bar{t} = kt \quad \bar{x} = x\left(\frac{k}{D}\right)^{\frac{1}{2}},$$

and omitting the bar for notational simplicity, we get

$$\frac{\partial u}{\partial t} = \frac{\partial^2 u}{\partial x^2} + u(1 - u). \quad (1.1.4)$$

Now if we substitute $u(x, t) = U(x - ct)$ in (1.1.4), we get an ordinary differential equation

$$\frac{d^2 U}{dz^2} + c \frac{dU}{dz} + U(1 - U) = 0. \quad (1.1.5)$$

Travelling wave solutions of (1.1.5) satisfy the boundary conditions

$$\lim_{z \rightarrow +\infty} U(z) = 0, \quad \lim_{z \rightarrow -\infty} U(z) = 1.$$

For the phase plane analysis, we rewrite (1.1.5) as a system of first order differential equations

$$\begin{aligned} \frac{dU}{dz} &= V, \\ \frac{dV}{dz} &= -cV - U(1 - U). \end{aligned} \quad (1.1.6)$$

A sketch of a particular solution in the phase plane is called the trajectory of the solution.

The trajectory can be found from the solution of (1.1.6) or

$$\frac{dV}{dU} = \frac{-cV - U(1 - U)}{V}. \quad (1.1.7)$$

It is clear that (1.1.7) has two singular points for (U, V) , namely $(0, 0)$ and $(1, 0)$ which are the equilibrium solutions. A linear stability analysis (for more details about stability analysis see Chapter 2) for the two equilibrium solutions show that the eigenvalues k_{\pm} satisfy

$$\begin{aligned} (0, 0) : \quad k_{\pm} &= \frac{1}{2}[-c \pm (c^2 - 4)^{\frac{1}{2}}], \\ (1, 0) : \quad k_{\pm} &= \frac{1}{2}[-c \pm (c^2 + 4)^{\frac{1}{2}}]. \end{aligned}$$

From the eigenvalues we can see that the origin is a stable node when $c^2 > 4$ and a stable spiral when $c^2 < 4$. Furthermore, $(1, 0)$ is a saddle point for all values of c . The sketch of a travelling wave solution is shown in Figure 1.1. Figure 1.2 shows a trapping region for all values of $c \geq c_{min} = 2$ in the region $U \geq 0, V \leq 0$ with $0 \leq U \leq 1$. The travelling wave solution for $c < 2$ has no physical meaning since $U < 0$, since it lies outside $0 \leq U \leq 1$, where the travelling wave is defined.

Analytical solutions of the Fisher equation were found for values of $c \geq 2$ in [AZ79, GC91]. Asymptotic and numerical methods are widely used to solve the Fisher equation and (1.1.2) for different $f(u)$, [LN04, Gou00, GC74, PB94].

1.1.2 Reaction-diffusion equation for generalized Fisher equation

In this section we study a reaction-diffusion equation for a single species with three equilibrium solutions. A general Fisher's genetic population model was studied by Hardler

CHAPTER 1: INTRODUCTION

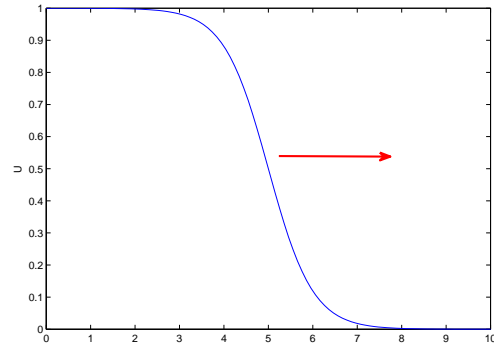


Figure 1.1: Travelling wavefront solution for the Fisher equation. The wave velocity $c \geq 2$.

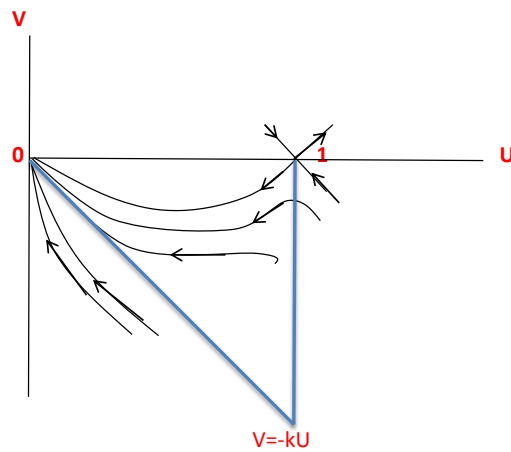


Figure 1.2: Phase plane trajectories for (1.1.5) for the travelling wavefront solution with $c^2 > 4$.

and Rothe in 1975 [HR75]. The travelling wave solution of (1.1.2) was studied analytically for some nonlinear reaction rates, $f(u)$. We show two of these types which we will use later in our work. The two types of $f(u)$ are,

- Case one:

$$f(u) = u(1 - u)(1 + vu), -1 \leq v \leq \infty. \quad (1.1.8)$$

In this case, it was shown that in [HR75], there exists a family of travelling waves that connect the two equilibrium solutions, $u = 1$ and $u = 0$ with a minimum wave speed (the least wave speed to have a solution satisfies $0 \leq u \leq 1$) that satisfies the relation

$$c_{min} = \begin{cases} 2, & \text{for } -1 \leq v \leq 2, \\ \frac{v+2}{\sqrt{2v}}, & \text{for } v \geq 2. \end{cases}$$

- Case two:

$$f(u) = u(1 - u)(u - \mu), 0 < \mu < 1. \quad (1.1.9)$$

In order to describe what types of travelling wave solutions exist in case two, we need the following definitions

$$\begin{aligned} c^* &= 2\sqrt{\mu(1 - \mu)}. \\ c_0 &= \begin{cases} \frac{1+\mu}{\sqrt{2}}, & \text{for } 0 < \mu \leq \frac{1}{3}, \\ c^*, & \text{for } \frac{1}{3} \leq \mu \leq \frac{1}{2}, \end{cases} \\ c_1 &= \frac{1}{\sqrt{2}} - \mu\sqrt{2}. \end{aligned} \quad (1.1.10)$$

There exists a monotone travelling wave for the following cases [HR75];

CHAPTER 1: INTRODUCTION

1. There exists a monotone decreasing wave when $c \geq c_0$, with boundary conditions

$$u(-\infty) = 1, \quad u(\infty) = \mu.$$

2. There exists a monotone increasing wave when $c \geq c^*$, with

$$u(-\infty) = 0, \quad u(\infty) = \mu.$$

3. There exists a unique monotone wave when $c = c_1$, with

$$u(-\infty) = 1, \quad u(\infty) = 0.$$

4. There exists an oscillating wave when $0 < c < c^*$, with

$$u(-\infty) = 0, \quad u(\infty) = \mu.$$

5. There exists an oscillating wave when $c_1 < c < c^*$, with

$$u(-\infty) = 1, \quad u(\infty) = \mu.$$

6. There exists a monotone decreasing wave when $\max(c_1, c^*) < c < c_0$, with

$$u(-\infty) = 1, \quad u(\infty) = \mu.$$

7. There are a unique non vanishing wave front when $c = 0$, with

$$u(-\infty) = u(\infty) = 0.$$

1.2 Lotka-Volterra system for interacting populations

When species interact, the population dynamics of each species is affected. There are three types of interactions that may occur between two species. An interaction is called

a predator-prey when the growth rate of one of the population species is increased and the other is decreased. If the growth rates of both populations are decreased, then the interaction is called a competition. If each population's growth rates are enhanced, then the interaction is called mutualism or symbiosis [VP09, Gop82, Hos03, Wan78].

A simple model defined for two species is the Lotka-Volterra system

$$\begin{aligned}\frac{du_1}{dt} &= r_1 u_1 \left(1 - \frac{u_1}{k_1} - \frac{\beta_{12} u_2}{k_1}\right), \\ \frac{du_2}{dt} &= r_2 u_2 \left(1 - \frac{u_2}{k_2} - \frac{\beta_{21} u_1}{k_2}\right),\end{aligned}\tag{1.2.1}$$

where r_i, k_i , ($i, j = 1, 2$) are positive which describe the intrinsic rates of growth and the carrying capacities of species u_i respectively [Neu98, Mur02, Gop82]. The interaction between the two species is given by the non-negative parameters β_{ij} , which describe the effect of species j on species i . The minus sign in front of β_{ij} corresponds to competition between the species which means that both species get negative effects when they compete for resources. In a predator-prey system for example, if the prey is u_1 and the predator is u_2 , the sign of β_{21} in this case should be a plus. If we set $\beta_{12} = \beta_{21} = 0$, then (1.2.1) decouples to two simple logistic growth equations. This system says nothing about the mechanism of competition or what the species are competing for. An interesting property of (1.2.1) is symmetry, i.e, if we replace the subscript for each term in the equation with the subscript for the other species, it will not change the model.

The analysis of (1.2.1) is shown in Figure 1.3 [Neu98]. There is a possibility of coexistence if $\beta_{12} < K_1/K_2$ and $\beta_{21} < K_2/K_1$. Species u_1 excludes u_2 , when $\beta_{12} < K_1/K_2$ and $\beta_{21} > K_2/K_1$ and vice versa when $\beta_{12} > K_1/K_2$, $\beta_{21} < K_2/K_1$. Furthermore, when $\beta_{12} > K_1/K_2$ and $\beta_{21} > K_2/K_1$ one species will exclude the other, but the winner depends on the initial densities of the two species, this is called founder control. Figure 1.4 shows

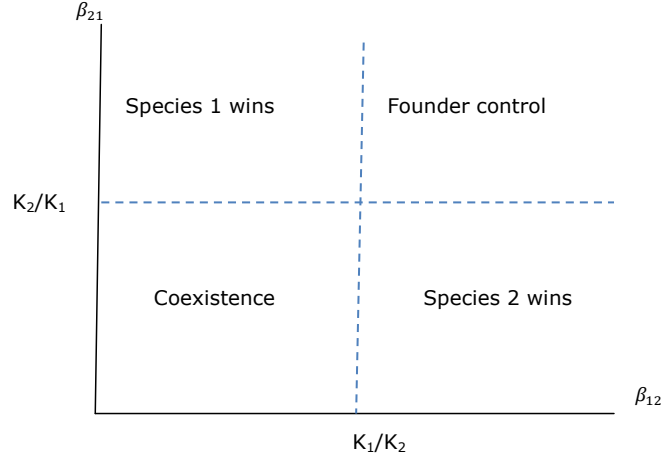


Figure 1.3: Phase diagram for the coexistence, the winning species and founder control depending on β_{ij} . [Neu98]

the phase portrait of (1.2.1). It was shown that there are four topologically different regions.

We will refer to the four topologically different regions as follows:

- RL_1 : $\beta_{12} < K_1/K_2$ and $\beta_{21} < K_2/K_1$.
- RL_2 : $\beta_{12} < K_1/K_2$ and $\beta_{21} > K_2/K_1$.
- RL_3 : $\beta_{12} > K_1/K_2$ and $\beta_{21} < K_2/K_1$.
- RL_4 : $\beta_{12} > K_1/K_2$ and $\beta_{21} > K_2/K_1$.

The equilibrium solutions for (1.2.1) were studied (for example in [Kot01]), and it was shown that for non dimensional Lotka-Volterra system there are two single species equilibrium solutions $(1, 0)$ and $(0, 1)$ and an extinction for both species $(0, 0)$. There is also a positive state (\bar{u}_1, \bar{u}_2) which is either a stable node or a saddle point. Both $(1, 0)$ and $(0, 1)$

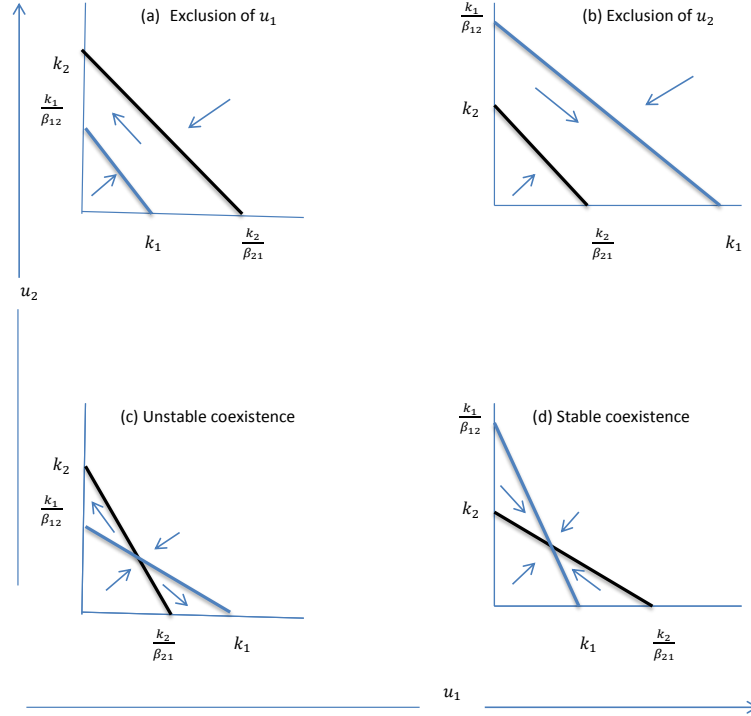


Figure 1.4: The description of competition between two populations in the Lotka-Volterra system. The population sizes of the two species are denoted by u_1 in the x-axis and u_2 in the y-axis. The lines are isoclines where population growth of one of the species is zero. There are four interspecific competition cases. Cases (a) and (b) show competitive dominance, where one species can exclude the other. In case (c), depending upon the starting size of the two populations, competitive dominance again occurs. In case (d), the two species reach a stable equilibrium. The arrows show changes in population size with time.

are stable when (\bar{u}_1, \bar{u}_2) is a saddle point (RL_4), while when (\bar{u}_1, \bar{u}_2) is a stable node, both single equilibrium solutions are unstable (RL_1). Furthermore, when (\bar{u}_1, \bar{u}_2) does not exist, one of the equilibrium solutions is stable and the other is unstable (RL_2 and RL_3). The equilibrium solution $(0, 0)$ is always unstable.

1.3 Travelling wave solutions of diffusion Lotka-Volterra system

The Lotka-Volterra system in a reaction-diffusion form needs the diffusion term. A diffusion Lotka-Volterra system for competing species is [VP09, Ked01]

$$\begin{aligned}\frac{\partial u_1}{\partial t} &= D_1 \frac{\partial^2 u_1}{\partial x^2} + r_1 u_1 \left(1 - \frac{u_1}{k_1} - \frac{\beta_{12} u_2}{k_1}\right), \\ \frac{\partial u_2}{\partial t} &= D_2 \frac{\partial^2 u_2}{\partial x^2} + r_2 u_2 \left(1 - \frac{u_2}{k_2} - \frac{\beta_{21} u_1}{k_2}\right),\end{aligned}\tag{1.3.1}$$

where D_i are diffusion coefficients. The type of travelling wave solution generated in (1.3.1) depends on the initial conditions. In [VP09], some types of travelling waves are shown where the initial conditions describe some biologically interesting cases. We show next two of these types of initial conditions which we will also use in our study. The first interesting biological case is when one of the species is invaded by the other. The initial conditions are shown to be,

$$u_1(x, 0) = 1 \quad \text{and} \quad u_2(x, 0) = \psi(x) \quad \forall x,$$

where $\psi(x)$ is a function with compact support for example a step function which can be written as

$$\psi(x) = \begin{cases} u_{10} & \text{for } x \leq L_0, \\ 0 & \text{for } x > L_0, \end{cases}$$

where L_0 is a width of the step function. This is the case where species u_1 is native, and species u_2 is introduced. There is a monotone travelling wavefront that connects the state $(1, 0)$ to the stable state (\bar{u}_1, \bar{u}_2) in RL_1 , and this is an invasion case. In RL_2 and RL_3 , (\bar{u}_1, \bar{u}_2) does not exist, but $(1, 0)$ is stable and $(0, 1)$ is unstable in RL_2 while $(1, 0)$ is unstable, and $(0, 1)$ is stable in RL_2 . A travelling front develops in RL_3 , which connects $(0, 1)$ to $(1, 0)$ and this means that the invasion of the second species succeeds. However, the invasion will fail in RL_2 . The equilibrium solution (\bar{u}_1, \bar{u}_2) exists but is unstable in RL_4 and the invasion of the first species will fail, while the invasion of the second species will succeed. The second interesting biological case is introducing a strong competition between species. For example let species u_1 be a virus whose spread needs to be controlled. The initial conditions corresponding to this case are

$$u_1(x, 0) = \begin{cases} u_{10} & \text{for } x \leq L_0, \\ 0 & \text{for } x > L_0, \end{cases}$$

$$u_2(x, 0) = \begin{cases} u_{20} & \text{for } x \leq L_0, \\ 0 & \text{for } x > L_0, \end{cases}$$

where $u_{20} \ll u_{10}$ (see [VP09]). The physical meaning for these conditions is that, both species are introduced. In RL_3 , where the second species excludes the first species and with the above initial conditions, the resulting travelling waves are, two wavefronts and represent an invasion of one of the species namely u_1 . In this case the speed of the wavefronts determine the different dynamics of the system. Lets c_0 be the speed of the trav-

elling wavefront of species u_1 , and c_1 be the speed of travelling wavefront of species u_2 . If $c_1 > c_0$, the travelling wave of species u_2 passes the one of species u_1 , and species u_1 dies out. If $c_1 < c_0$, the two travelling waves exist. The wave speed for both fronts are computed in [VP09], and it was shown that the travelling front of species u_1 is the same as the Fisher equation and arised from an initial condition, therefore $c_0 = 2\sqrt{D_1 r_1}$. The linearization of the second equation in (1.3.1) at the leading edge of the front and where the carrying capacity $u_1 = 1$, leads to

$$\frac{\partial u_2}{\partial t} = D_2 \frac{\partial^2 u_2}{\partial x^2} + r_2 u_2 \left(1 - \frac{\beta_{21}}{k_2}\right). \quad (1.3.2)$$

Therefore the speed of the travelling front of species u_2 (which can be deduce from (1.3.2)) is,

$$c_1 = 2\sqrt{D_2 r_2 \left(1 - \frac{\beta_{21}}{k_2}\right)}.$$

From the speed of both fronts, it was shown that when

$$D_2 r_2 > \frac{D_1 r_1}{\left(1 - \frac{\beta_{21}}{k_2}\right)}, \quad (1.3.3)$$

the species u_2 blocks the spread of species u_1 , but it can not be considered as a general condition. Example on that, when β_{21} is not small compare to k_2 , condition (1.3.3) can only hold if the diffusion coefficient and the growth rate of species u_2 exceed those of species u_1 considerably.

The travelling wave solutions for the diffusion Lotka-Volterra system are widely studied, examples of this, the exact travelling wave solutions using appropriate ansatz have been studied in [RM00, MT09]. The existence of at least one travelling wave at minimal

wave speed is proven in [FC03]. Perturbation methods are used in [Hos03] to study the travelling wave solutions for this model asymptotically, when there is only one stable equilibrium solution and the diffusion coefficient is small. In our present work we will study a reaction-diffusion system for competing and cooperating species. We will use similar initial conditions to those we showed above for the Lotka-Volterra system, in order to study the travelling wave solutions. We will consider a fast diffusion and slow reaction problem and we will use numerical and asymptotic methods to find the possible travelling waves.

1.4 Stability of travelling waves

The stability of travelling waves has applications in biology, ecology and others, and was studied by many authors (see for example [San98, Jon84, GJ91, SS01, Guo12]). There are several ways to investigate the stability of travelling waves depending on the type of partial differential equations, for more details see the reviews by [Xin00, San02, VV94]. In the two dimensional problem, the wavefront is examined for stability by putting a small perturbation at the head of the wavefront. If the wavefront returns to its original position then it is stable, otherwise it is unstable. Another method of studying the stability of travelling waves is by linearizing the partial differential equations about the wave. The resulting linear system of ordinary differential equations is useful to understand the stability of waves. The growth and decay of the solutions of the linearized system corresponds to the stable and unstable travelling waves.

Evans [Eva75] was the first to define a shooting and matching method to locate the spectrum of the linear differential operator for nerve axon equations. The Evans function was

used later to compute the stability of travelling waves of reaction-diffusion equations [AGJ90].

We use the shooting method to compute the Evans function by starting with a specific value of the spectral parameter and the correct boundary conditions. Shoot integrate towards the far end. Examine how close this solution is to satisfying the boundary conditions at the far end. Note that in practise we can match at either boundary or shoot from either end and match some where in-between to optimize accuracy. We can get accurate results when we use Evans function and it can be considered as a cheap costly tool with computations and saving time (see [Jon84, GJ91]). The idea of the stability of travelling wave in one dimension can be explained as follows (see for example [GMSW03, HZ06, DG05, PSW93, LLM11, SEs11]). Let us consider a single reaction-diffusion equation

$$\frac{\partial u}{\partial t} = D \frac{\partial^2 u}{\partial x^2} + F(u). \quad (1.4.1)$$

Substituting a new variable $z = x - ct$ in (1.4.1) we get

$$\frac{\partial u}{\partial t} = D \frac{\partial^2 u}{\partial z^2} + c \frac{\partial u}{\partial z} + F(u). \quad (1.4.2)$$

Let $Q(z)$ be a travelling wave solution of (1.4.2). We linearize (1.4.2) about $Q(z)$ by setting, $u(x, t) = Q(z) - \hat{u}(x - ct, t)$, and the linear perturbation equation is,

$$\frac{\partial \hat{u}}{\partial t} = D \frac{\partial^2 \hat{u}}{\partial z^2} + c \frac{\partial \hat{u}}{\partial z} + \frac{\partial}{\partial u} F(Q) \hat{u}. \quad (1.4.3)$$

If we substitute $\hat{u}(z, t) = \exp(\sigma t) \bar{u}(z)$ in (1.4.3), we get an eigenvalue problem

$$\sigma \bar{u}(z) = D \frac{d^2 \bar{u}}{dz^2} + c \frac{d \bar{u}}{dz} + \frac{\partial}{\partial u} F(Q) \bar{u} = L \bar{u}, \quad (1.4.4)$$

where L is a linear differential operator. We rewrite (1.4.4) as a system of first order,

$$U' = A(z, \sigma)U, \quad (1.4.5)$$

where

$$A(z, \sigma) = \begin{pmatrix} 0 & 1 \\ \frac{\sigma - \frac{\partial}{\partial u} F(Q)}{D} & \frac{-c}{D} \end{pmatrix},$$

subject to the boundary conditions

$$\bar{u}(z) \rightarrow \bar{u}(0) \quad \text{as } z \rightarrow \pm\infty.$$

To construct the Evans function, we need to find solutions of (1.4.5) that decay to zero as $z \rightarrow \pm\infty$. The limit matrices $A_{\pm}(\sigma)$ can be found from the boundary conditions,

$$\lim_{z \rightarrow \pm\infty} A(z, \sigma) = A_{\pm}(\sigma). \quad (1.4.6)$$

Let $\mu_{1,2}^{\pm}$ and $v_{1,2}^{\pm}$ be the eigenvalues and eigenvectors of the matrices $A_{\pm}(\sigma)$. From the eigenvalues and eigenvectors of the limit matrices A_{\pm} , we can construct eigensolutions of (1.4.6), say $\bar{u}_1^+, \dots, \bar{u}_i^+$ and $\bar{u}_{i+1}^-, \dots, \bar{u}_n^-$ as $z \rightarrow +\infty$ and $-\infty$ respectively. For example, if we have 2×2 matrices A_{\pm} , and let $\mu_{1,2}^{\pm}$ be the eigenvalues and $v_{1,2}^{\pm}$ the eigenvectors, then there exists an eigensolution $\bar{u}_1^-(z, \sigma)$ of (1.4.5) with respect to the limit matrices corresponding to the unstable subspace of A_- satisfying the conditions

$$\lim_{z \rightarrow -\infty} \exp(-\mu_1^- z) \bar{u}_1^-(z, \sigma) = v_1^-, \quad \text{Re}(\mu_1^-) > 0,$$

and an eigensolution $\bar{u}_2^+(z, \sigma)$ of (1.4.5) with respect to the limit matrices and corresponding to the stable subspace of A_+ satisfying the conditions

$$\lim_{z \rightarrow +\infty} \exp(-\mu_2^+ z) \bar{u}_2^+(z, \sigma) = v_2^+, \quad \text{Re}(\mu_2^+) < 0.$$

Then, σ is an eigenvalue of (1.4.5) if and only if the solutions \bar{u}_1^- and \bar{u}_2^+ are linearly dependent or, equivalently the Wronskian equals to zero which has the expression

$$W(\bar{u}_1, \bar{u}_2) = \begin{vmatrix} \bar{u}_1 & \bar{u}_2 \\ \bar{u}_1' & \bar{u}_2' \end{vmatrix} = 0.$$

The Evans function is defined by,

$$E(\sigma) = \det[\bar{u}_1^-(0, \sigma), \bar{u}_2^+(0, \sigma)].$$

$E(\sigma)$ is analytic in σ with zeroes corresponding in both location and multiplicity to the eigenvalues of the linear operator L . The instability of travelling wave solutions can be deduced from $E(\sigma)$. If $E(\sigma)$ has zeroes in the region $\text{Re}(\sigma) > 0$, then we can say that the travelling wave is unstable. The Evans function can be evaluated numerically by defining the solutions of (1.4.6) at $-\infty$ and $+\infty$, and shooting backward or forward towards $z = 0$. However, the numerical integration of a system of differential equations whose solutions grow exponentially should be treated carefully. In [PSW93], they deal with this problem by introducing the variable,

$$\bar{u}(z, \sigma) = \exp(-\mu z)u(z, \sigma),$$

where

$$\mu = \begin{cases} \mu_1^-, & \text{for } z \leq 0 \\ \mu_2^+, & \text{for } z > 0. \end{cases}$$

If we substitute $u(z, \sigma)$ in (1.4.6) we get

$$\frac{du}{dz} = [A(z, \sigma) - \mu I]u, \tag{1.4.7}$$

where I is the identity matrix. We will solve (1.4.7) in order to investigate the stability of travelling wave solutions. The Evans function has been computed analytically (see for example [FaP03, PW92, SE90, Ter90, HZ06]) and for complicated problems it has been computed numerically (see [MN08, AB01, BDG02, Bri01, HZ06]).

For two dimensional reaction-diffusion equations, we first make the substitutions

$$u(x, y, t) = u(x, t) \exp(iky), \tag{1.4.8}$$

where k is a wave number. The rest of the processes are the same as shown above for the one dimensional problem. The Evans function for the two dimensional stability problem has the form,

$$E(\sigma, k) = \text{Det}[u_1^-(0, \sigma, k)u_2^+(0, \sigma, k)].$$

An interesting reaction-diffusion system with an unstable wavefront in two dimensions is the Gray-Scott system

$$\begin{aligned}\frac{\partial u}{\partial t} &= D\nabla^2 u - uv^2 - \kappa uw, \\ \frac{\partial w}{\partial t} &= \nabla^2 w + uv^2 + \kappa uw,\end{aligned}\tag{1.4.9}$$

where κ is a parameter. In [ZF94, HPSS93, BCM99], it was shown that this system has an unstable wavefront when $\kappa = 0$ and for suitable values of D . We will apply our numerical methods which we will get in Chapter 5 to the Gray-Scott system and for the same values of the parameters shown above to test our methods.

1.5 Reaction-diffusion system

Consider the reaction-diffusion system

$$\begin{aligned}\frac{\partial u}{\partial t} &= D_u \frac{\partial^2 u}{\partial x^2} + k_u u(1 + l_u u - m_u u^2 - n_u w), \\ \frac{\partial w}{\partial t} &= D_w \frac{\partial^2 w}{\partial x^2} + k_w w(1 + l_w w - m_w w^2 - n_w u),\end{aligned}\tag{1.5.1}$$

where D_u and D_w are diffusion coefficients, and $k_u u(1 - m_u u^2)$ and $k_w w(1 - m_w w^2)$ are generalised logistic growth rates for the species u and w . In this model, the intra specific cooperation has the cooperative parameters l_u and l_w , whilst the inter specific competition has competitive coefficients n_u and n_w . When $n_w = n_u = 0$, (1.5.1) decouple and

each part is equivalent to the system studied in [Bri90]. Before we start to analyse this system, it is essential to write it in non dimensional terms. This make the units for variables unimportant and reduces the number of parameters. We define dimensionless variables

$$u = U\bar{u}, \quad w = W\bar{w}, \quad x = \left(\frac{D_u}{k_u}\right)^{1/2} \bar{x}, \quad t = \frac{\bar{t}}{k_u},$$

in terms of which (1.5.1) becomes

$$\begin{aligned} \frac{\partial \bar{u}}{\partial \bar{t}} &= \frac{\partial^2 \bar{u}}{\partial \bar{x}^2} + \bar{u}(1 + \alpha_1 \bar{u} - (1 + \alpha_1) \bar{u}^2 - \gamma_1 \bar{w}), \\ \frac{\partial \bar{w}}{\partial \bar{t}} &= \frac{D}{\lambda} \frac{\partial^2 \bar{w}}{\partial \bar{x}^2} + \lambda \bar{w}(1 + \alpha_2 \bar{w} - (1 + \alpha_2) \bar{w}^2 - \gamma_2 \bar{u}). \end{aligned} \quad (1.5.2)$$

Here U and W are the unique single species equilibrium solutions given by the positive solutions of

$$1 + l_u U - m_u U^2 = 0, \quad 1 + l_w W - m_w W^2 = 0.$$

The dimensionless parameters are

$$\alpha_1 = l_u U, \quad \gamma_1 = n_u W, \quad \frac{D}{\lambda} = \frac{D_w}{D_u}, \quad \lambda = \frac{k_w}{k_u}, \quad \alpha_2 = l_w W, \quad \gamma_2 = n_w U.$$

The two single species equilibrium solutions are the clear solutions for (1.5.1), therefore we non-dimensionalize it as explained above. All parameters are positive. For notational convenience we now omit the over bar, so that (1.5.2) becomes

$$\begin{aligned} \frac{\partial u}{\partial t} &= \frac{\partial^2 u}{\partial x^2} + u(1 + \alpha_1 u - (1 + \alpha_1) u^2 - \gamma_1 w), \\ \frac{\partial w}{\partial t} &= \frac{D}{\lambda} \frac{\partial^2 w}{\partial x^2} + \lambda w(1 + \alpha_2 w - (1 + \alpha_2) w^2 - \gamma_2 u). \end{aligned} \quad (1.5.3)$$

For $0 < \lambda \ll 1$, (1.5.3) is in the same range as in [Bil04], and we will discuss the reason later. Also, with small λ , w diffuses rapidly and grows slowly. The minus signs in front of $\gamma_1 w$ and $\gamma_2 u$ mean that both species are negatively affected when they compete with

CHAPTER 1: INTRODUCTION

each other for resources, whilst the plus signs in front of $\alpha_1 u$ and $\alpha_2 w$ reflect cooperation within species.

We will study three ecologically important initial conditions and also the bifurcations of the spatially uniform solutions of (1.5.3). We will assume that the initial conditions are symmetric about the origin, so we consider the problem for $x \geq 0$ and $t \geq 0$,

$$u(x, 0) = u_0(x), \quad w(x, 0) = w_0(x),$$

and boundary conditions

$$\frac{\partial u}{\partial x}(0, t) = 0, \quad \frac{\partial w}{\partial x}(0, t) = 0.$$

We will consider initial conditions of three types, which describe the most common cases in population ecology:

- I.C. A:

$$u_0(x) = \begin{cases} 1 & \text{for } x \leq L_0, \\ 0 & \text{for } x > L_0, \end{cases}$$

$$w_0(x) = 1,$$

where L_0 is a width of step function. The far field boundary conditions are therefore $u \rightarrow 0$ and $w \rightarrow w_\infty$ as $x \rightarrow \infty$. The physical meaning for this case is that species w is native and species u is introduced.

- I.C. B:

$$u_0(x) = 1,$$

$$w_0(x) = \begin{cases} 1 & \text{for } x \leq L_0, \\ 0 & \text{for } x > L_0. \end{cases}$$

The far field boundary conditions are therefore, $u \rightarrow u_\infty$ and $w \rightarrow 0$ as $x \rightarrow \infty$. The physical meaning for this case is that species u is native and species w is introduced.

- I.C. C:

$$u_0(x) = \begin{cases} 1 & \text{for } x \leq L_0, \\ 0 & \text{for } x > L_0, \end{cases}$$

$$w_0(x) = \begin{cases} 1 & \text{for } x \leq L_0, \\ 0 & \text{for } x > L_0, \end{cases}$$

We have chosen in the initial condition to have a value ($u_0 = 1$ or $w_0 = 1$) consistent with the value of the equilibrium solutions as we will see later. This will help of getting a stable numerical solutions as we will see in Chapter 3. The far field boundary conditions are therefore, $u \rightarrow 0$ and $w \rightarrow 0$ as $x \rightarrow \infty$. The physical meaning for this case is that species u and w are both introduced.

The initial conditions of types A and B correspond to the invasion of one species into a region already inhabited by the other. The case with two invasions is reflected in the initial condition C . In Chapter 2, we will study (1.5.3), the reaction-diffusion system for competing and cooperating species and compare it to the Lotka-Volterra system. We will compare the number and stability of equilibrium solutions and the type of travelling wave solutions in both systems. In Chapter 3, we will compute the numerical solutions for the travelling waves of (1.5.3) using the three types of initial conditions, A , B and C . We will study the dynamics of the process of change from one dominant travelling wave to another in the case of initial condition C using numerical and asymptotic methods.

CHAPTER 1: INTRODUCTION

In Chapter 4, we will use asymptotic methods to find the three types of travelling wave solutions. Furthermore, we will investigate the existence of unsteady travelling wave solutions similar to what was found in [Bil04] for $t = O(\lambda^{-1})$, $\lambda \ll 1$. We will study the stability of travelling waves of the reaction-diffusion model for competing and cooperating species in two dimensions numerically in Chapter 5, and we will use asymptotic methods and Evans function to analyse the stability of travelling waves.

Equilibrium solutions

In this chapter we study the dynamics of a reaction-diffusion system that represents competition between two species and cooperation within species. We begin by studying the types and stability of equilibrium solutions. We study the types of bifurcations, and we use the phase portrait to show the possible connections between equilibrium solutions.

2.1 Equilibrium solutions and bifurcation

We study the equilibrium solutions of (1.5.3)

$$\begin{aligned}\frac{du}{dt} &= u(1 + \alpha_1 u - (1 + \alpha_1)u^2 - \gamma_1 w) \equiv u(f(u) - \gamma_1 w), \\ \frac{dw}{dt} &= \lambda w(1 + \alpha_2 w - (1 + \alpha_2)w^2 - \gamma_2 u) \equiv \lambda w(g(w) - \gamma_2 u),\end{aligned}\tag{2.1.1}$$

where

$$f(u) = 1 + \alpha_1 u - (1 + \alpha_1)u^2, \quad g(w) = 1 + \alpha_2 w - (1 + \alpha_2)w^2.$$

The convenient way to analyse these solutions and get a qualitative picture of the dynamics of the ordinary differential equations (2.1.1) is using nullclines. The nullclines

CHAPTER 2: EQUILIBRIUM SOLUTIONS

are

$$\begin{aligned}u(f(u) - \gamma_1 w) &= 0, \\w(g(w) - \gamma_2 u) &= 0.\end{aligned}\tag{2.1.2}$$

The intersection of $\gamma_1 w = f(u)$ and $\gamma_2 u = g(w)$ or the values of u and w for which the time derivatives in (2.1.1) are equal to zero are the spatially uniform solutions or the equilibrium solutions. Thus, the obvious equilibrium solutions are,

- $(u, w) = (0, 1)$ and $(u, w) = (1, 0)$, which are single species equilibrium points.
- $(u, w) = (0, 0)$, which is an extinction of both species.

In addition, there may be up to three other equilibrium solutions given by the intersections of the quadratic curves

$$w = f(u)/\gamma_1, \quad u = g(w)/\gamma_2.\tag{2.1.3}$$

There are seven topologically different arrangements of the curves, shown in Figure 2.1 and denoted by R_1 - R_7 . In cases R_3 and R_7 there are no additional equilibria, in R_1 and R_6 there is one, in R_2 and R_4 there are two, and in R_5 there are three additional equilibrium solutions.

CHAPTER 2: EQUILIBRIUM SOLUTIONS

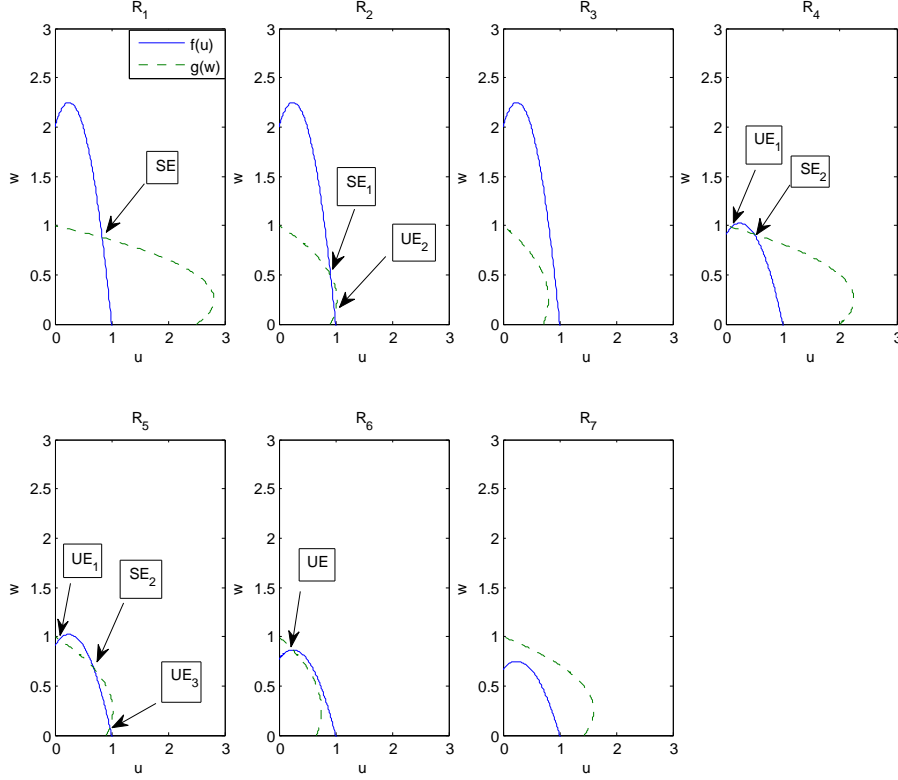


Figure 2.1: The intersection of the two curves $w = f(u)/\gamma_1$ and $u = g(w)/\gamma_2$ in each of the topologically distinct cases R_1 to R_7 . The stable and unstable interior equilibrium points are labelled SE and UE.

In order to study the stability of the equilibrium points, we need to consider the Jacobian matrix

$$J = \begin{pmatrix} \frac{\partial f_1(u, w)}{\partial u} & \frac{\partial f_1(u, w)}{\partial w} \\ \frac{\partial f_2(u, w)}{\partial u} & \frac{\partial f_2(u, w)}{\partial w} \end{pmatrix},$$

$$f_1(u, w) = u(f(u) - \gamma_1 w),$$

$$f_2(u, w) = \lambda w(g(w) - \gamma_2 u),$$

CHAPTER 2: EQUILIBRIUM SOLUTIONS

where $f_1(u, w) = 0$ and $f_2(u, w) = 0$ are the nullclines. From the determinant of the Jacobian we can find the characteristic equation

$$K^2 - \text{tr}J K + \det J = 0, \quad (2.1.4)$$

where $\text{tr}J$ and $\det J$ are the trace and determinant of J respectively, and in general

$$\text{tr}J = \frac{\partial f_1(u, w)}{\partial u} + \frac{\partial f_2(u, w)}{\partial w}, \quad \det J = \frac{\partial f_1(u, w)}{\partial u} \frac{\partial f_2(u, w)}{\partial w} - \frac{\partial f_1(u, w)}{\partial w} \frac{\partial f_2(u, w)}{\partial u}.$$

The eigenvalues of the Jacobian are the solutions of the quadratic equation (2.1.4)

$$K_{1,2} = \frac{\text{tr}J \pm \sqrt{(\text{tr}J)^2 - 4\det J}}{2}. \quad (2.1.5)$$

The stability of the equilibrium points depends on the sign of the eigenvalues at (2.1.5). Figure 2.2 (see for example [Kot01]) shows the type of an equilibrium point depending on the trace and the determinant. The line $\det J = 0$ separates saddles from nodes, and the curve $(\text{tr}J)^2 = 4\det J$ separates nodes from foci.

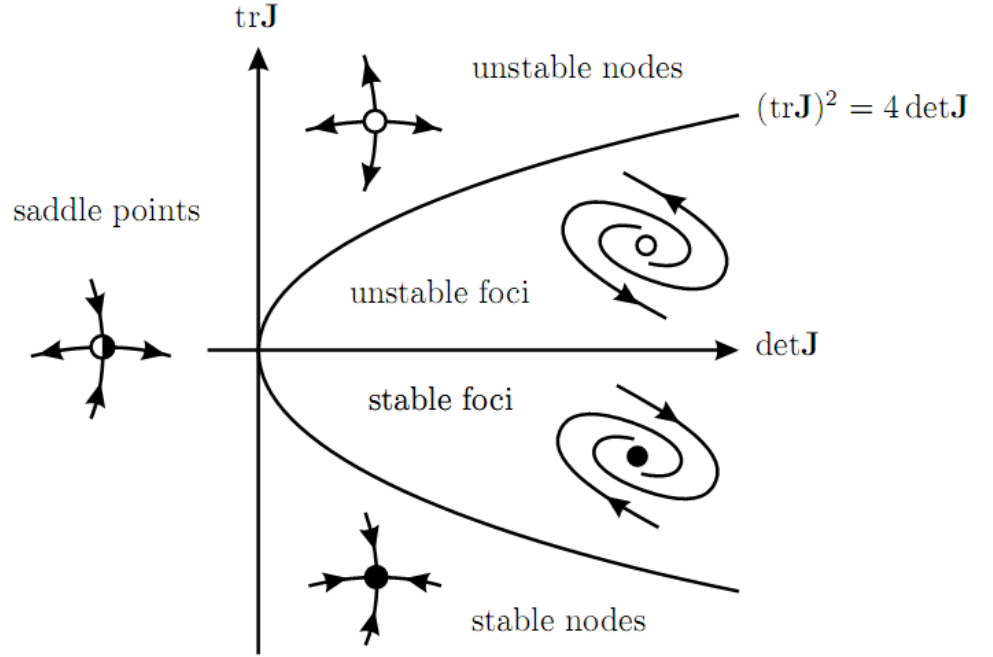


Figure 2.2: The type of equilibrium point found from the eigenvalues of the Jacobian.

The Jacobian of (2.1.1) is

$$J = \begin{pmatrix} f'(u) - \gamma_1 w & -\gamma_1 u \\ -\lambda \gamma_2 w & \lambda(g'(w) - \gamma_2 u) \end{pmatrix}$$

where

$$f' = \frac{df}{du}, \quad g' = \frac{dg}{dw}.$$

Also

$$\text{tr} J = f'(u) - \gamma_1 w + \lambda(g'(w) - \gamma_2 u),$$

CHAPTER 2: EQUILIBRIUM SOLUTIONS

$$\det J = (f'(u) - \gamma_1 w) \lambda (g'(w) - \gamma_2 u) - (\gamma_1 u \lambda \gamma_2 w),$$

where

$$f'(u) = 1 + 2\alpha_1 u - 3(1 + \alpha_1)u^2,$$

$$g'(w) = 1 + 2\alpha_2 w - 3(1 + \alpha_2)w^2.$$

The stability analysis for the equilibrium solutions show that,

- $(0,0)$:

Eigenvalues	Eigenvectors
1	$(1,0)^T$
λ	$(0,1)^T$

This is an unstable node for all positive values of λ .

- $(1,0)$:

Eigenvalues	Eigenvectors
$-(2 + \alpha_1)$	$(1,0)^T$
$\lambda(1 - \gamma_2)$	$(1, \frac{-2-\alpha_1-\lambda(1-\gamma_2)}{\gamma_1})^T$

This is a stable node if $\gamma_2 > 1$ and a saddle point if $\gamma_2 < 1$. Note that this is the unique stable equilibrium state with $u > 0$ and $w = 0$ if $\gamma_2 > 1$.

- $(0,1)$:

Eigenvalues	Eigenvectors
$-\lambda(2 + \alpha_2)$	$(0,1)^T$
$(1 - \gamma_1)$	$(1, \frac{\lambda(2+\alpha_2)-(1-\gamma_1)}{\lambda\gamma_2})^T$

This is a stable node if $\gamma_1 > 1$ and a saddle point if $\gamma_1 < 1$. Note that this is the unique stable equilibrium solution with $w > 0$ and $u = 0$ if $\gamma_1 > 1$. From the stability of the previous equilibrium points we deduce that there are transcritical bifurcations at $\gamma_{1,2} = 1$

(for more details see the next section). If (\hat{u}, \hat{w}) is an intersection point of the two curves $u = g(w)/\gamma_2$ and $w = f(u)/\gamma_1$, then

$$J(\hat{u}, \hat{w}) = \begin{pmatrix} \hat{u}f'(\hat{u}) & -\gamma_1\hat{u} \\ -\lambda\gamma_2\hat{w} & \lambda\hat{w}g'(\hat{w}) \end{pmatrix},$$

and the eigenvalues satisfy

$$K_{1,2} = \frac{(\hat{u}f' + \lambda\hat{w}g') \pm \sqrt{(\hat{u}f' + \lambda\hat{w}g')^2 - 4\hat{u}\hat{w}\lambda(g'f' - \gamma_1\gamma_2)}}{2}. \quad (2.1.6)$$

The equilibrium solution (\hat{u}, \hat{w}) is a stable node if $f'(\hat{u})g'(\hat{u}) - \gamma_1\gamma_2 > 0$ and $(\hat{u}f' + \lambda\hat{w}g') < 0$, and a saddle point if $f'(\hat{u})g'(\hat{u}) - \gamma_1\gamma_2 < 0$ and $(\hat{u}f' + \lambda\hat{w}g') > 0$. Note that the slopes of the curves shown in Figure 2.1 are f'/γ_1 and γ_2/g' , so the stability of each equilibrium point can be determined from these slopes at each point of intersection. There are seven regions formulated depending on the number of intersection points. Some of the boundaries of these regions are given by the transcritical bifurcations $\gamma_1 = 1$ and $\gamma_2 = 1$ which we noted above. The remaining boundaries are given when the two quadratics, $u = g(w)/\gamma_2$ and $w = f(u)/\gamma_1$, are tangent. At this tangency:

$$\frac{f'(u)}{\gamma_1} = \frac{\gamma_2}{g'(w)}, \quad (2.1.7)$$

which is consistent with the fact that the nature of the equilibrium point changes at this value of the parameters. By substituting (2.1.7) into (2.1.3), we can eliminate w and obtain the two cubic equations

$$a_3u^3 + a_2u^2 + a_1u + a_0 = 0, \quad (2.1.8)$$

$$b_3u^3 + b_2u^2 + b_1u + b_0 = 0,$$

where

$$\begin{aligned}
 a_3 &= \frac{-2}{(1+\alpha_2)}(4\alpha_1 + \alpha_2 + \alpha_2^2 + 4\alpha_2\alpha_1 + \alpha_2\alpha_1^2 + 1), \\
 a_2 &= \frac{3}{(1+\alpha_2)}(\alpha_1 + \alpha_1^2 + \alpha_2\alpha_1 + \alpha_2\alpha_1^2), \\
 a_1 &= \frac{-1}{(1+\alpha_2)}(-2\alpha_1 - 2\alpha_2 + \alpha_1^2 - 2 + \gamma_1\alpha_2\alpha_1 - 2\alpha_2\alpha_1 + \alpha_2\alpha_1^2 + \gamma_1\alpha_2), \\
 a_0 &= \frac{-1}{2(1+\alpha_2)}(\gamma_2\gamma_1^2 + 2\alpha_2\alpha_1 + 2\alpha_1 - \gamma_1\alpha_2\alpha_1), \\
 b_3 &= (4\gamma_2 + 8\gamma_2\alpha_2\alpha_1 + 4\gamma_2\alpha_2\alpha_1^2 + 4\gamma_2\alpha_1^2 + 4\gamma_2\alpha_2 + 8\gamma_2\alpha_1), \\
 b_2 &= (-8\alpha_1 - 4\alpha_1^2 - 4\alpha_2 - \alpha_2^2 - 4\gamma_2\alpha_2\alpha_1 - 4\gamma_2\alpha_2\alpha_1^2 - 8\alpha_2\alpha_1 - \\
 &\quad 4\alpha_2\alpha_1^2 - 4\gamma_2\alpha_1 - 4\gamma_2\alpha_1^2 - 2\alpha_2^2\alpha_1 - 2\alpha_2^2\alpha_1^2 - 4), \\
 b_1 &= (4\alpha_1 + 4\alpha_1^2 + \gamma_2\alpha_2\alpha_1^2 + 4\alpha_2 - \alpha_1 + 4\alpha_2 - \alpha_1^2 + \gamma_2\alpha_1^2 + \alpha_2^2\alpha_1 + \alpha_2^2 + \alpha_1^2), \\
 b_0 &= (-\alpha_1^2 + \frac{\gamma_2^2\gamma_1^2}{4} - \alpha_2\alpha_1^2 - \frac{-\alpha_2^2\alpha_1^2}{4}).
 \end{aligned}$$

A solution of (2.1.8) is possible when the determinant of the Sylvester matrix (see, for example, [Afo95]) vanishes, so that

$$\begin{vmatrix}
 a_3 & a_2 & a_1 & a_0 & 0 & 0 \\
 0 & a_3 & a_2 & a_1 & a_0 & 0 \\
 0 & 0 & a_3 & a_2 & a_1 & a_0 \\
 b_3 & b_2 & b_1 & b_0 & 0 & 0 \\
 0 & b_3 & b_2 & b_1 & b_0 & 0 \\
 0 & 0 & b_3 & b_2 & b_1 & b_0
 \end{vmatrix} = 0. \tag{2.1.9}$$

Even with the help of a computer algebra package, it is difficult to make analytical progress with this equation. However, by plotting the solution for various values of the parameters, we find that the general picture is as shown in Figure 2.3, where the blue line is

the solution of 6.2.5 and represent saddle-node bifurcation boundary. There are two distinct saddle node bifurcation boundaries, which meet at a cusp where there is a codimension two point (a pitchfork). In the Figures 2.4(a), 2.4(b), 2.4(c), 2.4(d), 2.5(a), 2.5(b), 2.5(c), 2.5(d) and 2.5(e), we show the nullclines $w = f(u)/\gamma_1$ and $u = g(w)/\gamma_2$ are at the boundary of the seven regions. We plot the negative intersection points of the two curves in order to explain how the coexistence equilibrium points are moving around the origin. Figure 2.4(a), shows that the coexistence equilibrium point changes from negative to positive when it moves from $R1$ to $R2$, in other words, it moves from the left of the origin to the right. Thus, there is a transcritical bifurcation between $R1$ and $R2$. Similar behaviour can be found in Figures 2.4(a), 2.4(b), 2.4(c), 2.4(d), 2.5(a) and 2.5(b) which show the behaviour of coexistence equilibrium points around the origin on either side of the boundaries $R1 - R4$, $R4 - R5$, $R2 - R5$, $R3 - R6$ and $R6 - R7$ respectively. It is clear that, in Figures 2.5(c) and 2.5(e), the number of coexistence equilibrium points changes from zero to two between the regions $R2 - R3$ and $R4 - R7$, and this is a saddle-node bifurcation. The final Figure (2.5(d)), shows that there is a saddle-node bifurcation between regions $R5 - R6$.

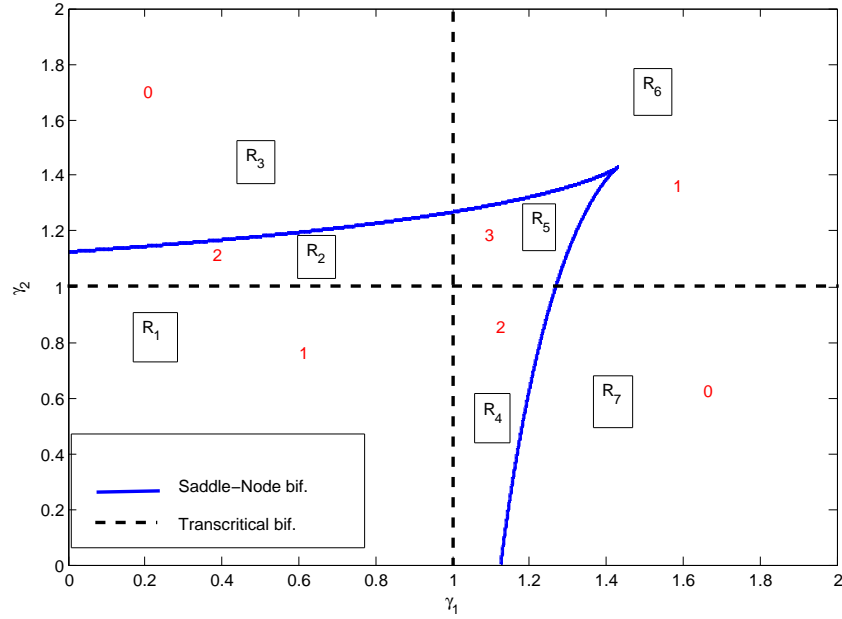


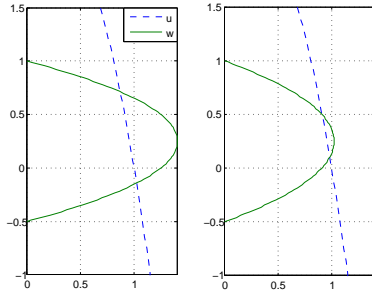
Figure 2.3: The bifurcation boundaries when $\alpha_{1,2} = 1$. The number of interior equilibrium points in each region is also shown.

2.1.1 Stability of the equilibrium points and the phase portrait in the regions

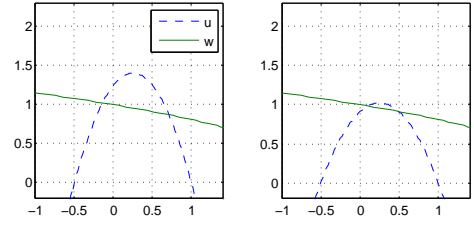
$R_1 - R_7$

From the stability of the equilibrium points $(1, 0)$ and $(0, 1)$, we can deduce the stability of the coexistence equilibrium points in each region. We have shown that $(1, 0)$ is a stable node if $\gamma_2 > 1$ and a saddle point if $\gamma_2 < 1$, while $(0, 1)$ is a stable node if $\gamma_1 > 1$ and a saddle point if $\gamma_1 < 1$. Also $(0, 0)$ is always an unstable node, therefore, the phase portrait and stability in the regions $R_1 - R_7$ are shown in Figures 2.6(a), 2.6(b), 2.6(c), 2.6(d), 2.6(e), 2.6(f) and 2.6(g). The equilibrium solution $(0, 1)$ at the boundary $\gamma_1 = 1$ (this occurs when we move between $R_1 - R_4$ or $R_2 - R_5$ or $R_3 - R_6$) collides with one of the unstable coexistence equilibrium solution at $\gamma_1 = 1$ and then the unstable coexistence equilibrium

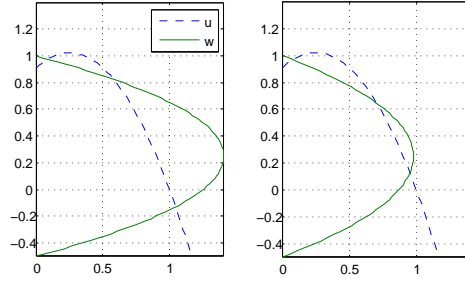
CHAPTER 2: EQUILIBRIUM SOLUTIONS



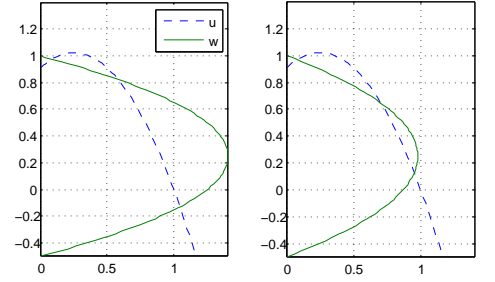
(a) The nullclines of (2.1.2) in $R1$ and $R2$.



(b) The nullclines of (2.1.2) in $R1$ and $R4$.

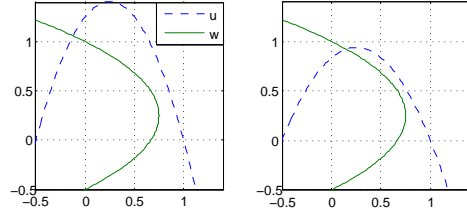


(c) The nullclines of (2.1.2) in $R4$ and $R5$.

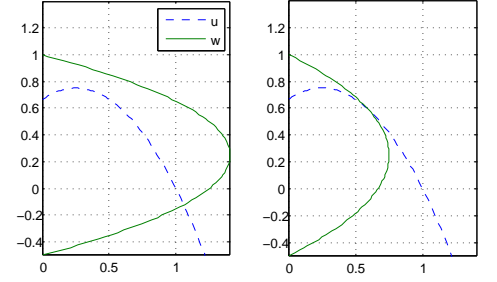


(d) The nullclines of (2.1.2) in $R2$ and $R5$.

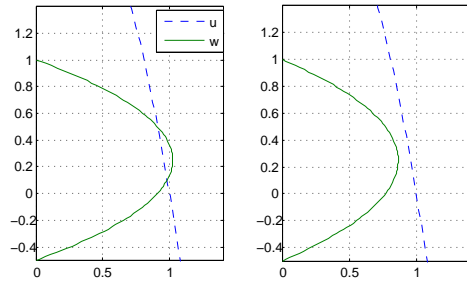
Figure 2.4: Description of the types of bifurcation, when the number of the intersection points of $u = g(w)/\gamma_2$ and $w = f(u)/\gamma_1$ are changed corresponding to the parameter values.



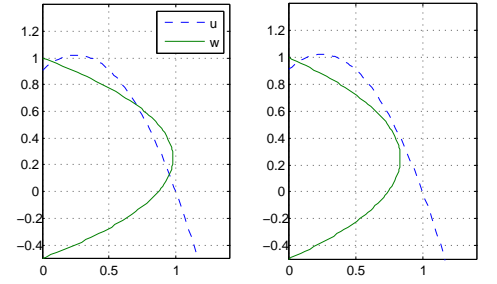
(a) The nullclines of (2.1.2) in R_3 and R_6 .



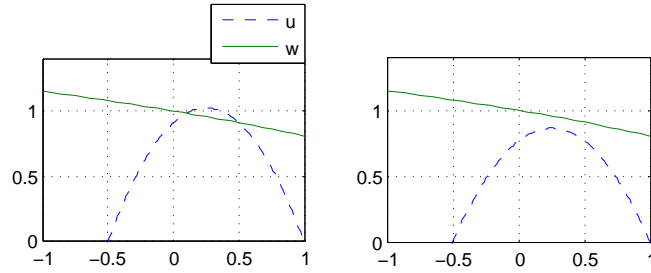
(b) The nullclines of (2.1.2) in R_6 and R_7 .



(c) The nullclines of (2.1.2) in R_2 and R_3 .



(d) The nullclines of (2.1.2) in R_5 and R_6 .



(e) The nullclines of (2.1.2) in R_4 and R_7 .

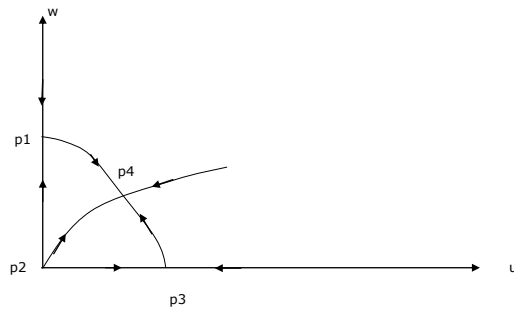
Figure 2.5: Description of the types of bifurcation, when the number of the intersection points of the two curves $u = g(w)/\gamma_2$ and $w = f(u)/\gamma_1$ are changed corresponding to the parameter values.

solution annihilate at $(0,1)$ when we cross the boundary (see 2.6(a) and 2.6(d) or 2.6(b) and 2.6(e) or 2.6(c) and 2.6(f)). Similar thing happen when we move cross $\gamma_2 = 1$ (this occurs when we move between $R_1 - R_2$ or $R_4 - R_5$ or $R_6 - R_7$) but this time the unstable coexistence equilibrium solution annihilate at $(1,0)$ (see 2.6(a) and 2.6(b) or 2.6(d) and 2.6(e) or 2.6(f) and 2.6(g)). Both $(1,0)$ and $(0,1)$ are changing their stability and the above analysis show that $\gamma_1 = 1$ and $\gamma_2 = 1$ are transcritical bifurcation. The blue lines in figure 2.3 is the saddle-node bifurcation boundaries as we mentioned above separate the regions $R_2 - R_3$, $R_5 - R_6$ and $R_4 - R_7$. At the blue boundaries, two of the coexistence equilibrium points (one stable and the other unstable) collide and annihilate each other (see 2.6(b) and 2.6(c) or 2.6(e) and 2.6(f) or 2.6(d) and 2.6(g)).

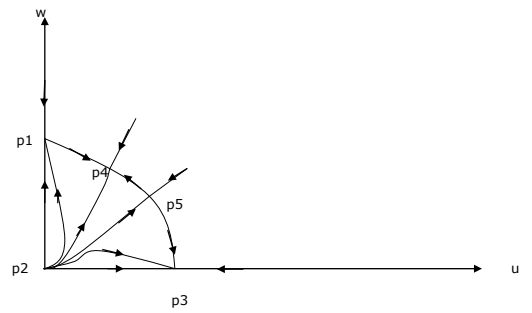
As discussed in chapter one, in the Lotka-Volterra system there are four topologically different regions as shown in Figure 1.3, whilst there are seven topologically different regions for (1.5.3) as shown in Figure 2.3. The regions R_1 , R_3 , R_6 and R_7 are similar to the four regions in the Lotka-Volterra system. In R_1 , there exists a stable coexistence state, and both single equilibrium solutions $(1,0)$ and $(0,1)$ are unstable. The single species $(1,0)$ excludes $(0,1)$ in R_3 , whilst $(0,1)$ excludes $(1,0)$ in R_7 . In R_6 both single species are stable, and the winner depends on the initial densities of the two species. The major difference between the two systems is the three regions R_2 , R_4 and R_5 which can be found in (1.5.3) but do not exist in the Lotka-Volterra system. The key feature of the three regions is the existence of only one stable coexistence equilibrium state. Beside the stable coexistence state, one of the single species wins, $(1,0)$ wins in R_2 , whilst $(0,1)$ wins in R_4 . The other coexistence equilibrium point in both R_2 and R_4 is unstable. In R_5 , there is a strong competition between $(1,0)$ and $(0,1)$ and the winner depends on the initial condition. There are also two unstable and one stable coexistence equilibrium points of

CHAPTER 2: EQUILIBRIUM SOLUTIONS

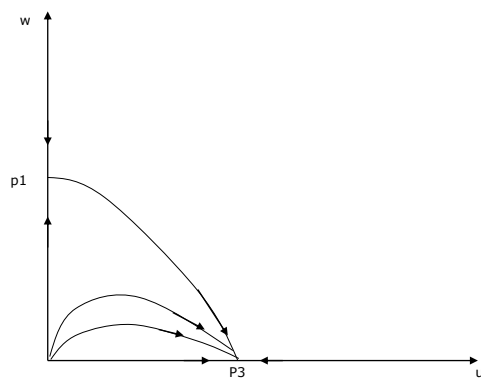
R_5 .



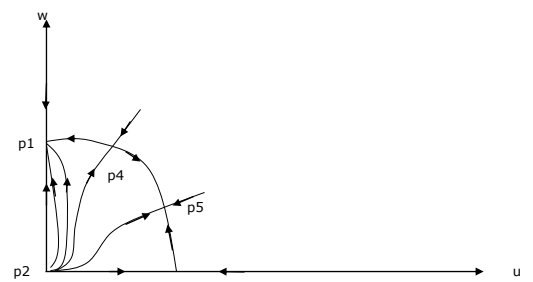
(a) Phase portrait in R_1 .



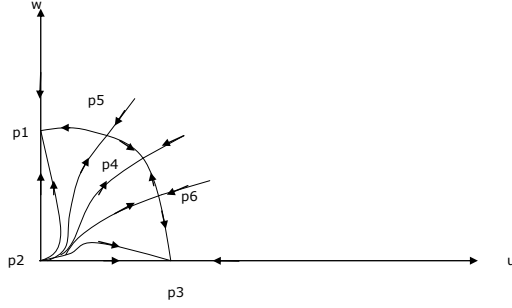
(b) Phase portrait in R_2 .



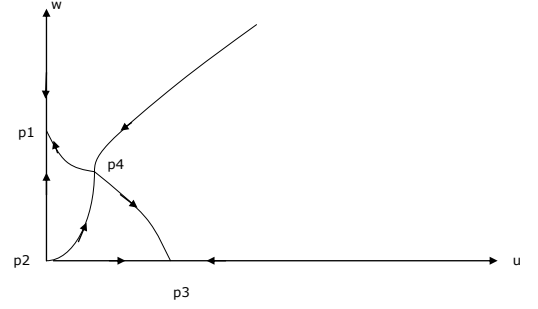
(c) Phase portrait in R_3 .



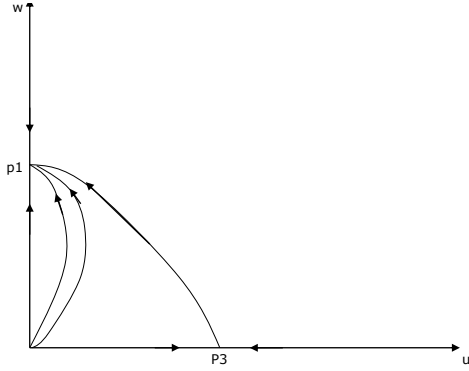
(d) Phase portrait in R_4 .



(e) Phase portrait in R_5 .



(f) Phase portrait in R_6 .



(g) Phase portrait in R_7 .

Figure 2.6: Phase portrait in the seven regions, $R_1 - R_7$.

2.2 The effect of the parameters $\alpha_{1,2}$ on the bifurcation boundaries

In this section we examine how the cooperative coefficients $\alpha_{1,2}$ affect the boundaries of regions $R_1 - R_7$. If we assume that the reaction-diffusion system in (1.5.3) is only for competing species, in other words, there is no cooperation within species and $\alpha_{1,2} = 0$, then (2.1.1) becomes,

$$\begin{aligned}\frac{du}{dt} &= u(1 - u^2 - \gamma_1 w) \equiv u(f(u) - \gamma_1 w), \\ \frac{dw}{dt} &= \lambda w(1 - w^2 - \gamma_2 u) \equiv \lambda w(g(w) - \gamma_2 u).\end{aligned}\tag{2.2.1}$$

The spatially uniform solutions for (2.2.1) are, $(0,0)$, $(1,0)$ and $(0,1)$, the same as in (2.1.1), besides the number of the intersection points of the two curves in (2.1.3). The stability analysis of the equilibrium points $(1,0)$ and $(0,1)$ shows again there are transcritical bifurcations at $\gamma_{1,2} = 1$. A similar analysis of the tangency of the two curve shown in (2.1.7) with help of Sylvester matrix produces a quartic equation,

$$27\gamma_1^4\gamma_2^4 - 288\gamma_1^2\gamma_2^2 + 256\gamma_1^2 + 256\gamma_2^2 - 256 = 0.\tag{2.2.2}$$

This plot of (2.2.2) is shown in Figure 2.7. We can find that the bifurcation boundaries are qualitatively the same as in the case $\alpha_{1,2} = 1$ in Figure 2.3. The seven regions $R_1 - R_7$ still exist for this special case with a narrowing of the regions R_2 and R_4 .

Similar analysis in the case $\alpha_1 \rightarrow \infty$ and $\alpha_2 = 1$, shows an extension in the regions R_4 and R_5 , whilst, R_2 shrinks when α_1 increases, as shown in Figure 2.8. The case is opposite when $\alpha_1 = 1$ and $\alpha_2 \rightarrow \infty$, R_2 is extending and both R_4 and R_5 are shrinking as we can see in Figure 2.9. The final case is when $\alpha_{1,2} \rightarrow \infty$, there is an extension in R_2 , R_4 and R_5 . This case is shown in Figure 2.10. In summary, the parameters $\alpha_{1,2}$ have no effect on the qualitative bifurcation boundaries. There are seven topologically different regions of (1.5.3) for all the values of $\alpha_{1,2}$, including $\alpha_{1,2} = 0$. However, when α_1 increases both regions R_4 and R_5 are increased and the region R_2 is reduced. The opposite occurs when α_2 increases.

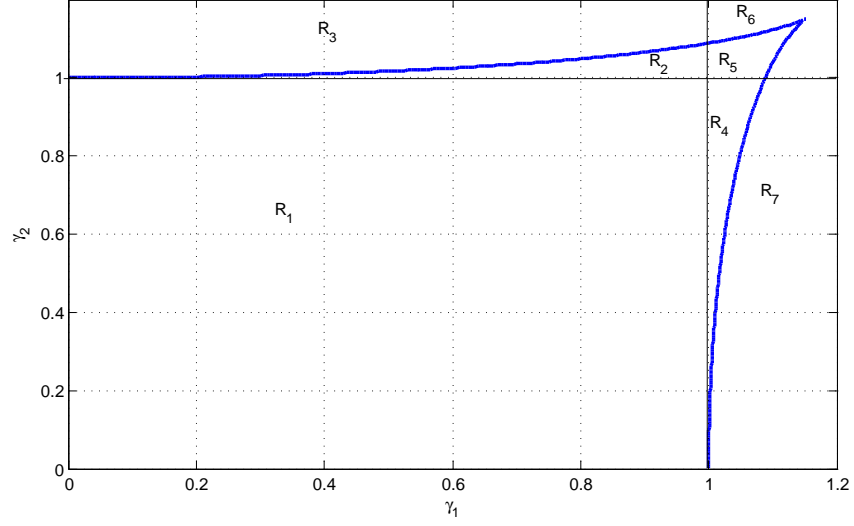


Figure 2.7: The bifurcation boundaries produced from the tangency of the two curves in (2.2.1) and the lines $\gamma_{1,2} = 1$. The parameter values, $\alpha_{1,2} = 0$.

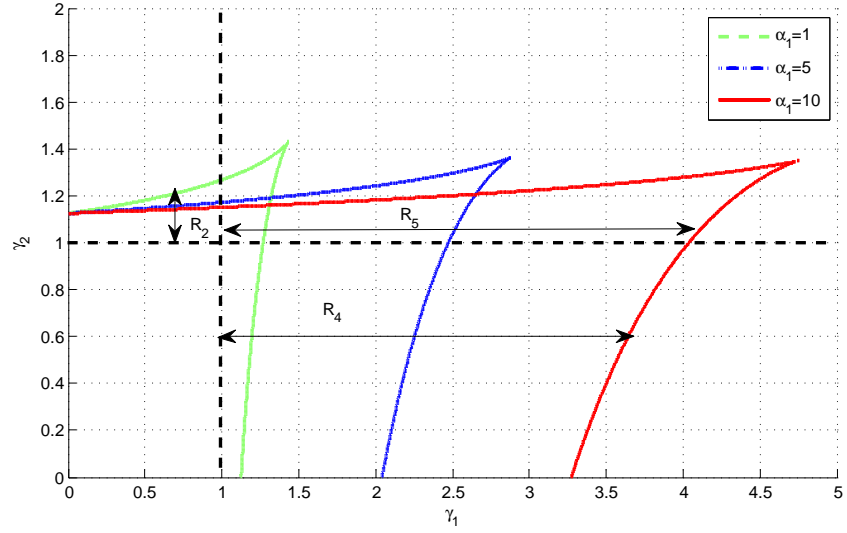


Figure 2.8: The bifurcation boundaries produced from the tangency of the two curves in (2.2.1) and the lines $\gamma_{1,2} = 1$. The parameter values, $\alpha_1 = 10$ and $\alpha_2 = 1$.

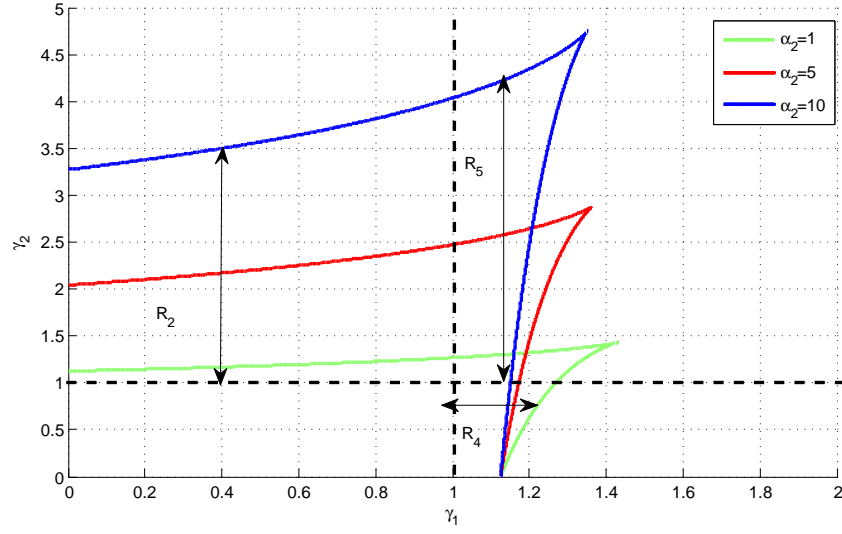


Figure 2.9: The bifurcation boundaries produced from the tangency of the two curves in (2.2.1) and the lines $\gamma_{1,2} = 1$. The parameter values, $\alpha_1 = 1$ and $\alpha_2 = 10$.

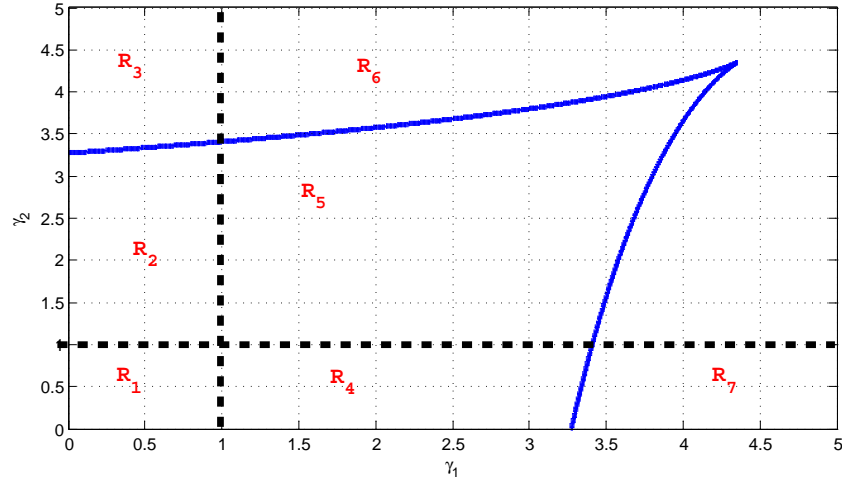


Figure 2.10: The bifurcation boundaries produced from the tangency of the two curves in (2.2.1) and the lines $\gamma_{1,2} = 1$. The parameter values, $\alpha_1 = 10$ and $\alpha_2 = 10$.

Travelling wave solutions for the initial value problem (1.5.3)

In this chapter, we study the types of travelling wave solution for the initial value problem (1.5.3) with the help of MATLAB. Also we investigate the dynamics of the growth of and the development of a travelling wave after a long time in the case of initial condition C , and we compare between numerical and asymptotic solutions for this case.

3.1 Travelling wave solutions

Typical solutions of reaction-diffusion system are travelling waves that connect equilibrium solutions. We concentrate on the case when the travelling wave move to the right. The three types of travelling wave that we study are

- Type (I_a) , the travelling wave connects the positive coexistence equilibrium solution (u_0, w_0) to $(0, 1)$.
- Type (I_b) , the travelling wave connects the positive coexistence equilibrium solu-

tion (u_0, w_0) to $(1, 0)$.

- Type (II_a) , the travelling wave connects $(1, 0)$ to $(0, 0)$.
- Type (II_b) , the travelling wave connects $(0, 1)$ to $(0, 0)$.
- Type (III) , the travelling wave connects $(1, 0)$ to $(0, 1)$, which we also split into type (III_r) when $(1, 0)$ is a stable and behind the wave, and type (III_l) when $(0, 1)$ is a stable and behind the wave.

These travelling wave solutions connect a stable equilibrium solution behind the wave to get a steady wave to another equilibrium solution. Waves of type (I) can only exist if the coexistence state (u_0, w_0) is stable (regions R_1, R_2, R_4 and R_5). Waves of type (II_a) and (III_r) require $(1, 0)$ to be stable (regions R_3 and R_6), whilst waves of type (II_b) and (III_l) require that $(0, 1)$ is stable (regions R_6 and R_7). Waves of type (III) do not exist in regions where (u_0, w_0) is stable, although these satisfy the condition $(1, 0)$ is stable for type (III_r) and $(0, 1)$ is stable for (III_l) . These results are illustrated in Figure 3.1.

Another type of travelling wave that we might expect to exist is one that connects (u_0, w_0) to $(0, 0)$, and this may emerge as a solution of the initial value problem with initial conditions of type C. However, we have found that, not only does such a travelling wave not develop in any numerical simulation we have made, we have been unable to construct such a solution in the asymptotic limit $\lambda \ll 1$. The reasons for this are unclear. This type of travelling wave solutions can be found in (1.5.3) only when $\lambda = 1$ and $D = 1$, which we will discuss later. Note also that travelling wave solutions that connect to unstable coexistence equilibrium solution also exist, but will not be realised in any physically meaningful initial value problem.

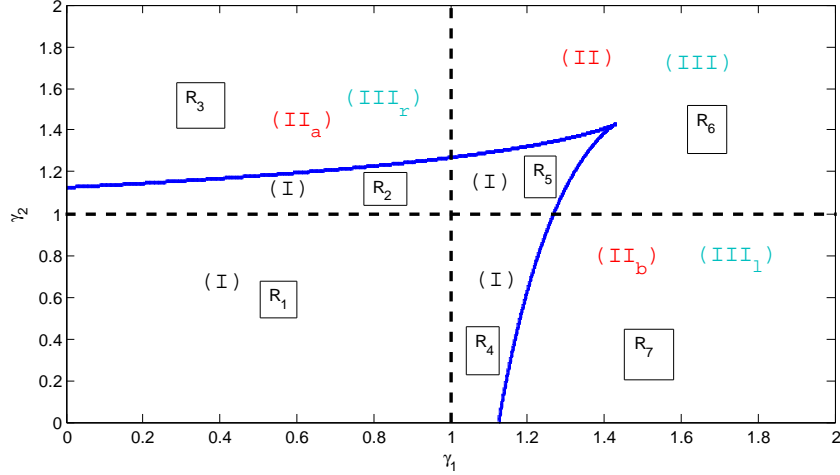


Figure 3.1: An overview of the types of travelling wave that may exist in regions, $R_1 - R_7$. The figure is related to the diagram shown in Fig.2.3.

3.2 Numerical solutions

In this section we solve (1.5.3) numerically and try to find the different types of travelling wave solutions that are generated by the different initial conditions. A semi-implicit finite difference method provides a sufficiently accurate numerical solution since it is unconditionally stable. An implicit method is used to discretise the diffusion operator. For the non linear reaction part we use an explicit method. Finite difference method can be derived using a Taylor series expansion for $u(x_0 + \Delta x)$ and $u(x_0 - \Delta x)$, where Δx is

the step size of x . The discretization equation of (1.5.3) is:

$$\begin{aligned} \frac{u_n^{t+\Delta t} - u_n^t}{\Delta t} &= \frac{u_{n+\Delta x}^{t+\Delta t} - 2u_n^{t+\Delta t} + u_{n-\Delta x}^{t+\Delta t}}{(\Delta x)^2} + \\ &u_n^t(1 + \alpha_1 u_n^t - (1 + \alpha_1)(u_n^t)^2 - \gamma_1 w_n^t), \\ \frac{w_n^{t+\Delta t} - w_n^t}{\Delta t} &= \frac{D}{\lambda} \left(\frac{w_{n+\Delta x}^{t+\Delta t} - 2w_n^{t+\Delta t} + w_{n-\Delta x}^{t+\Delta t}}{(\Delta x)^2} \right) + \\ &\lambda w_n^t(1 + \alpha_2 w_n^t - (1 + \alpha_2)(w_n^t)^2 - \gamma_2 u_n^t). \end{aligned}$$

These equations simplify to give us

$$\begin{aligned} ru_{n+\Delta x}^{t+\Delta t} - (1 + 2r)u_n^{t+\Delta t} + ru_{n-\Delta x}^{t+\Delta t} &= -u_n^t \\ &- (\Delta t)u_n^t(1 + \alpha_1 u_n^t - (1 + \alpha_1)(u_n^t)^2 - \gamma_1 w_n^t), \\ \left(\frac{Dr}{\lambda}\right)w_{n+\Delta x}^{t+\Delta t} - \left(1 + \frac{2Dr}{\lambda}\right)w_n^{t+\Delta t} + \left(\frac{Dr}{\lambda}\right)w_{n-\Delta x}^{t+\Delta t} &= -w_n^t \\ &- (\Delta t)\lambda w_n^t(1 + \alpha_2 w_n^t - (1 + \alpha_2)(w_n^t)^2 - \gamma_2 u_n^t), \end{aligned}$$

where $r = \frac{\Delta t}{(\Delta x)^2}$. The domain of solution $0 < x < l$ is divided into N discrete equally spaced points $x = x_i = (i - 1)\Delta x$, where $i = 1, 2, \dots, N$ and $\Delta x = l/(N - 1)$. The length of domain l should be much larger than $O(\frac{1}{\lambda})$, when $\lambda \ll 1$ to capture the travelling wave solutions. The initial conditions are $u(x, 0) = u_0(x)$ and $w(x, 0) = w_0(x)$. The boundary conditions are no flux Neumann boundary conditions, $u_x = w_x = 0$ at $x = 0, l$, which are imposed using a three point formula (this is a second order accuracy stable)

$$\begin{aligned} u'(x) &= \frac{-3u_n^{t+\Delta t} + 4u_{n+\Delta x}^{t+\Delta t} - u_{n+2\Delta x}^{t+\Delta t}}{2\Delta x} = 0, \\ w'(Y) &= \frac{-3w_n^{t+\Delta t} + 4w_{n+\Delta x}^{t+\Delta t} - w_{n+2\Delta x}^{t+\Delta t}}{2\Delta x} = 0. \end{aligned} \quad (3.2.1)$$

From discretization we get a system of algebraic equations which can be written in the form

$$AU^{t+1} = bU^t, \quad (3.2.2)$$

$$BW^{t+1} = cW^t,$$

$$\begin{bmatrix} 3 & -4 & 1 \\ -r & (1+2r) & -r \\ \ddots & \ddots & \ddots \\ & -r & (1+2r) & -r \\ & 1 & -4 & 3 \end{bmatrix} \begin{bmatrix} u_1^{t+1} \\ u_2^{t+1} \\ \vdots \\ u_{N-1}^{t+1} \\ u_N^{t+1} \end{bmatrix} = \begin{bmatrix} 0 \\ u_2^t + (\Delta t)u_2^t(1 + \alpha_1 u_2^t \\ -(1 + \alpha_1)(u_2^t)^2 - \gamma_1 w_2^t) \\ \vdots \\ u_{N-1}^t + (\Delta t)u_{N-1}^t(1 + \alpha_1 u_{N-1}^t \\ -(1 + \alpha_1)(u_{N-1}^t)^2 - \gamma_1 w_{N-1}^t) \\ 0 \end{bmatrix},$$

where

$$A = \begin{pmatrix} 3 & -4 & 1 \\ -r & (1+2r) & -r \\ \ddots & \ddots & \ddots \\ & -r & (1+2r) & -r \\ & 1 & -4 & 3 \end{pmatrix},$$

$$bU^t = \begin{bmatrix} 0 \\ u_2^t + (\Delta t)u_2^t(1 + \alpha_1 u_2^t) \\ -(1 + \alpha_1)(u_2^t)^2 - \gamma_1 w_2^t \\ \vdots \\ u_{N-1}^t + (\Delta t)u_{N-1}^t(1 + \alpha_1 u_{N-1}^t) \\ -(1 + \alpha_1)(u_{N-1}^t)^2 - \gamma_1 w_{N-1}^t \\ 0 \end{bmatrix}, U^{t+1} = \begin{bmatrix} u_1^{t+1} \\ u_2^{t+1} \\ \vdots \\ u_{N-1}^{t+1} \\ u_N^{t+1} \end{bmatrix}.$$

In the case of w

$$B = \begin{pmatrix} 3 & -4 & 1 \\ -\frac{Dr}{\lambda} & (1 + \frac{2Dr}{\lambda}) & -\frac{Dr}{\lambda} \\ \ddots & \ddots & \ddots \\ & -\frac{Dr}{\lambda} & (1 + \frac{2Dr}{\lambda}) & -\frac{Dr}{\lambda} \\ & 1 & -4 & 3 \end{pmatrix},$$

$$cW^t = \begin{bmatrix} 0 \\ w_2^t + (\Delta t)w_2^t(1 + \alpha_2 w_2^t) \\ -(1 + \alpha_2)(w_2^t)^2 - \gamma_2 u_2^t \\ \vdots \\ w_{N-1}^t + (\Delta t)w_{N-1}^t(1 + \alpha_2 w_{N-1}^t) \\ -(1 + \alpha_2)(w_{N-1}^t)^2 - \gamma_2 u_{N-1}^t \\ 0 \end{bmatrix}, W^{t+1} = \begin{bmatrix} w_1^{t+1} \\ w_2^{t+1} \\ \vdots \\ w_{N-1}^{t+1} \\ w_N^{t+1} \end{bmatrix}.$$

We solve the linear system (3.2.2) at each timestep using the backslash operator in MATLAB. To obtain the wave speed numerically, we consider one of the values of u in the position of the head of the wave front namely $u = 0.5$. Also, when time $t_0 = 0$, then

$t_1 = t_0 + \Delta t$, where Δt is the time step. At the time $t = t_1$, the head of the wave front will be in the position $x = x_1$ and then it moves to $x = x_2$ at time $t = t_2$, where $x_2 = x_1 + \Delta x$. So we can estimate the total distance $\Delta x = x_2 - x_1$ travelled by the wave in the time interval $\Delta t = t_2 - t_1$. Thus

$$\text{Wave speed} = \frac{\text{total distance}}{\text{total time}} = \frac{\Delta x}{\Delta t}.$$

3.3 Numerical solutions of the initial value problem

The aim of this section is to solve the system of algebraic equations(1.5.3) numerically and to find the types of travelling wave solution working in a frame of reference that moves with any travelling waves that develop. In each case we find that at least one and sometimes three travelling waves are generated depending upon the initial conditions and choice of parameters ($R_1 - R_7$).

3.3.1 Initial Condition A : $u_0(x)$ is a step function and $w_0(x) = 1$

We find that there are three qualitatively different types of behaviour. If the parameters lie in R_3 or R_7 , where there are no coexistence equilibria, or in R_6 , where the single coexistence equilibrium state is unstable, a simple travelling wave is generated, which connects $(1, 0)$ to $(0, 1)$, as shown in Figure 3.2.

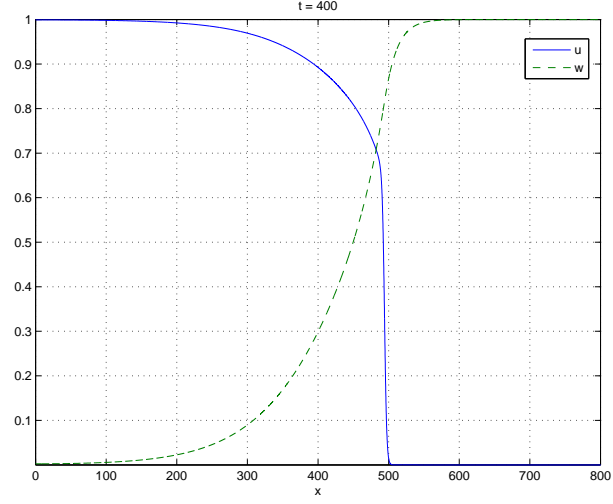


Figure 3.2: From initial condition A and (1.5.3), a travelling wave solution of type (III) is generated when $\alpha_1 = 0.7$, $\alpha_2 = 0.6$, $\gamma_1 = 0.9$, $\gamma_2 = 1.5$, $\lambda = 0.05$ and $D = 2.5$. (R_3 in figure 2.3)

If the parameters lie in R_1 , in which case there is a single, stable coexistence equilibrium, again, a simple travelling wave is generated, but now this connects (u_0, w_0) to $(0, 1)$, as shown in Figure 3.3.

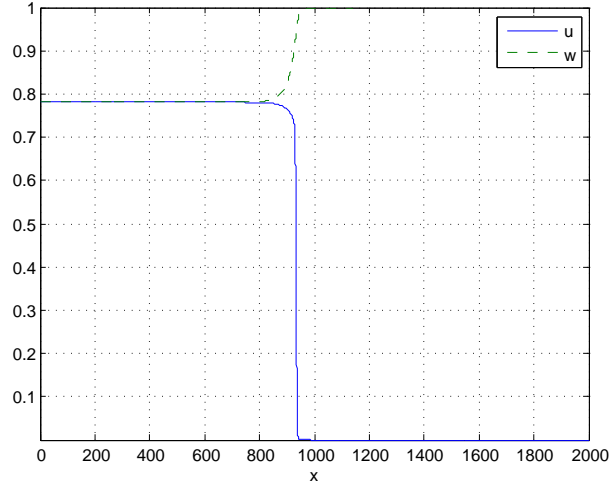


Figure 3.3: From initial condition A and (1.5.3), a travelling wave solution of type (I_a) is generated when $\alpha_{1,2} = 0.6404$, $\gamma_{1,2} = 0.6404$, $\lambda = 0.05$ and $D = 1$. (R_1 in figure 2.3)

Finally, if the parameters lie in R_2 , R_4 or R_5 , more than one coexistence equilibrium state exists, of which exactly one is stable, which we label (u_0, w_0) . This leads to the generation of either one or two travelling waves, depending on the initial values of u and w and also the value of parameters $\gamma_{1,2}$ in these regions. If these are such that, in the spatially-uniform system the initial conditions lie in the basin of attraction of the coexistence state, solutions are similar to those discussed above when the parameters lie in R_1 . If the initial conditions are attracted to $(1, 0)$, two travelling waves are generated, one connecting $(1, 0)$ to (u_0, w_0) , and one connecting (u_0, w_0) to $(0, 1)$, as shown in Figure 3.4. It is clear that with initial condition A we have an invasion case, and the invader is the species u . It can be seen that the initial conditions plays an important role of determining the final state at $t \rightarrow \infty$. After a long time there will be only the equilibrium solution

behind the wave which left from travelling wave solution.

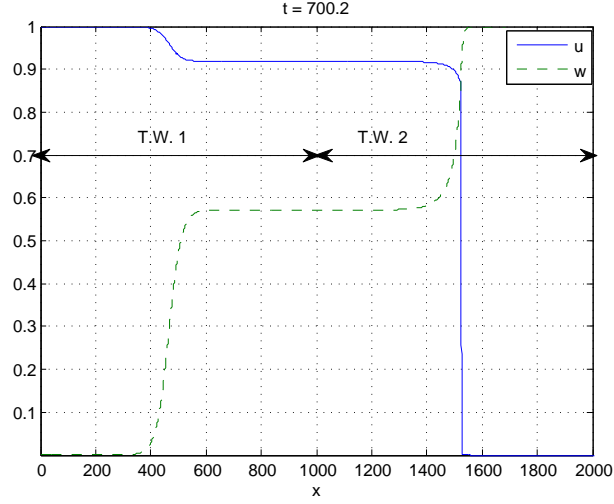


Figure 3.4: From initial condition A and (1.5.3), two travelling wave solutions are generated when $\lambda = 0.05$, $\alpha_1 = 4$, $\alpha_2 = 4$, $\gamma_1 = 0.8$, $\gamma_2 = 1.8$, $\lambda = 0.05$ and $D = 1$. (R_2 in figure 2.3)

3.3.2 Initial Condition B : $u_0(x) = 1$ and $w_0(x)$ is a step function

With initial condition B, the situation is similar to that for initial condition A. The same three qualitatively different cases are possible, which we illustrate in Figures 3.5 to 3.7.

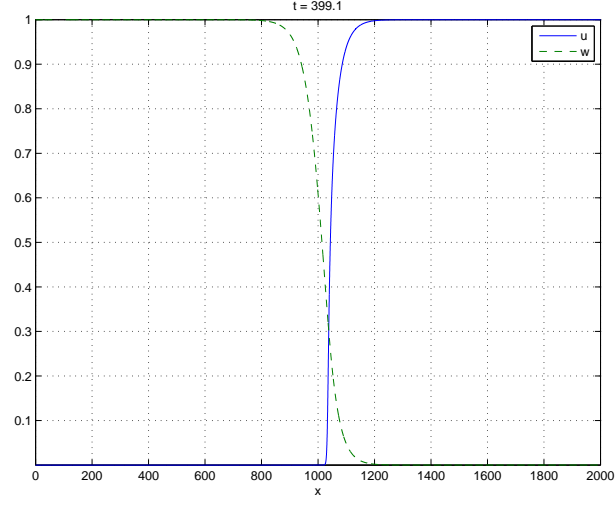


Figure 3.5: From initial condition B and (1.5.3), a travelling wave solution of type (III) is generated when $\alpha_1 = 2.8$, $\alpha_2 = 0.1$, $\gamma_1 = 6$, $\gamma_2 = 0.8$, $\lambda = 0.05$ and $D = 2.8$. (R_7 in figure 2.3)

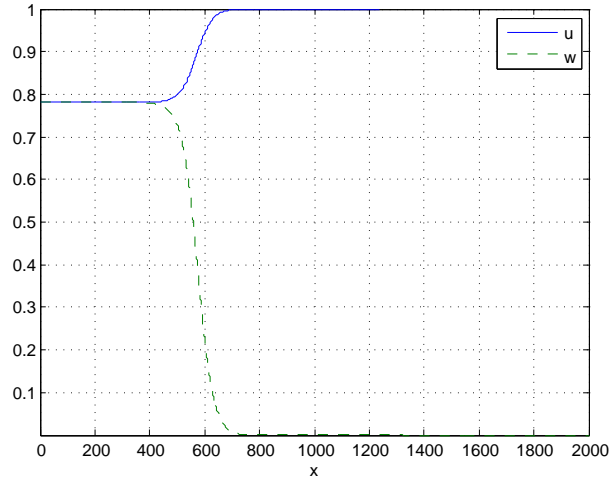


Figure 3.6: From initial condition B and (1.5.3), a travelling wave solution of type (I_b) is generated when $\alpha_{1,2} = 0.6404$, $\gamma_{1,2} = 0.6404$, $\lambda = 0.05$ and $D = 1$. (R_1 in figure 2.3)

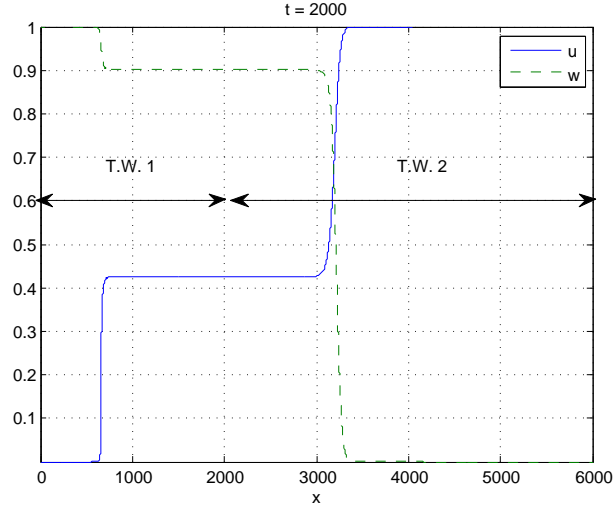


Figure 3.7: From initial condition B and (1.5.3), two travelling wave solutions are generated when $\lambda = 0.05$, $\alpha_1 = 1$, $\alpha_2 = 1$, $\gamma_1 = 1.2$, $\gamma_2 = 0.7$ and $D = 2.8$. (R_4 in figure 2.3)

The invasion of one of the species occurs again with initial condition B, and the invader is the species w . Notice that in all of these typical solutions we have taken $\lambda = 0.05$. As we shall see in chapter 4, when $\lambda \ll 1$, travelling wave solutions develop on an $O(\lambda^{-1})$ lengthscale, with the exception of those that involve an equilibrium state with $u = 0$, in which case there is an inner region at the wavefront where u changes on an $O(1)$ lengthscale.

3.3.3 Initial Condition C: $u_0(x)$ and $w_0(x)$ are step functions

In all cases, the state left behind the wave is determined by the initial conditions and the spatially-uniform system. The main difference from initial conditions A and B is that a travelling wave of type (II) is always generated, and propagates into the region where $u = w = 0$. Whether this is of type (II_a) or (II_b) it depends upon their wavespeed. The faster wave from (II_a) or (II_b) is the one that is generated. For example, Figures 3.8 and 3.9 show the solution when the parameters lie in R_1 , and differ only in the choice of D . In Figure 3.8, the wave of type (II_a) is faster than type (II_b) , and vice versa for Figure 3.9. We compare the wave speed of the travelling wave of types (II_a) and (II_b) in Figure 3.10 for the same value of parameters and different values of D . It can be seen that D plays the crucial role of determining the speed of travelling wave of type (II). Also, Figures 3.11 and 3.12 show two travelling waves are generated of type (III) in addition to (II). The parameters for both figures lie in R_6 . Furthermore, in Figures 3.13 and 3.14 three travelling waves are generated. In addition to type (II) there are two travelling waves that connect $(1,0)$ to (u_0, w_0) and (u_0, w_0) to $(0,1)$ in Figure 3.13, and $(0,1)$ to (u_0, w_0) and (u_0, w_0) to $(1,0)$ in Figure 3.14. The parameters for Figures 3.13 and 3.14 lie in (R_2) and (R_4) respectively. There are always two invaders species u and w with this type of initial condition.

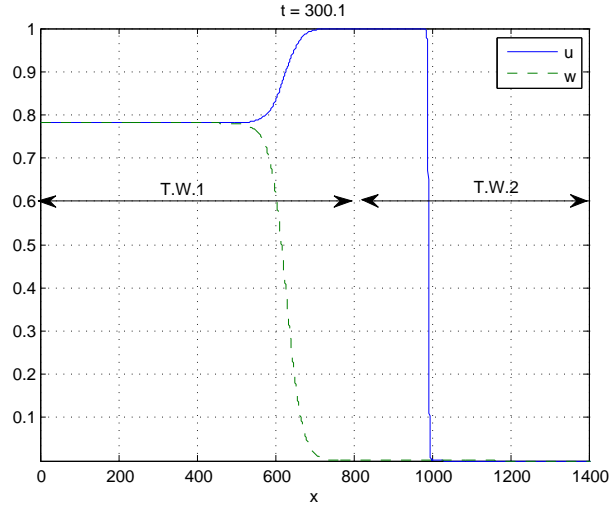


Figure 3.8: From initial condition C and (1.5.3), two travelling waves are generated when $\lambda = 0.05$, $\alpha_{1,2} = 0.6404$, $\gamma_{1,2} = 0.6404$ and $D = 0.5$. The coexistence equilibrium state value is $(u_0, w_0) = (0.78, 0.78)$. (R_1 in figure 2.3)

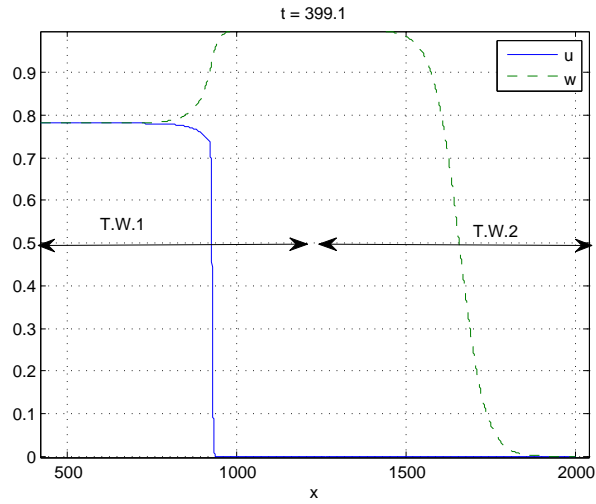


Figure 3.9: From initial condition C and (1.5.3), two travelling waves are generated when $\alpha_{1,2} = 0.6404$, $\gamma_{1,2} = 0.6404$ and $D = 3$. The coexistence equilibrium state value is $(u_0, w_0) = (0.78, 0.78)$. (R_1 in figure 2.3)

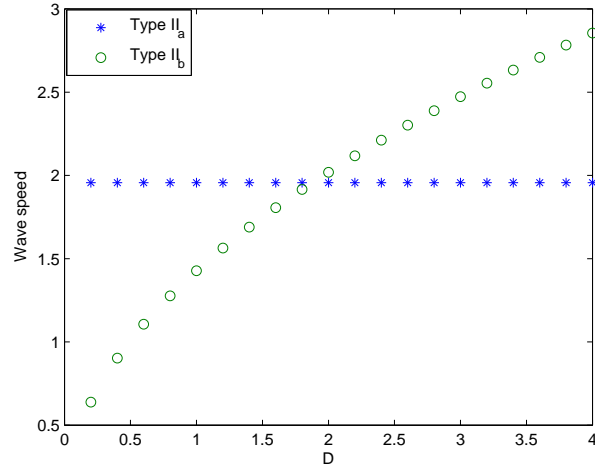


Figure 3.10: The speed of the travelling wave of type (II) that generated from initial condition C and (1.5.3), plotted as a function of D , with $\lambda = 0.05$, $\alpha_{1,2} = 0.6404$, $\gamma_1 = 0.6404$ and $\gamma_2 = 0.6404$. (R_1 in figure 2.3)

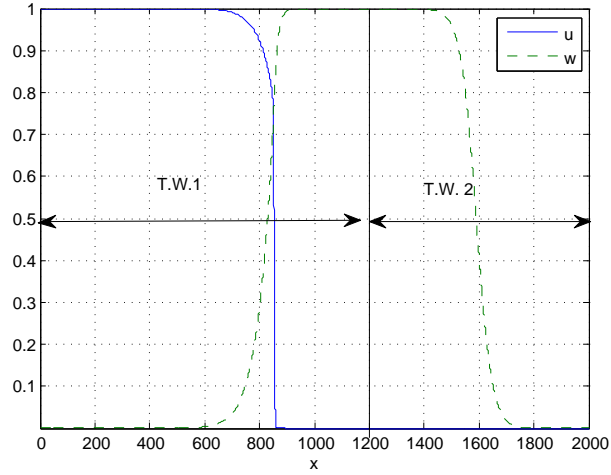


Figure 3.11: From initial condition C and (1.5.3), two travelling waves are generated when $\lambda = 0.05$, $\alpha_1 = 1$, $\alpha_2 = 1$, $\gamma_1 = 1.5$, $\gamma_2 = 0.5$ and $D = 1.2$. (R_6 in figure 2.3)

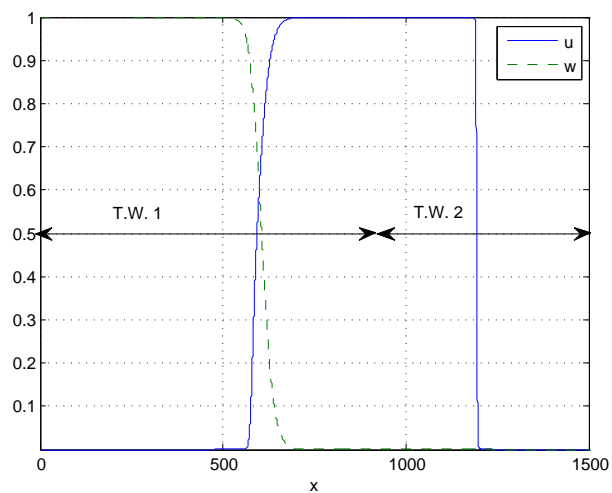


Figure 3.12: From initial condition C and (1.5.3), two travelling waves are generated when $\lambda = 0.05$, $\alpha_1 = 1$, $\alpha_2 = 1$, $\gamma_1 = 1.5$, $\gamma_2 = 0.5$ and $D = 0.5$. ((R_6) in figure 2.3)

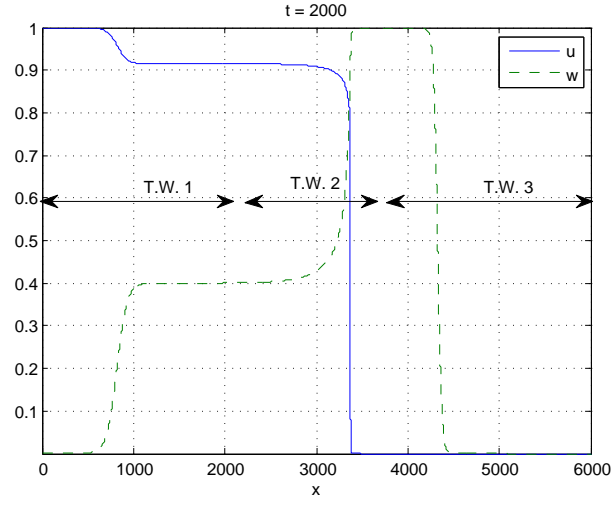


Figure 3.13: Three travelling waves are generated from initial condition C when $\lambda = 0.05$, $\alpha_1 = 1.2817$, $\alpha_2 = 6.1501$, $\gamma_1 = 0.3548$, $\gamma_2 = 2.4567$ and $D = 2$. ((R_2) in figure 2.3).

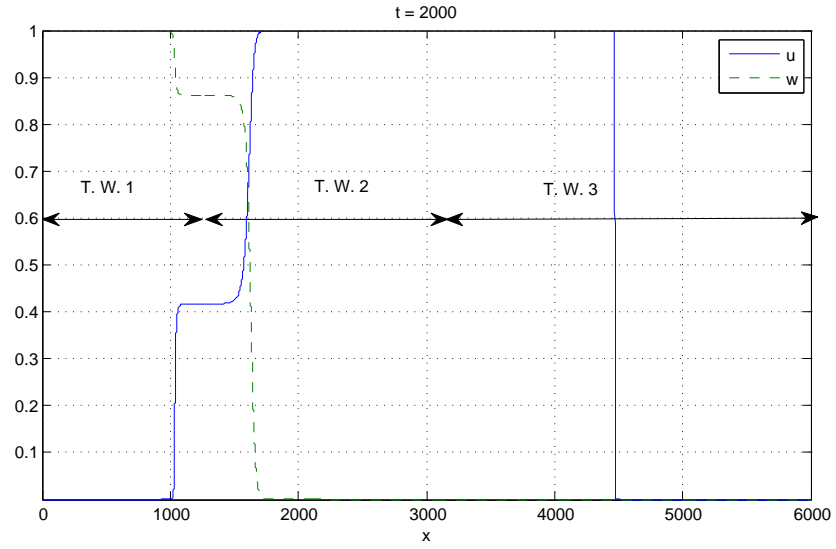


Figure 3.14: From initial condition C and (1.5.3), three travelling waves are generated when $\lambda = 0.05$, $\alpha_1 = 1$, $\alpha_2 = 1$, $\gamma_1 = 1.24$, $\gamma_2 = 0.9$ and $D = 0.4$. ((R_4) in figure 2.3).

3.4 Symmetry properties of (1.5.3) when $\lambda = 1$

The Reaction-diffusion system in (1.5.3) reduces to a single equation when $D = 1$, $\lambda = 1$, $\alpha_1 = \alpha_2$, $\gamma_1 = \gamma_2$ and $u = w$, and can be written as,

$$\frac{\partial u}{\partial t} = \frac{\partial^2 u}{\partial x^2} + u(1 + (\alpha_1 - \gamma_1)u - (1 + \alpha_1)u^2). \quad (3.4.1)$$

This is similar to the equation studied in [HR75] as we showed in Chapter 1 and has travelling wave solution connecting the coexistence equilibrium solution $u = u_0$ to the equilibrium solution $u = 0$. Thus we can deduce from the symmetry that there exists a travelling wave solution in (1.5.3) when $\lambda = 1$ connecting the coexistence equilibrium solution $(u, w) = (u_0, w_0)$ to the $(u, w) = (0, 0)$. We were unable to find this type of travelling wave when $\lambda \ll 1$. Also, it can be seen numerically for (1.5.3) that this type of travelling wave solution exists as shown in figure 3.15.

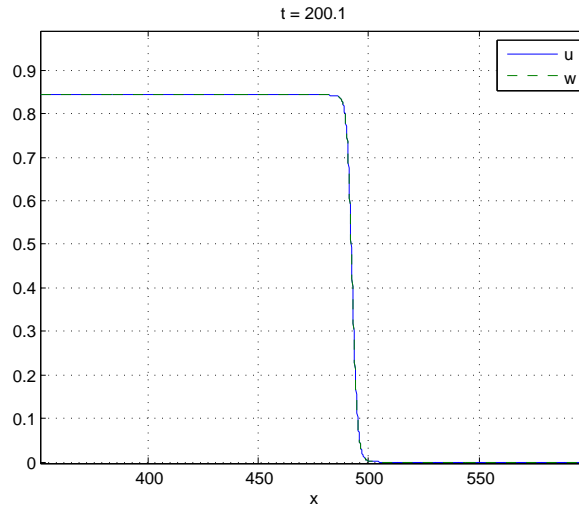


Figure 3.15: From initial condition C and (1.5.3), two travelling waves are generated

when $\lambda = 1$, $\alpha_1 = 1$, $\alpha_2 = 1$, $\gamma_1 = 0.5$, $\gamma_2 = 0.5$ and $D = 1$.

3.5 The impact of the cooperative and competitive coefficients on the wave speed

In this subsection, we show how the parameters $\alpha_{1,2}$ and $\gamma_{1,2}$ affect the speed of the travelling waves. We consider travelling waves of type (III), where the invader is species u . We have computed the wave speed for different values of α_1 in figure 3.16, and we found that as α_1 increases the wave speed increases. This ecologically means when α_1 increases the cooperation in species u increases and therefore the invader spreads out faster. The opposite happens when α_2 increases and it negatively affects the spread of the invader. We see in Figure 3.17 that the wave speed decreases as α_2 increases. The competition coefficient γ_1 measures the effect of w on the growth rate of u , whilst γ_2 measures the effect of u on the growth rate of w . As we increase γ_1 the wave speed decreases as shown in Figure 3.18. This is because when γ_1 increases the effect of species w on the invader species u increases. When γ_2 increases the effect will be negative on the growth rate of species w , whilst it increases the effect of the invasion of species u which increases the wave speed as shown in Figure 3.19.

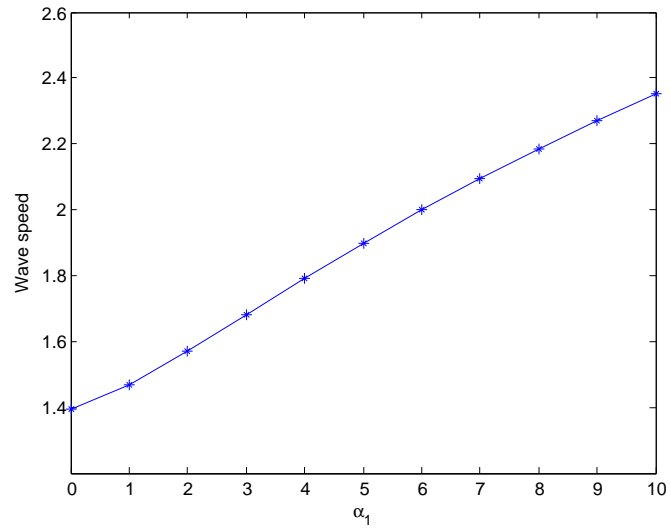


Figure 3.16: The affect of α_1 in the speed of the travelling wave of type (III_r) when $\alpha_2 = 1$, $\gamma_1 = 0.5$, $\gamma_2 = 1.5$, $D = 1$ and $\lambda = 0.05$.

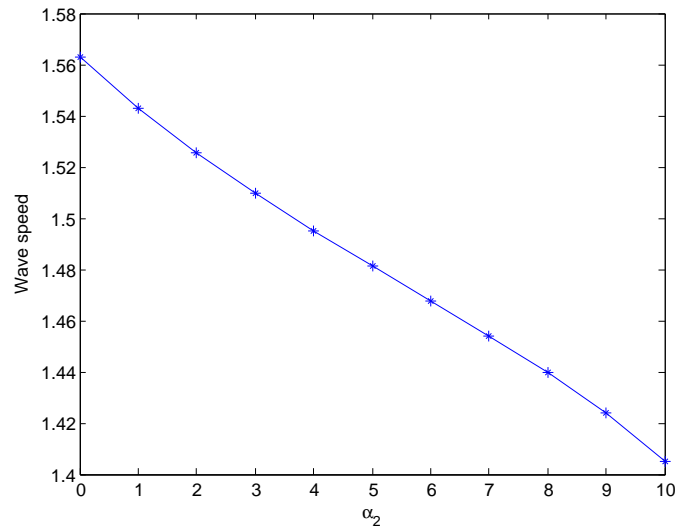


Figure 3.17: The effect of α_2 on the speed of the travelling wave of type (III_r) when $\alpha_1 = 1$, $\gamma_1 = 0.5$, $\gamma_2 = 1.5$, $D = 1$ and $\lambda = 0.05$.

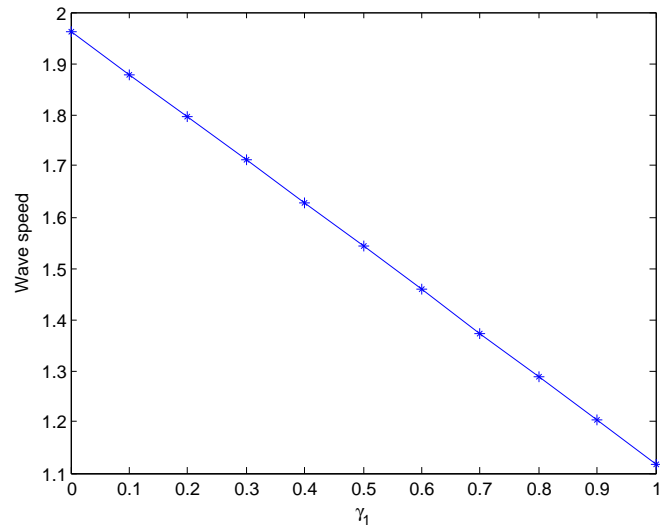


Figure 3.18: The effect of γ_1 on the speed of the travelling wave of type (III_r) when $\alpha_1 = 1, \alpha_2 = 1, \gamma_2 = 1.5, D = 1$ and $\lambda = 0.05$.

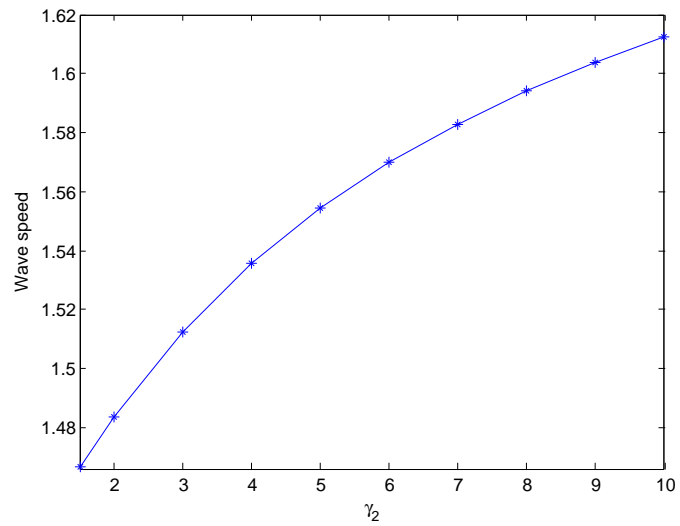


Figure 3.19: The effect of γ_2 on the speed of the travelling wave of type (III_r) when $\alpha_1 = 1, \alpha_2 = 1, \gamma_1 = 0.5, D = 1$ and $\lambda = 0.05$.

3.6 Founder control case

In Chapter 1 we showed that in the Lotka-Volterra system, when the single species equilibrium solutions $(1, 0)$ and $(0, 1)$ are stable, the initial condition may decide the winner. This case is called the founder control case. We study whether founder control occurs in (1.5.3). In R_6 , where both single species equilibrium solutions are stable, there is strong competition between both species and the winner depends on the initial conditions of type A and B . We found that with initial condition A , $(1, 0)$ wins and the travelling wave of type (III_r) develops, whilst $(0, 1)$ wins in the case of initial condition B and we get the travelling wave of type (III_l) . However, this is not always true, because the parameters $\gamma_{1,2}$ plays a significant role in growth or extinctions of the populations of species and then affect on the existence of the travelling wave solutions. In Figure 3.23, we show that the travelling wave of type (III_r) develops with initial conditions A when $\gamma_2 = 9$ and failed for $\gamma_2 = 1.5$ and 6 . A travelling wave of type (III_l) develop with initial conditions of type B in Figure 3.27 when $\gamma_1 = 3$, and failed when $\gamma_1 = 1.5$. We conclude that a founder control occurs in (1.5.3), and depends on both initial conditions and the parameters $\gamma_{1,2}$.

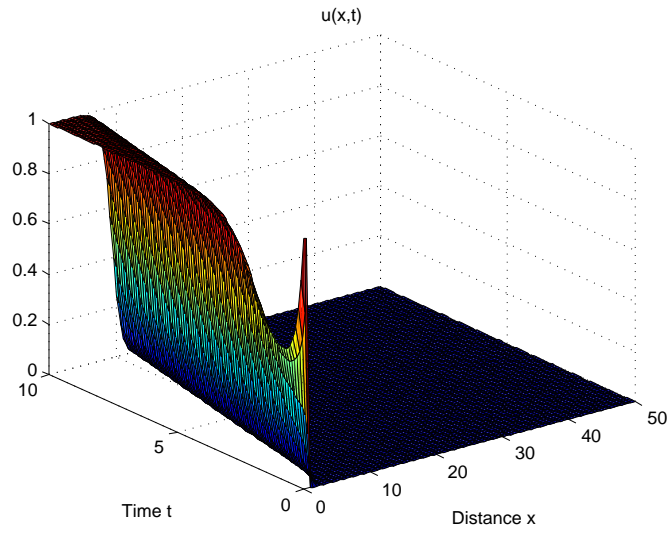


Figure 3.20: The founder control case, the development of the travelling wave of type (III_r) for u with initial condition A , when $\alpha_1 = 1$, $\alpha_2 = 1$, $\gamma_1 = 2$, $\gamma_2 = 9$, $D = 1$, $\lambda = 0.05$.

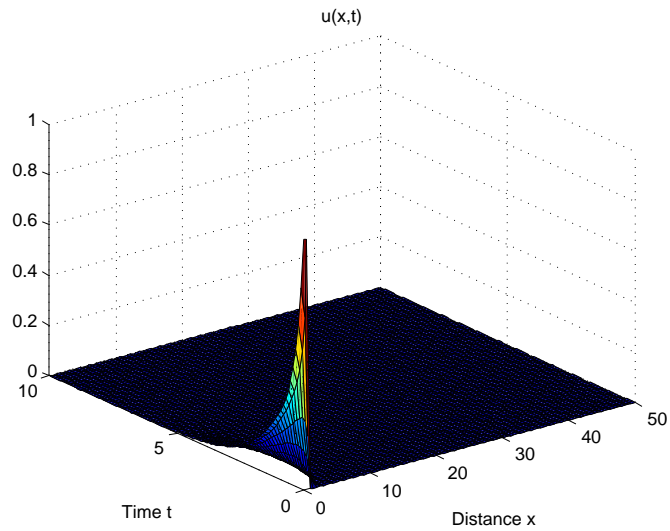


Figure 3.21: The founder control case, the development of the travelling wave of type (III_r) for u with initial condition A , when $\alpha_1 = 1$, $\alpha_2 = 1$, $\gamma_1 = 2$, $\gamma_2 = 1.5$, $D = 1$, $\lambda = 0.05$.

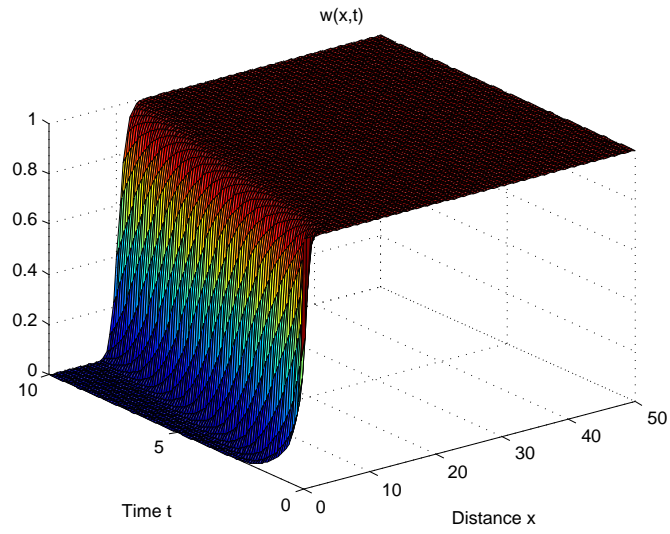


Figure 3.22: The founder control case, the development of the travelling wave of type (III_r) for w with initial condition A , when $\alpha_1 = 1$, $\alpha_2 = 1$, $\gamma_1 = 2$, $\gamma_2 = 9$, $D = 1$, $\lambda = 0.05$.

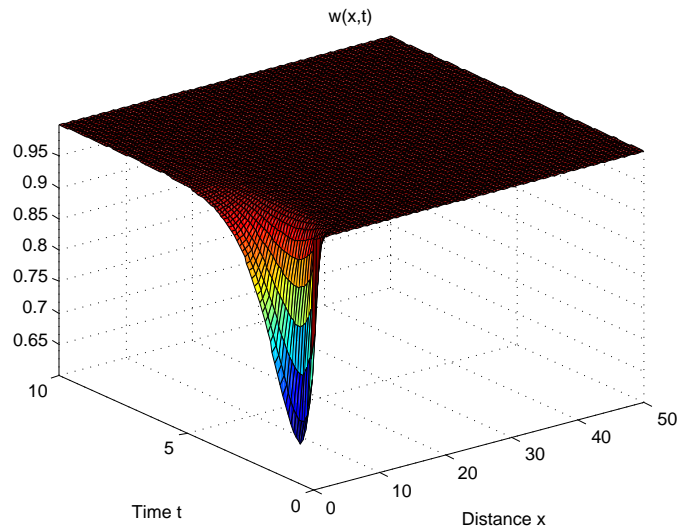


Figure 3.23: The founder control case, the development of the travelling wave of type (III_r) for w with initial condition A , when $\alpha_1 = 1$, $\alpha_2 = 1$, $\gamma_1 = 2$, $\gamma_2 = 1.5$, $D = 1$, $\lambda = 0.05$.

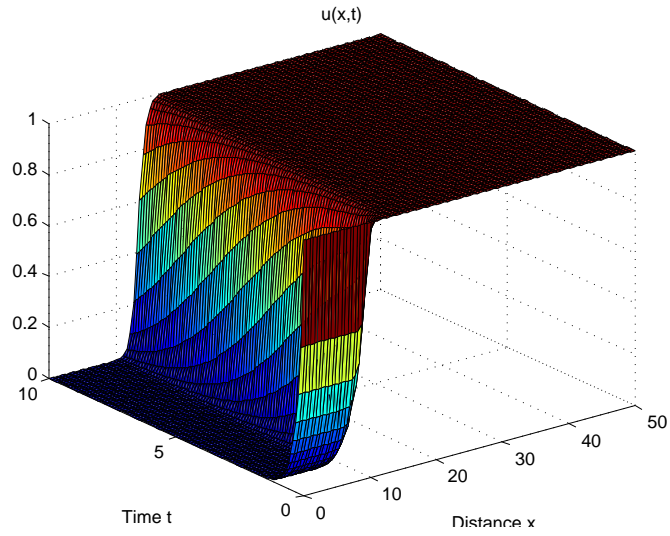


Figure 3.24: The founder control case, the development of the travelling wave of type (III_l) for u with initial condition B , when $\alpha_1 = 1$, $\alpha_2 = 1$, $\gamma_1 = 3$, $\gamma_2 = 4$, $D = 1$ and $\lambda = 0.05$.

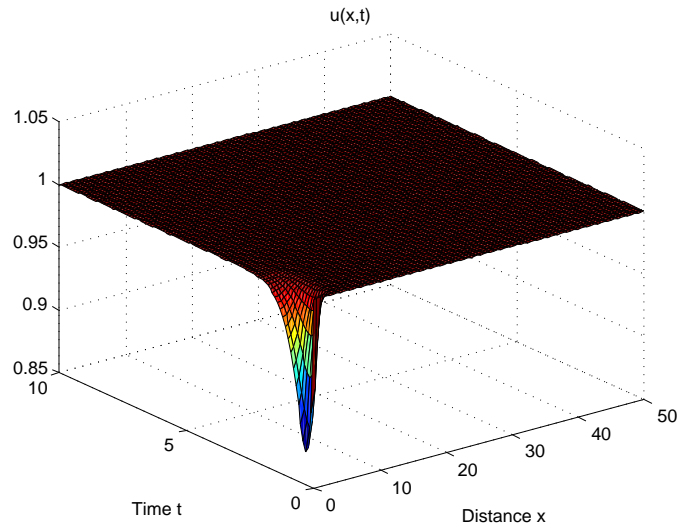


Figure 3.25: The founder control case, the development of the travelling wave of type (III_l) for u with initial condition B , when $\alpha_1 = 1$, $\alpha_2 = 1$, $\gamma_1 = 1.5$, $\gamma_2 = 4$, $D = 1$ and $\lambda = 0.05$.

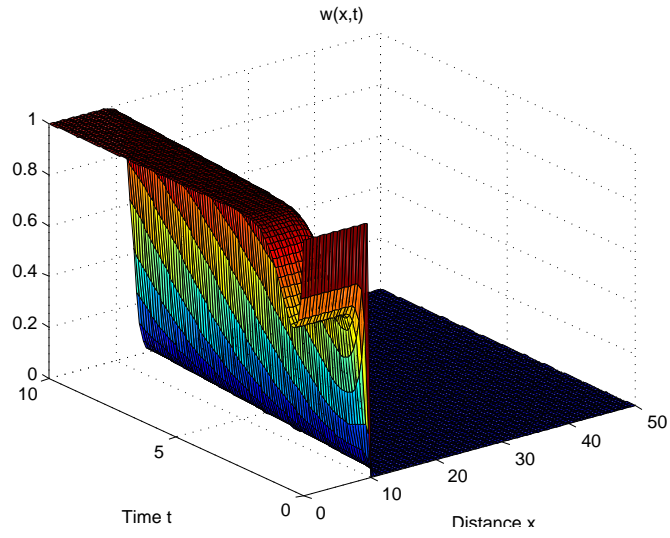


Figure 3.26: The founder control case, the development of the travelling wave of type (III_l) for w with initial condition B , when $\alpha_1 = 1$, $\alpha_2 = 1$, $\gamma_1 = 3$, $\gamma_2 = 4$, $D = 1$ and $\lambda = 0.05$.

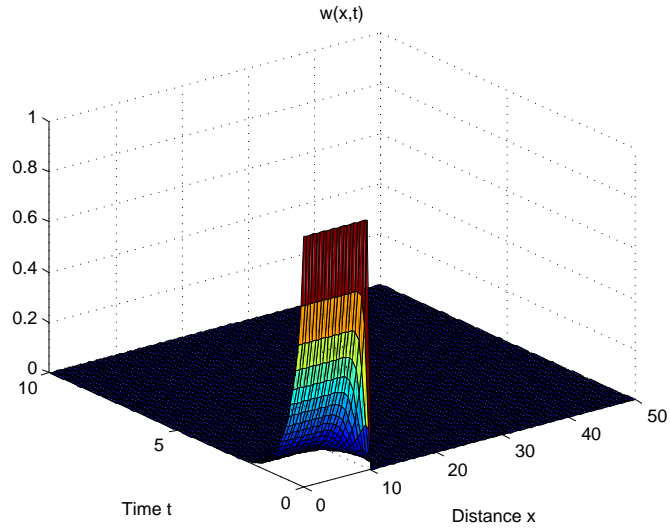


Figure 3.27: The founder control case, the development of the travelling wave of type (III_l) for w with initial condition B , when $\alpha_1 = 1$, $\alpha_2 = 1$, $\gamma_1 = 1.5$, $\gamma_2 = 4$, $D = 1$ and $\lambda = 0.05$.

3.7 The effect of the diffusion coefficient D on the travelling wave solutions

In this section we show the effect of the diffusion coefficient on the travelling wave solutions with initial conditions of type C. In this case we get two travelling wavefront solutions for specific values of parameters. The ecological explanation for this case is there is an invading species introduced and represented by two wavefronts in both species, u and w . In Figure 3.28, there are two wavefronts and the faster is the wavefront of species u , when $D = 1$. Now if we make $D = 2$, then the wavefront of u can be caught by the front of the invader w and species u starts to decrease and dies out (the new travelling wave is of type II). This case is shown in Figures 3.29 and 3.30, where the parameters are the same but we only changed D . This increases the speed of the front of species w . In Figures 3.31 and 3.32, the invader species w moves faster than the front of species u , and then disappears when D decreases (the new travelling wave is of type II). Thus, the wavefront in w spreads faster than the front of species u when D increases and vice versa, for some values of parameters and initial conditions of type C. It can be seen that the diffusion coefficient affects the existence of the type of travelling wave solutions with initial condition C.

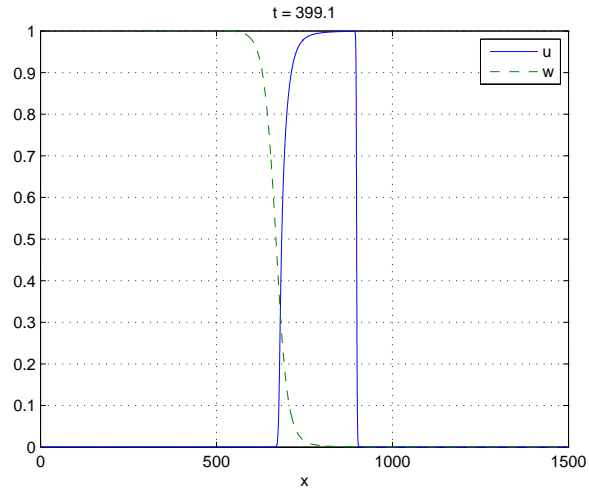


Figure 3.28: The effect of D in the development of travelling waves with initial condition

C , when $\alpha_1 = 2$, $\alpha_2 = 1$, $\gamma_1 = 5$, $\gamma_2 = 0.5$, $D = 1$ and $\lambda = 0.05$.

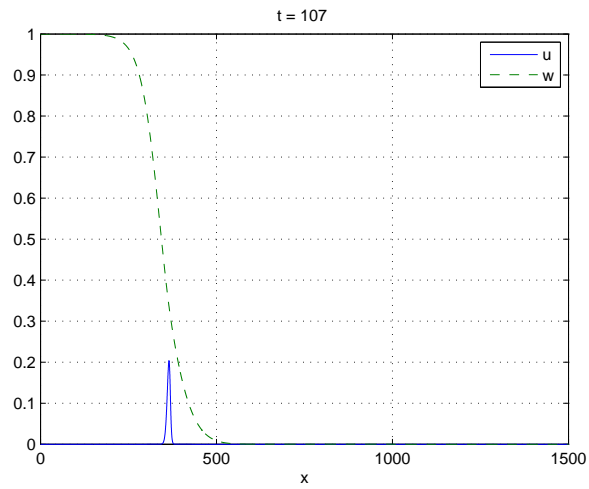


Figure 3.29: The effect of D in the development of travelling waves with initial condition

C , when $\alpha_1 = 2$, $\alpha_2 = 1$, $\gamma_1 = 5$, $\gamma_2 = 0.5$, $D = 2$ and $\lambda = 0.05$.

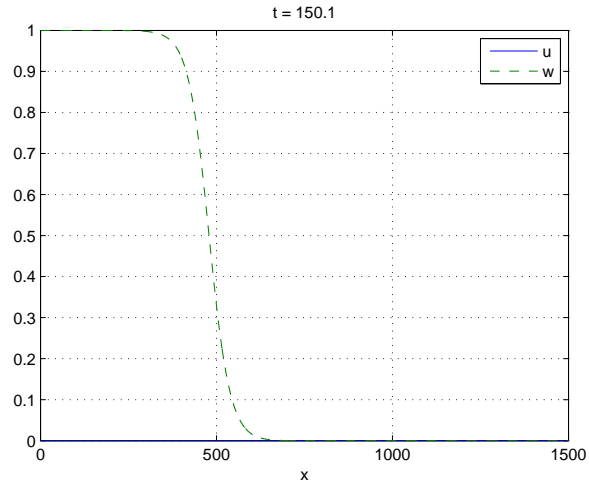


Figure 3.30: The effect of D in the development of travelling waves with initial condition

C , when $\alpha_1 = 2, \alpha_2 = 1, \gamma_1 = 5, \gamma_2 = 0.5, D = 2$ and $\lambda = 0.05$.

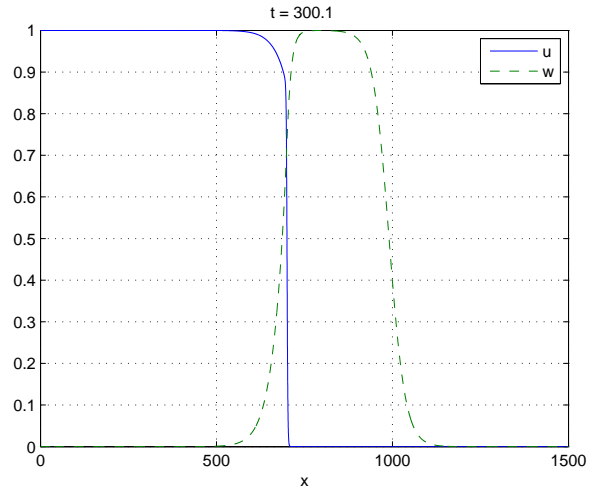


Figure 3.31: The effect of D in the development of travelling waves with initial condition

C , when $\alpha_1 = 1, \alpha_2 = 2, \gamma_1 = 0.5, \gamma_2 = 3, D = 2$ and $\lambda = 0.05$.

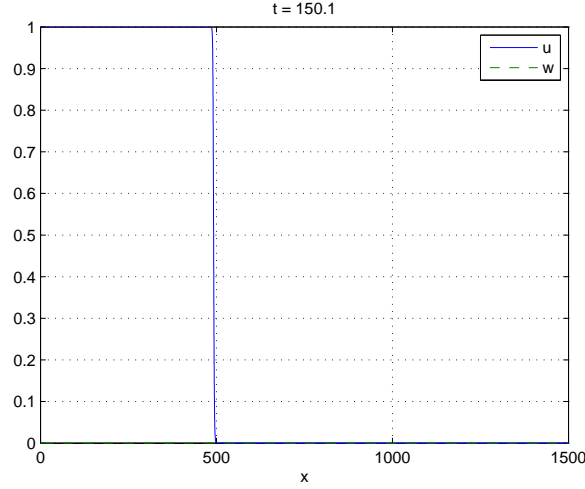


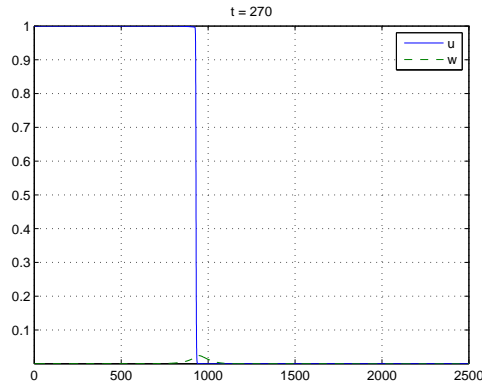
Figure 3.32: The effect of D in the development of travelling waves with initial condition

C , when $\alpha_1 = 1$, $\alpha_2 = 2$, $\gamma_1 = 0.5$, $\gamma_2 = 3$, $D = 0.5$, $\lambda = 0.05$.

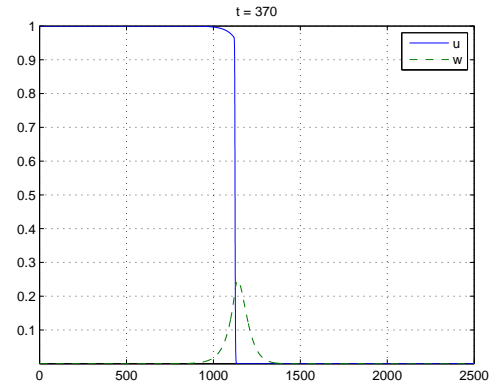
3.8 Dynamics of the growth and development of travelling wave solutions with initial condition C

In this section, we study the dynamics of the initial growth and development of travelling wave solutions for (1.5.3) with initial condition C . Figure 3.33 and 3.34 show the dynamics of the growth of a travelling wave solution for typical parameter values. In Figure 3.33, initially, w is small and u propagates into the domain as a travelling wave. However, after a long induction period, w begins to grow at the wavefront. Then w expands and finally forms a new wavefront that allows w to propagate into $x > 0$, followed by a slower wavefront. Figure 3.34 shows the same process but u grows as a spike and develops after long induction as a wave front, whilst w propagates into the domain as a travelling wave slower than the wave front u .

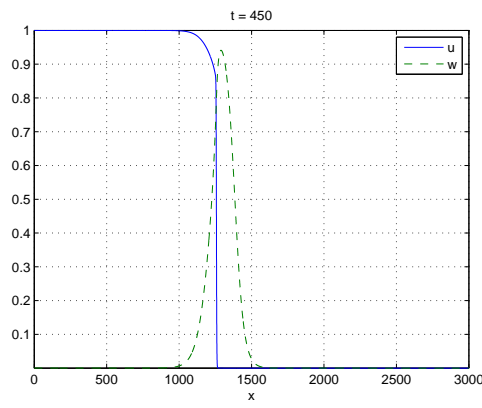
CHAPTER 3: TRAVELLING WAVE SOLUTIONS FOR THE INITIAL VALUE PROBLEM (1.5.3)



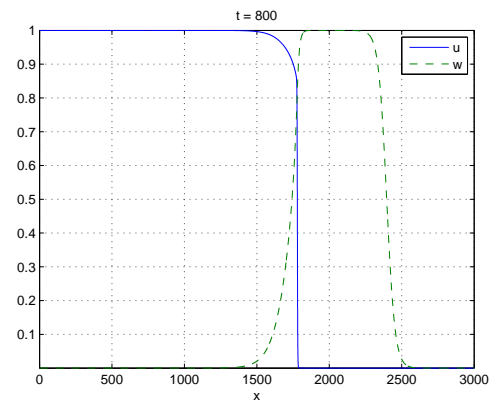
(a)



(b)



(c)



(d)

Figure 3.33: Detail of the development of a travelling wave in w from one in u , when

$$\lambda = 0.05, \alpha_{1,2} = 1, D = 2, \gamma_1 = 0.5 \text{ and } \gamma_2 = 1.64.$$

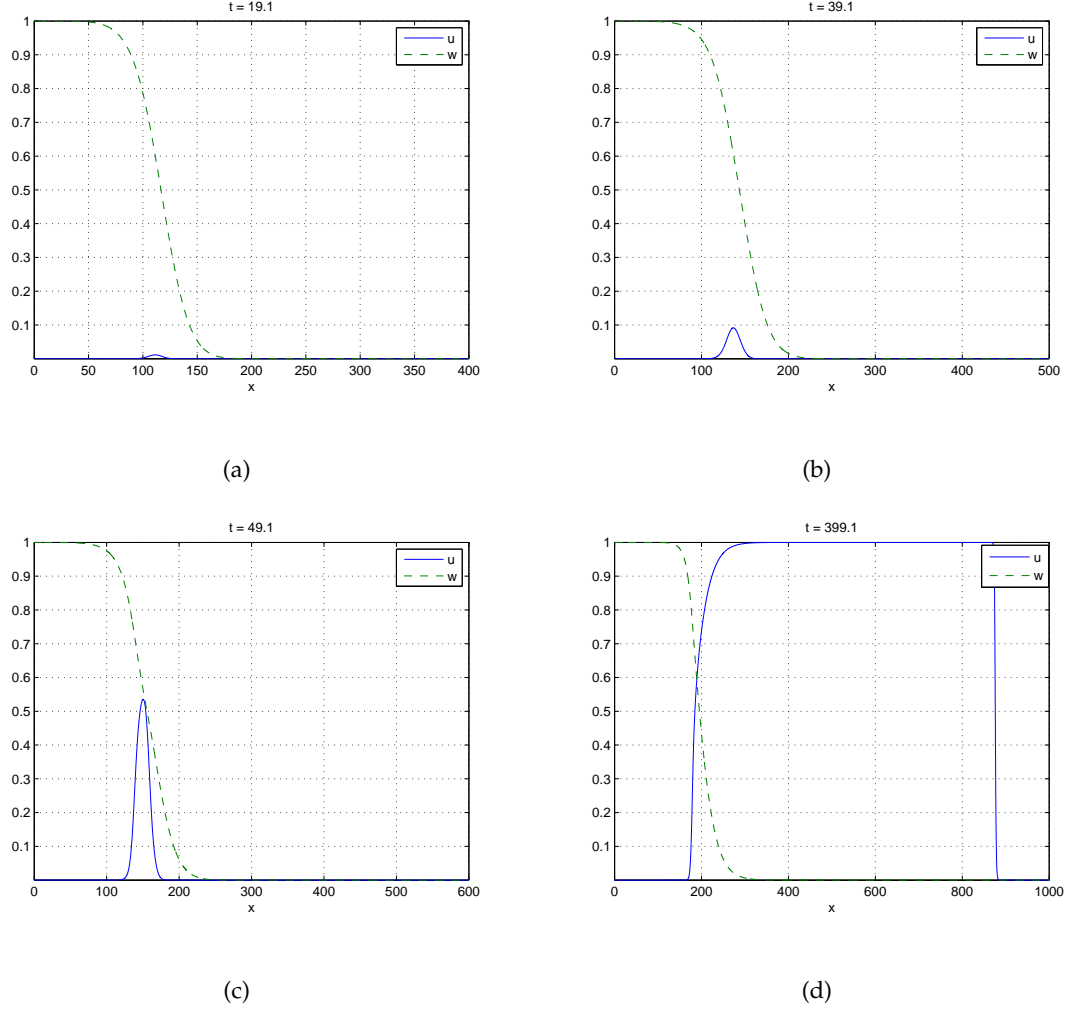


Figure 3.34: Details of the development of a travelling wave in u from one in w , when

$$\lambda = 0.05, \alpha_{1,2} = 1, \gamma_1 = 1.5, \gamma_2 = 1.6 \text{ and } D = 0.5.$$

3.8.1 Asymptotic solutions

In order to gain some insight into this process in the case of Figure 3.33, we consider a system problem in which we treat the initial travelling wave in u as simply a Heaviside function $H(-x)$, and consider the dynamics of this system when w is initially small and also a Heaviside function $H(-x)$. We use an asymptotic method to find the solution for w in the limit of $0 < \lambda \ll 1$. Specifically, we rescale using

$$w = \lambda \bar{w} \quad x = \frac{\bar{x}}{\lambda}, \quad t = \frac{\bar{t}}{\lambda}, \quad u = H(ct - x)$$

where

$$H(-x) = \begin{cases} 0, & \text{if } x \geq L_0 \\ 1, & \text{if } x < L_0, \end{cases}$$

c is the initial travelling wave speed, and where L_0 is a constant. At leading order as $\lambda \rightarrow 0$,

$$\frac{\partial \bar{w}}{\partial \bar{t}} = D \frac{\partial^2 \bar{w}}{\partial \bar{x}^2} + \bar{w}(1 - \gamma_2 H(ct - x)), \quad (3.8.1)$$

subject to

$$\bar{w}(x, 0) = w_0 H(-x). \quad (3.8.2)$$

For convenience we omit the over bar from (3.8.1) and then we solve it analytically. We assume that the position of the wavefront of species u is $L_0 + ct$, where L_0 is the position of a head of the wavefront in u at time t . Thus when $x > L_0 + ct$, (3.8.1) becomes

$$\frac{\partial w}{\partial t} = D \frac{\partial^2 w}{\partial x^2} + w. \quad (3.8.3)$$

While if $x < L_0 + ct$,

$$\frac{\partial w}{\partial t} = D \frac{\partial^2 w}{\partial x^2} - Kw, \quad (3.8.4)$$

where $K = \gamma_2 - 1 > 0$ and $\gamma_2 > 1$.

We solve (3.8.3) and (3.8.4) analytically using the Laplace transform method. We begin by defining $Z = x - L_0 - ct$, so that (3.8.3) becomes

$$\frac{\partial w(Z, t)}{\partial t} - c \frac{\partial w(Z, t)}{\partial Z} = D \frac{\partial^2 w(Z, t)}{\partial Z^2} + w(Z, t), \quad Z > 0, \quad (3.8.5)$$

with initial conditions $w(Z, 0) = 0$.

Similarly (3.8.4) becomes

$$\frac{\partial w(Z, t)}{\partial t} - c \frac{\partial w(Z, t)}{\partial Z} = D \frac{\partial^2 w(Z, t)}{\partial Z^2} - Kw(Z, t), Z < 0, \quad (3.8.6)$$

with initial conditions $w(Z, 0) = 1$, and

$$w(0, t) \quad \text{and} \quad \frac{\partial w(0, t)}{\partial Z} \quad \text{are continuous at} \quad Z = 0. \quad (3.8.7)$$

3.8.2 Laplace transform method

In order to solve (3.8.5) and (3.8.6), we use the Laplace transform for $w(Z, s)$,

$$L\{w(Z, t)\} = w(Z, s) = \int_0^\infty e^{-st} w(Z, t) dt.$$

Thus we get

$$D \frac{d^2 w(Z, s)}{dZ^2} + c \frac{dw(Z, s)}{dZ} + (1 - s)w(Z, s) = 0. \quad (3.8.8)$$

This is a homogeneous differential equation and the general solution is

$$w(Z, s) = A_1(s) e^{Z(\frac{-c + \sqrt{c^2 - 4D(1-s)}}{2D})} + A_2(s) e^{Z(\frac{-c - \sqrt{c^2 - 4D(1-s)}}{2D})},$$

where $s = 1 - \frac{c^2}{4D}$ is a branch point in the complex s - plane. Moreover, $A_1(s)$ and $A_2(s)$ are functions of s , and we need the condition $w(Z, 0) = 0$, as $Z \rightarrow \infty$, so that $A_1(s) = 0$.

Thus we get

$$w(Z, s) = A_2(s) e^{Z(\frac{-c - \sqrt{c^2 - 4D(1-s)}}{2D})}. \quad (3.8.9)$$

To solve (3.8.6) for $Z < 0$, again using the Laplace transform method we get

$$D \frac{d^2 w(Z, s)}{dZ^2} + c \frac{dw(Z, s)}{dZ} - (K + s)w(Z, s) = -1. \quad (3.8.10)$$

The general solution is

$$w(Z, s) = B_1(s)e^{z\left(\frac{-c+\sqrt{c^2+4D(K+s)}}{2D}\right)} + B_2(s)e^{z\left(\frac{-c-\sqrt{c^2+4D(K+s)}}{2D}\right)} + \frac{1}{s+K}. \quad (3.8.11)$$

The branch point $s = \frac{c^2}{4D} - k$ lies in the complex-s plane. This holds for $Z < 0$, so that

$$B_2(s)e^{z\left(\frac{-c-\sqrt{c^2+4D(K+s)}}{2D}\right)} \rightarrow 0 \quad \text{as } Z \rightarrow -\infty.$$

Thus $B_2 = 0$ and

$$w(Z, s) = B_1(s)e^{z\left(\frac{-c+\sqrt{c^2+4D(K+s)}}{2D}\right)} + \frac{1}{s+K}. \quad (3.8.12)$$

The branch points are shown on the negative real axis or the branch cut in Figure 3.35.

Now we have (3.8.11) and (3.8.12) with two unknown functions which we can determine using (3.8.7) to be

$$A_1(s) = \frac{(c + \sqrt{c^2 - 4D(1-s)})}{(-\sqrt{c^2 - 4D(1-s)} - \sqrt{c^2 + 4D(K+s)})(K+s)}$$

$$B_1(s) = \frac{(c + \sqrt{c^2 - 4D(1-s)})}{(-\sqrt{c^2 - 4D(1-s)} - \sqrt{c^2 + 4D(K+s)})(K+s)} + \frac{1}{s+K}.$$

After simplification, we get

$$\begin{aligned} w(Z, s) = & \frac{(c + \sqrt{c^2 - 4D(1-s)})(\sqrt{c^2 - 4D(1-s)} - \sqrt{c^2 + 4D(K+s)})}{4D(1+K)(s+K)} e^{z\left(\frac{-c-\sqrt{c^2-4D(1-s)}}{2D}\right)} \\ & + \frac{1}{s+K} e^{z\left(\frac{-c-\sqrt{c^2-4D(1-s)}}{2D}\right)}, \end{aligned}$$

which holds for $Z > 0$ and

$$\begin{aligned} w(Z, s) = & \left(\frac{(c + \sqrt{c^2 - 4D(1-s)})(\sqrt{c^2 - 4D(1-s)} - \sqrt{c^2 + 4D(K+s)})}{4D(1+K)(s+K)} \right) e^{z\left(\frac{-c+\sqrt{c^2+4D(K+s)}}{2D}\right)} \\ & + \frac{1}{s+K}, \end{aligned}$$

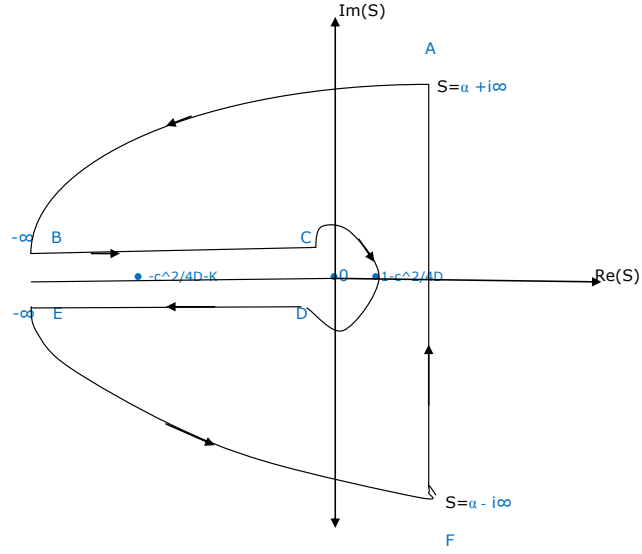


Figure 3.35: Branch points at the negative real axis in the complex s -plane.

for $Z < 0$. We use the inverse Laplace transform, to obtain

$$w(Z, t) = L^{-1}\{w(Z, s)\} = \frac{1}{2\pi i} \int_{\alpha - i\infty}^{\alpha + i\infty} e^{st} w(Z, s) ds.$$

This is the Bromwich inversion integral and the contour of integration is a vertical line in the complex s -plane, from $\alpha - i\infty$ to $\alpha + i\infty$ as shown in Figure 3.35, where α should be larger than the real part of all the branch points. It is also possible to simplify the problem by closing the contour of integration using a large semicircle in the left half plane enclosing the branch points. We can then determine an integral expression for the solution (note that there is no pole at $s = -K$). The inversion integral of $w(Z, s)$ is

$$w(Z, t) = \int_{C_R} e^{st} w(Z, s) ds.$$

Thus

$$\begin{aligned} w(Z, t) &= \frac{1}{2\pi i} \int_{\gamma-i\infty}^{\gamma+i\infty} e^{st} w(Z, s) ds \\ &= -\frac{1}{2\pi i} \left(\int_{BC} + \int_{CD} + \int_{DE} \right) e^{st} w(Z, s) ds. \end{aligned} \quad (3.8.13)$$

The integral around CD can be calculated by parametrising with $s = \epsilon e^{i\Theta}$ that goes from π to $-\pi$. The integration around CD as $\epsilon \rightarrow 0$ is equal to zero, therefore we need to know the integral around BC and DE. To simplify our problem we will solve the integral in the form

$$\begin{aligned} \int_{BC} + \int_{DE} &= \frac{1}{2\pi i} \left(\int_{-\infty}^{\frac{-c^2}{4D}-K} + \int_{\frac{-c^2}{4D}-K}^{-\infty} \right) + \left(\int_{1-\frac{c^2}{4D}}^{\frac{-c^2}{4D}-K} + \int_{\frac{-c^2}{4D}-K}^{1-\frac{c^2}{4D}} \right). \\ \int_{BC} &= \frac{1}{2\pi i} \int_{-\infty}^{\frac{-c^2}{4D}-K} e^{st} w_{p1}(Z, s) e^{Z(\frac{-c}{2D} - i\frac{\sqrt{4D(1-s)-c^2}}{2D})} ds \\ &\quad + \frac{1}{2\pi i} \int_{\frac{-c^2}{4D}-K}^{-\infty} e^{st} w_{p2}(Z, s) e^{Z(\frac{-c}{2D} + i\frac{\sqrt{4D(1-s)-c^2}}{2D})} ds, \end{aligned}$$

where

$$w_{p1}(Z, s) = \frac{(c + i\sqrt{4D(1-s)-c^2})(i\sqrt{4D(1-s)-c^2} - i\sqrt{4D(-k-s)-c^2})}{4D(1+K)(s+K)},$$

$$w_{p2}(Z, s) = \frac{(c - i\sqrt{4D(1-s)-c^2})(-i\sqrt{4D(1-s)-c^2} + i\sqrt{4D(-k-s)-c^2})}{4D(1+K)(s+K)}.$$

After some calculations and simplification we get

$$\int_{BC} = \frac{e^{\frac{-cZ}{2D}}}{8\pi D(1+K)(s+K)} \int_{-\infty}^{\frac{-c^2}{4D}-K} e^{st} w_{p3}(Z, s) ds,$$

where

$$\begin{aligned}
 w_{p3}(Z, s) = & c(\sqrt{4D(1-s-c^2)} - \sqrt{4D(-K-s)-c^2}) \cos\left(\frac{Z\sqrt{4D(1-s)-c^2}}{2D}\right) + \\
 & (4D(1-s)-c^2 - \sqrt{4D(1-s)-c^2}\sqrt{4D(-k-s)-c^2}) \sin\left(\frac{Z\sqrt{4D(1-s)-c^2}}{2D}\right) - \\
 & 4D(1+K) \sin\left(\frac{Z\sqrt{4D(1-s)-c^2}}{2D}\right).
 \end{aligned}$$

In the same way we can find the integral along DE in the form where

$$\begin{aligned}
 w_{p4}(Z, s) = & (c\sqrt{c^2 + 4D(K+s)} + 4D(1-s) - c^2) \cos\left(\frac{Z\sqrt{4D(1-s)-c^2}}{2D}\right) \\
 & + (c\sqrt{4D(1-s)-c^2} - \sqrt{4D(1-s)-c^2}\sqrt{c^2 + 4D(K+s)}) \\
 \sin\left(\frac{Z\sqrt{4D(1-s)-c^2}}{2D}\right) & + 4D(1+K) \sin\left(\frac{Z\sqrt{4D(1-s)-c^2}}{2D}\right).
 \end{aligned}$$

Although this is a complicated expression, the presence of a term e^{st} in the integrand means that the solution will decay exponentially if the ranges of integration do not extend into $s > 0$, which will occur if $1 - c^2/4D < 0$, and hence $c > 2\sqrt{D}$. Since $2\sqrt{D}$ is the linearized wave speed of the wavefront in w , this suggests that if the wavefront in u moves faster than that in w , w will decay to zero, otherwise, w will grow and (once nonlinear terms become important) form a wavefront.

We can evaluate the solution of (3.8.13) numerically using MATLAB. In Figure 3.36 we show the spike of w which we get from numerical integration. The solid line represents w when $Z > 0$, while dashed lines represent w when $Z < 0$. Figure 3.36 shows the solution once w starts to grow, evaluated numerically, and clearly shows that the growth is localised at the wavefront. Figure 3.37 shows a comparison between the numerical solution of the full initial value problem and the asymptotic solution, which is in reasonable agreement considering that the wavefront is not precisely a Heaviside function.

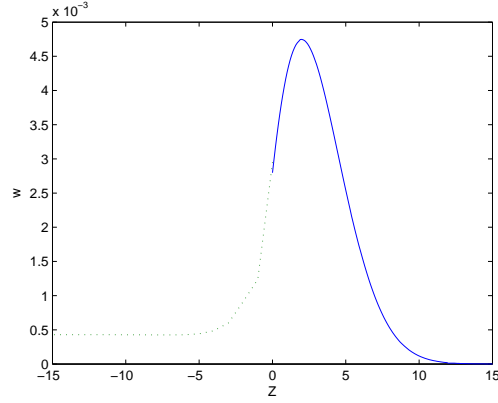


Figure 3.36: The solution (3.8.13) with $c = 0.5$, $K = 5.98$, $t = 0.8$ and $D = 7$. The dashed line represents the solution for $Z < 0$, and the solution for $Z > 0$ denoted by the solid line.

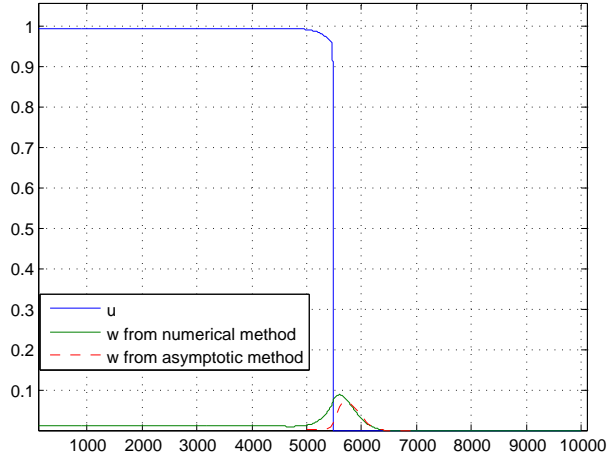


Figure 3.37: Comparison between the numerical solutions of the initial value problem and (3.8.13) when $\lambda = 0.02$, $\alpha_{1,2} = 0.1, 0.2$, $D = 8$, $c = 1$, $t = 0.8$ and $K = 8$.

Travelling wave solutions for $\lambda \ll 1$ and $\lambda = O(1)$

In this chapter, we will study the asymptotic solutions for the three types of travelling waves in the limit of small λ . We will show that there are two types of problem to solve asymptotically; a regular perturbation problem and a singular perturbation problem. In the singular perturbation problem, there is one inner and two outer regions.

4.1 Asymptotic solutions for $\lambda \ll 1$

We have seen that a variety of travelling waves develops as solutions of the initial value problem, so we will study their structure, focusing on the analytically tractable case, $\lambda \ll 1$. We define $z = x - ct$, and seek permanent form travelling wave solutions $u = \hat{u}(z)$ and $w = \hat{w}(z)$ with wave speed $c > 0$, so that (1.5.3) becomes

$$\begin{aligned} \frac{d^2 \hat{u}}{dz^2} + c \frac{d\hat{u}}{dz} + \hat{u}(1 + \alpha_1 \hat{u} - (1 + \alpha_1) \hat{u}^2 - \gamma_1 \hat{w}) &= 0, \\ \frac{D}{\lambda} \frac{d^2 \hat{w}}{dz^2} + c \frac{d\hat{w}}{dz} + \lambda \hat{w}(1 + \alpha_2 \hat{w} - (1 + \alpha_2) \hat{w}^2 - \gamma_2 \hat{u}) &= 0. \end{aligned} \tag{4.1.1}$$

The appropriate boundary conditions depend upon which equilibrium solution are connected by the travelling wave solution, and we shall return to this question later.

This is a fourth order system of ordinary differential equations, which is difficult to study analytically. A limit where we can make some progress is $\lambda \ll 1$. The system is similar to that studied in [Bil04], where it was shown that the asymptotic structure of the solution consists of an inner region with lengthscale of $O(1)$ at the wavefront, which we can place without loss of generality in the neighbourhood of $z = 0$, with outer solutions ahead of and behind the wavefront with lengthscale of $O(\lambda^{-1})$. The inner region is only needed when one of the equilibrium solutions associated with the travelling wave has $u = 0$, so, in contrast to the system studied in [Bil04], some travelling wave solutions can be described without the need to resort to the method of matched asymptotic expansions. We therefore begin by defining scaled outer variables as $Z = \lambda z$, $\hat{u} = U(Z)$, $\hat{w} = W(Z)$ with U, W, Z of $O(1)$ as $\lambda \rightarrow 0$. In terms of these new variables, (4.1.1) become

$$\begin{aligned} \lambda^2 \frac{d^2 U}{dZ^2} + \lambda c \frac{dU}{dZ} + U(1 + \alpha_1 U - (1 + \alpha_1)U^2 - \gamma_1 W) &= 0, \\ D \frac{d^2 W}{dZ^2} + c \frac{dW}{dZ} + W(1 + \alpha_2 W - (1 + \alpha_2)W^2 - \gamma_2 U) &= 0. \end{aligned} \quad (4.1.2)$$

Although we can take any wavespeed above the minimum wavespeed when we compare between the wavespeed of numerical and asymptotic solutions, we have chosen the minimum wavespeed in what follows and we found a good agreement between the wavespeed for both solutions.

4.2 Regular perturbation solutions

At leading order, provided that $U \not\rightarrow 0$ as $Z \rightarrow \pm\infty$, this is a regular perturbation problem, with the leading order equations

$$D \frac{d^2 W}{dZ^2} + c \frac{dW}{dZ} + W(1 + \alpha_2 W - (1 + \alpha_2)W^2 - \gamma_2 U) = 0, \quad (4.2.1)$$

$$W = \frac{1 + \alpha_1 U - (1 + \alpha_1)U^2}{\gamma_1}, \quad (4.2.2)$$

or equivalently

$$\begin{aligned} \frac{dW}{dZ} &= V, \\ \frac{dV}{dZ} &= -\frac{1}{D}cV - \frac{W}{D}(g(W) - \gamma_2 U), \end{aligned} \quad (4.2.3)$$

$$\gamma_1 W = f(U). \quad (4.2.4)$$

In the (W, V) phase plane, this system has equilibrium points at $(0, 0)$, which corresponds to the equilibrium solutions $U = 1$, $W = 0$, and $(w_0, 0)$, where w_0 is such that (u_0, w_0) is a coexistence equilibrium state (an intersection of the curves $\gamma_1 w = f(u)$ and $\gamma_2 u = g(w)$, as discussed previously). Possible travelling wave solutions with this structure therefore connect these two equilibria.

4.2.1 Asymptotic solutions for type (I_b)

We will focus on travelling wave solutions that satisfy $(W, V) \rightarrow (w_0, 0)$ as $Z \rightarrow -\infty$ and $(W, V) \rightarrow (0, 0)$ as $Z \rightarrow \infty$, since these emerge as solutions from initial conditions A and B in regions R_1, R_2, R_4 and R_5 .

By linearizing about $(w_0, 0)$, we find that this is a saddle point if $\gamma_1/f' > g'/\gamma_2$, and a stable node if $\gamma_1/f' < g'/\gamma_2$. This is a condition on the relative slopes of the quadratics

shown in Figure 2.1, and in each case we find that the stable coexistence equilibrium point corresponds to a saddle point in (4.2.3). If a travelling wave solution exists it is therefore represented by the unstable separatrix of $(w_0, 0)$ that points into $V < 0$.

We solve (4.2.3) using ODE45 in Matlab by integrating forward near $(w_0, 0)$ and as $z \rightarrow -\infty$. We get a family of travelling wave solutions by solving (4.2.3), we will choose the travelling wave solution which has a minimum wave speed c satisfying $W > 0$. The asymptotic solution for travelling wave of type (I_b) as a result of integrating (4.2.3) is shown in Figure 4.1. In Figure 4.2, we compare the asymptotic and numerical solutions for the travelling waves of type (I_b) in a typical case and find that there is excellent agreement. Figure 4.3, shows the numerical and asymptotic solutions for type I_b with typical parameters and two stable equilibrium points, $(1, 0)$ and $(0.9182, 0.5716)$.

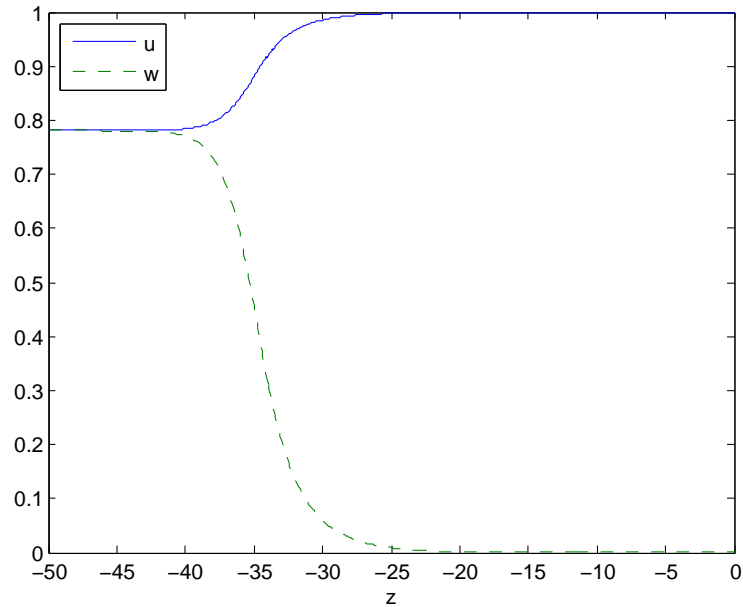


Figure 4.1: Travelling waves from asymptotic solutions of (4.2.3) for type (I_b) , $\alpha_{1,2} = 0.6404$, $\gamma_{1,2} = 0.6404$, $D = 1$, $c = 1.3$ and $\lambda = 0.05$.

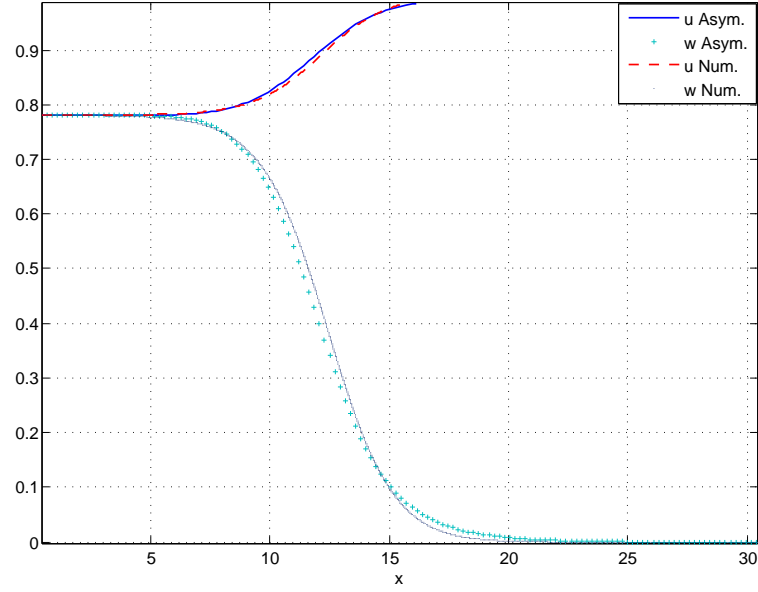


Figure 4.2: Comparison between the asymptotic solution of (4.2.3) and a numerical solution of the initial value problem with $\alpha_1 = 0.6404$, $\alpha_2 = 0.6404$, $\gamma_{1,2} = 0.6404$, $D = 1$, $\lambda = 0.05$ and $(u_0, w_0) = (0.78, 0.78)$.

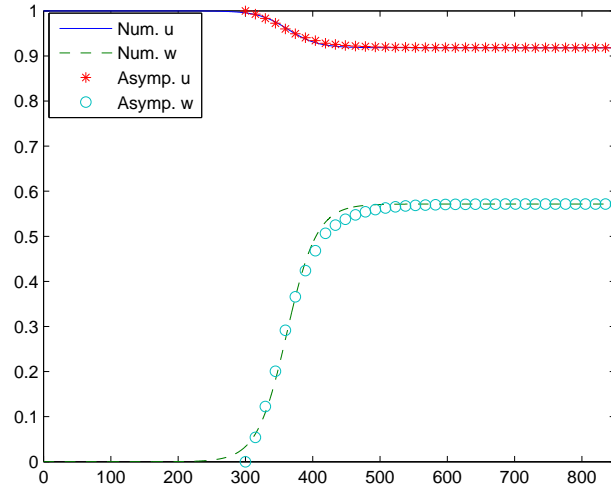


Figure 4.3: Asymptotic and numerical solutions for type I_b , the parameters are, $\alpha_{1,2} = 4$, $\gamma_1 = 0.8$, $\gamma_2 = 1.8$, $D = 1$ and $(u_0, w_0) = (0.9182, 0.5716)$.

When $\gamma_2 < 1$, $(W, V) = (0, 0)$ is a stable node provided that $c^2 > 4D(1 - \gamma_2)$, and a stable focus for $c^2 < 4D(1 - \gamma_2)$. Since we require $W > 0$, this provides a lower bound, $c \geq c_{lb} \equiv 2\sqrt{D(1 - \gamma_2)}$, on the wavespeed. In this case we would expect a spectrum of wave speeds to exist, bounded below by some $c_{min} \geq c_{lb}$. When $\gamma_2 > 1$ we find that $(0, 0)$ is a saddle point, and hence if a travelling wave solution exists, it will be a saddle-saddle connection between $(w_0, 0)$ and $(0, 0)$, which we would expect to exist for a single value of c .

4.2.2 $\gamma_2 < 1$, R_1 and R_4 : saddle-node connection

In this case, we can try to construct a trapping region for the unstable separatrix of $(w_0, 0)$, and use the Poincare-Bendixson theorem to show that it must enter the stable node at $(0, 0)$. If such a trapping region exists for all $c \geq c_{lb}$ we will have shown that

$$c_{min} = c_{lb} \equiv 2\sqrt{D(1 - \gamma_2)}. \quad (4.2.5)$$

Consider the triangular region OAB shown in Figure 4.4, which is bounded by OA , the W -axis, AB , the line $W = w_0$, and OB , the line $V = -KW$, where $K > 0$ is a constant that we shall choose below to maximize the range of values of c for which OAB is a trapping region. On OA , trajectories enter OAB if $\frac{dV}{dZ} < 0$, or equivalently, when $g(W) > \gamma_2 U$. We can see graphically in Figure 2.1 that this condition holds in regions R_1 and R_4 . On AB , $dW/dZ = V < 0$, so all trajectories enter OAB there.

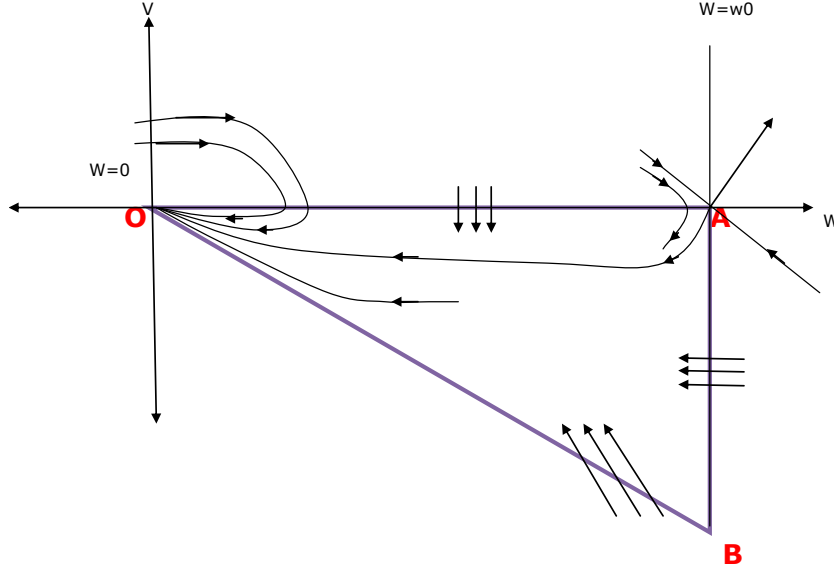


Figure 4.4: Trapping region for the equilibrium points $(W, V) = (w_0, 0)$ and $(W, V) = (0, 0)$.

On OB , a trajectory enters OAB if $\frac{dV}{dW} - \frac{V}{W} < 0$, or equivalently

$$F(K) = K^2 - \frac{c}{D}K + \frac{(g(W) - \gamma_2 U)}{D} < 0.$$

Since $F(0) > 0$, we can choose some K such that $F(K) < 0$ provided that $c^2 \geq 4D(g(W) - \gamma_2 U)$ at each point on AB . We can therefore guarantee that OAB is a trapping region provided that

$$c > c_{ub} \equiv 2\sqrt{D \max_{\gamma_1 W=f(U)} (g(W) - \gamma_2 U)}. \quad (4.2.6)$$

A simple graphical argument shows that a unique maximiser exists, and is easy to compute numerically as shown in Figure 4.5. Note that $c_{ub} \geq c_{min} \geq c_{lb}$. Figure 4.6 shows the numerically determined wave speed, the upper and lower bounds on the minimum wavespeed given by c_{ub} and c_{lb} , along with the minimum wavespeed (minimum wavespeed

satisfying $W > 0$) determined numerically from (4.2.3) and the speed of the wave generated in the initial value problem with initial conditions B. Note that the numerically calculated wavespeed is consistent with the asymptotic estimate of the wavespeed, and is correctly bounded between the asymptotic estimates of the upper and lower bounds, although these bounds are not tight.

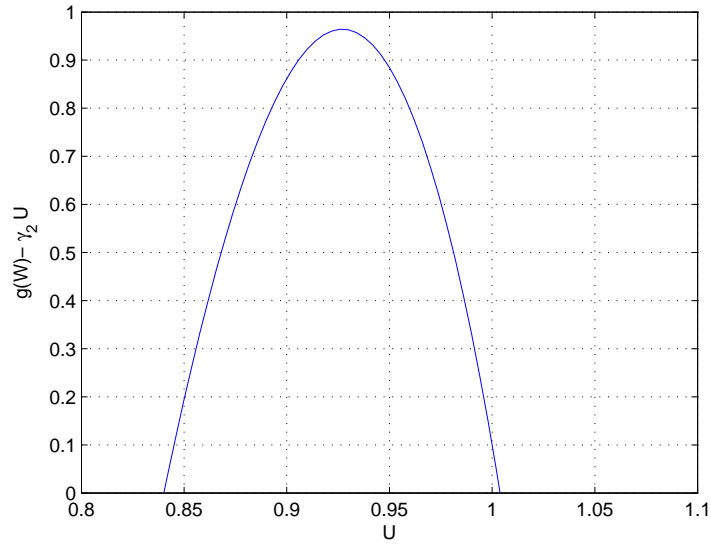


Figure 4.5: A plot of $\max_{\gamma_1 W=f(U)}(g(W) - \gamma_2 U)$, when $\alpha_1 = 1$, $\alpha_2 = 4$, $\gamma_1 = 0.5$ and $\gamma_2 = 0.9$.

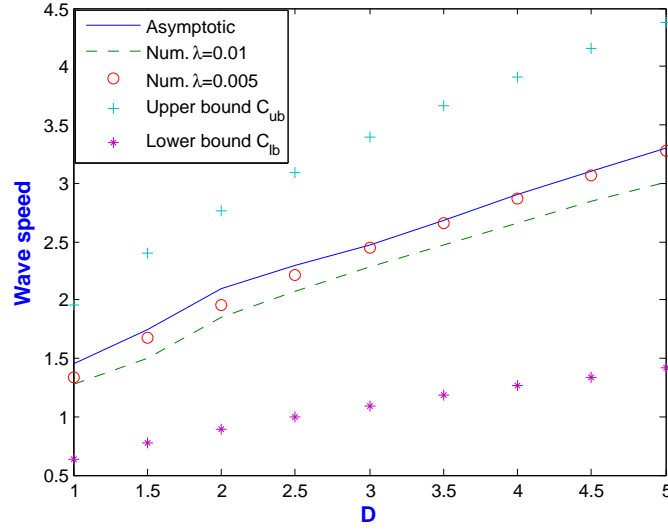


Figure 4.6: The wavespeed determined from the solution of the initial value problem for $\lambda = 0.005$ and 0.01 , the small λ asymptotic minimum wave speed (solid line), and the upper and lower bounds c_{ub} and c_{lb} , when $\alpha_1 = 1$, $\alpha_2 = 4$, $\gamma_1 = 0.5$ and $\gamma_2 = 0.9$.

4.2.3 $\gamma_2 > 1$, R_2 and R_5 : saddle-saddle connection

In order to investigate whether there exists a value of c for which there exists a travelling wave solution, we adapt the method presented in [BN91] to the differential-algebraic system (4.2.3). Let S_1 be the stable separatrix of $(0,0)$ that lies in $W > 0$ and let be S_2 the unstable separatrix of $(w_0,0)$ that lies in $V < 0$. A travelling wave solution exists for values of c for which $S_1 = S_2$.

We begin by defining the line L to be

$$L = \{(W, V), : V = 0, 0 \leq W \leq w_0\} \cup \{(W, V) : V \leq 0, W = w_0\}.$$

Since $\frac{dW}{dZ} < 0$ when $V < 0$ and $\frac{dV}{dW}$ is bounded for $0 \leq W \leq w_0$, S_1 must intersect the line L at a unique point. We can therefore construct the well-defined, continuous function

$f(c)$ as

- Case (a), S_1 intersects with L on the W -axis at $W = W_1$: $G(c) = W_1 < w_0$.
- Case (b), $S_1 = S_2$: $G(c) = w_0$.
- Case (c), S_1 intersects with L on the line $W = w_0$ at $V = -V_0$: $G(c) = w_0 + V_0$.

This definition is illustrated in Figure 4.7.

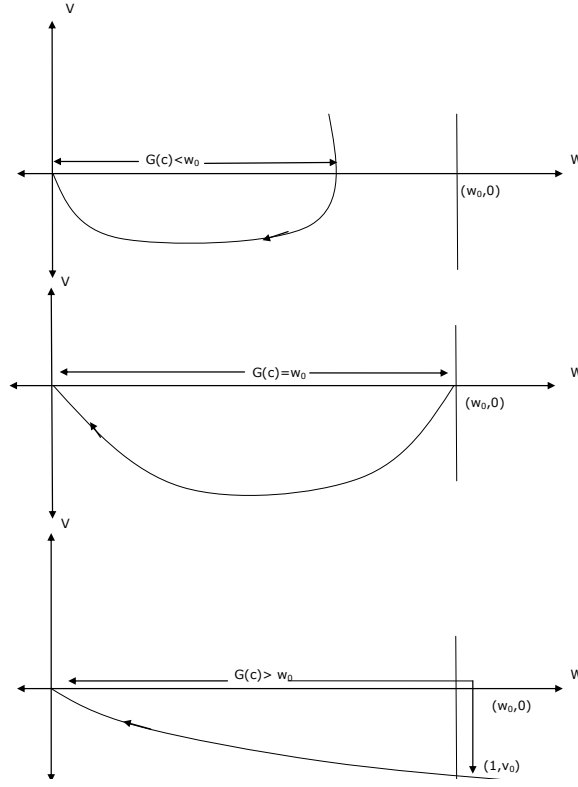


Figure 4.7: The definition of the function $G(c)$.

The behaviour of S_1 and S_2 in each case is illustrated in Figure 4.8.

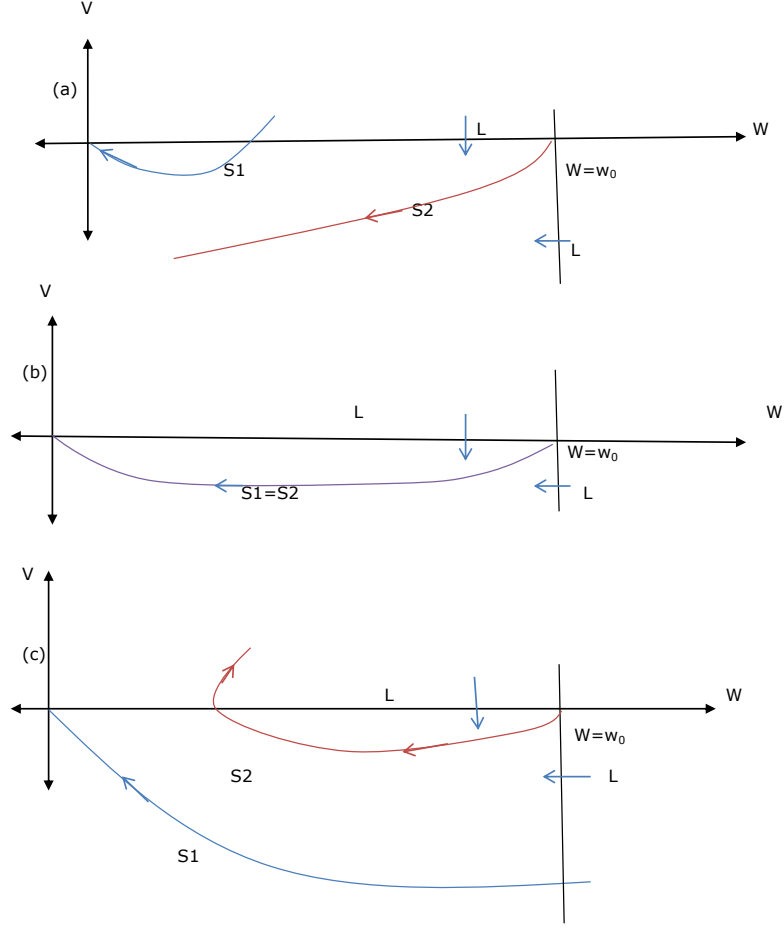


Figure 4.8: The behaviour of S_1 and S_2 in cases (a), (b) and (c).

We will now show that there is a unique value of c for which $G(c) = w_0$, and hence a unique travelling wave solution. We begin by showing that $G(c)$ is strictly monotone increasing. Consider the region $D(c_0)$ defined by

$$D(c_0) = \{(W, V) : 0 \geq V \geq V_{S_1}(W)|_{c=c_0}, 0 \leq W \leq w_0\},$$

where $V = V_{S_1}(W)$ is the equation of S_1 . Since

$$\frac{\partial}{\partial c} \left(\frac{dV}{dW} \right) = -\frac{1}{D} < 0,$$

the slope of the integral paths that meet the boundary of $D(c_0)$ rotate in a clockwise direction as c increases. When $c = c_1 > c_0$, S_1 cannot pass through the boundary of $D(c_0)$, and therefore must meet L outside $D(c_0)$. The function $G(c)$ is therefore strictly monotonically increasing.

When $c \gg 1$, it is straightforward to show that the equation of S_1 is given by $V = -cW/D$ at the leading order, and hence that $G(c) \sim w_0 + cw_0/D > w_0$ as $c \rightarrow \infty$. We therefore conclude that no more than one travelling wave solution can exist, and that it exists if and only if $G(0) < w_0$. When $c = 0$, we can solve (4.2.3), and find that the equation of S_1 is

$$V = -\sqrt{\frac{2}{D} \int_0^W w (\gamma_2 U - g(w)) dw}, \quad \gamma_1 w = f(U). \quad (4.2.7)$$

We conclude that S_1 meets the W -axis in $0 < W < w_0$, and hence that a travelling wave solution exists if and only if

$$\int_0^{w_0} W (\gamma_2 U - g(W)) dW < 0, \quad \gamma_1 W = f(U). \quad (4.2.8)$$

Although it is possible to evaluate this integral and obtain a polynomial in u_0 and w_0 , we have been unable to demonstrate that the condition (4.2.8) is satisfied for all values of the parameters. However, numerical evaluation suggests that it is always satisfied.

4.3 Singular perturbation solutions

When one of the equilibrium solutions connected by the travelling wave solution has $U = 0$, we must solve a singular perturbation problem similar to that described in [Bil04].

This is because the leading order problem in the outer region has, from (4.1.2):

$$U(1 + \alpha_1 U - (1 + \alpha_1)U^2 - \gamma_1 W) = 0.$$

The solution must smoothly connect a state with $U = 0$ to one with $1 + \alpha_1 U - (1 + \alpha_1)U^2 - \gamma_1 W = 0$, so an inner asymptotic region is required.

4.4 Asymptotic solutions for type (I_a)

For this type of travelling wave, $U \rightarrow U_0$ as $Z \rightarrow -\infty$ and $U \rightarrow 0$ as $Z \rightarrow \infty$, so for $Z < 0$, the solution must satisfy (4.2.1) and (4.2.2), whilst for $Z > 0$, $U \equiv 0$ (strictly speaking $U = o(1)$) and W satisfies

$$D \frac{d^2 W}{dZ^2} + c \frac{dW}{dZ} + Wg(W) = 0, \quad (4.4.1)$$

or equivalently

$$\begin{aligned} \frac{dW}{dZ} &= V, \\ \frac{dV}{dZ} &= -\frac{1}{D}cV - \frac{W}{D}g(W). \end{aligned} \quad (4.4.2)$$

In the (W, V) phase plane, this system has equilibrium points at $(1, 0)$, which corresponds to the equilibrium solution $U = 0$, $W = 1$, and $(0, 0)$, which correspond to the equilibrium solution $U = 0$, $W = 0$. The equilibrium points, eigenvalues and eigenvectors of (4.4.2) are

Equilibrium point	Eigenvalues	Eigenvectors
$(0, 0)$	$\frac{-c}{2D} \pm \frac{\sqrt{\frac{c^2}{D^2} - \frac{4g'(0)}{D}}}{2}$	$(1, \frac{c}{2D} \pm \frac{\sqrt{\frac{c^2}{D^2} - \frac{4g'(0)}{D}}}{2})^T$
$(1, 0)$	$\frac{-c}{2D} \pm \frac{\sqrt{\frac{c^2}{D^2} - \frac{4g'(1)}{D}}}{2}$	$(1, \frac{c}{2D} \pm \frac{\sqrt{\frac{c^2}{D^2} - \frac{4g'(1)}{D}}}{2})^T$

where

$$g'(0) = 1 \text{ and } g'(1) = -2 - \alpha_2.$$

The origin is a stable node for $c > 2\sqrt{g'(0)D}$, and a stable focus for $c < 2\sqrt{g'(0)D}$, while $(1, 0)$ is a saddle point. We need to solve either (4.4.2) for $Z > 0$ and (4.2.3) for $Z < 0$ or (4.2.3) for $Z > 0$ and (4.4.2) for $Z < 0$, subject to the boundary conditions as $Z \rightarrow \pm\infty$ and satisfy the connection conditions that W and dW/dZ should be continuous at $Z = 0$. We can solve each system of differential or differential-algebraic equations in MATLAB, shooting from close to the equilibrium points at infinity towards $Z = 0$ by using Newton's method to adjust the initial conditions to satisfy the connection conditions at $Z = 0$.

The asymptotic solutions for type (I_a) satisfy the solutions of (4.4.2) for $Z > 0$ and (4.2.3) for $Z < 0$, subject to the boundary conditions,

$$W \rightarrow 1, \quad V \rightarrow 0, \quad \text{as } Z \rightarrow \infty,$$

$$W \rightarrow W_0, \quad V \rightarrow 0, \quad \text{as } Z \rightarrow -\infty.$$

If we assume the solution (4.4.2) for $Z > 0$ is $W_1(Z)$ and the solution of (4.2.3) for $Z < 0$ is $W_2(Z)$, then we need to solve the connection conditions

$$W_1(0) - W_2(0) = 0, \quad \frac{dW_1}{dZ} - \frac{dW_2}{dZ},$$

at $Z = 0$ by the help of Newton method. The resulting solutions are shown in the following figures, Figure 4.9 shows the outer solution in both $Z < 0$ and $Z > 0$ in a typical case, whilst Figure 4.10 shows good agreement between the asymptotic and numerical solutions.

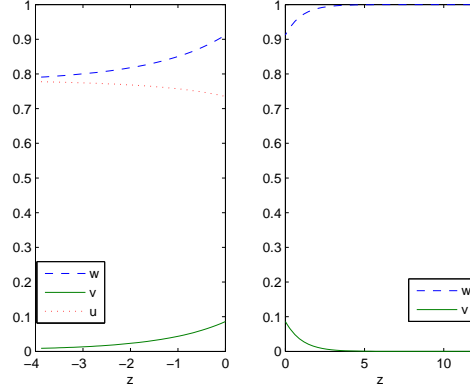


Figure 4.9: Outer solutions of type (I_a) , $\alpha_{1,2} = 0.6404$, $\gamma_{1,2} = 0.6404$ and $D = 3$.

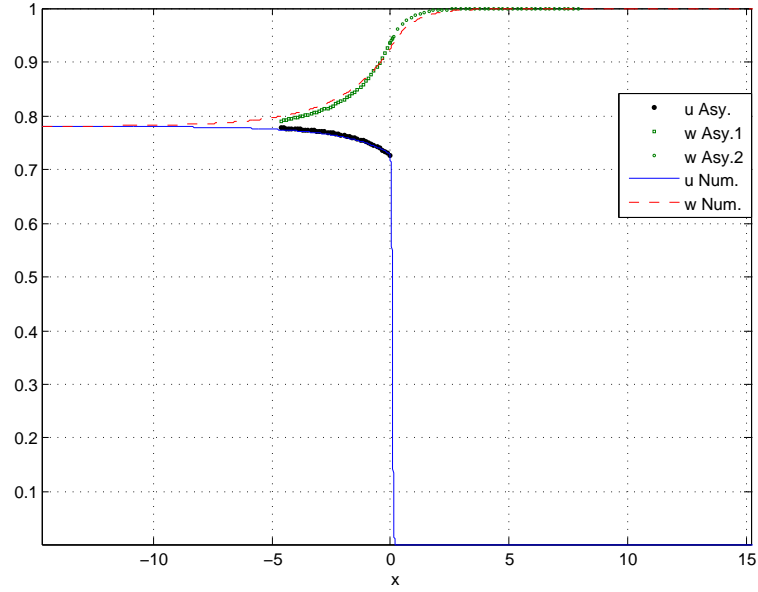


Figure 4.10: Comparison between the asymptotic travelling wave solution (also shown in Figure 4.9), and a numerical solution of (??) with $\alpha_1 = 0.6404$, $\alpha_2 = 0.6404$, $\gamma_1 = 0.6404$, $\gamma_2 = 0.6404$ and $D = 4$.

4.4.1 Inner solution for (I_a)

In the inner region, $z = O(1)$ and \hat{w} is constant at leading order, with value \hat{w}_0 determined by matching with the outer solution. At leading order, (4.1.2) is reduced to an ordinary differential equation for \hat{u} ,

$$\frac{d^2 \hat{u}}{dz^2} + c \frac{d \hat{u}}{dz} + \hat{u}(L + \alpha_1 \hat{u} - (1 + \alpha_1) \hat{u}^2) = 0, \quad (4.4.3)$$

where $L = 1 - \gamma_1 \hat{w}_0$, subject to the boundary conditions

$$\begin{aligned} \hat{u} &\rightarrow 0 \quad \text{as } z \rightarrow \infty, \\ \hat{u} &\rightarrow \frac{\alpha_1 + \sqrt{\alpha_1^2 + 4(1 + \alpha_1)L}}{2(1 + \alpha_1)} \quad \text{as } z \rightarrow -\infty. \end{aligned} \quad (4.4.4)$$

Since the wavefront in type I_a moves to the right, we need $L > 0$. In chapter one, we showed that in [HR75] a similar equation to (4.4.3) was studied with reaction term,

$$F(u) = u(1 - u)(1 + vu), \quad -1 \leq v \leq \infty. \quad (4.4.5)$$

It was shown in [HR75], that the minimum wave speed for this case satisfies,

$$c_0 = \begin{cases} 2 & -1 \leq v \leq 1, \\ \frac{v+2}{\sqrt{2v}} & v \geq 2. \end{cases} \quad (4.4.6)$$

If we rescale (4.4.5) and match the parameters with (4.4.3), we can deduce two possibilities (In [Bil04], the same equation (4.4.3) was studied and the results are derived from [HR75]),

1. When $L > 0$ there is a travelling wave solution for each $c \geq c_m(L)$,
2. When $L \leq 0$ there is a unique travelling wave solution for $c = c_m(L)$,

where the function $c_m(L, \alpha_1)$ is defined by

$$c_m(L, \alpha_1) = \begin{cases} 2\sqrt{L} & \frac{2\alpha_1^2}{(1+\alpha_1)} \leq L < 1, \\ \frac{3\sqrt{\alpha_1^2 + 4(1+\alpha_1)L - \alpha_1}}{\sqrt{8(1+\alpha_1)}} & L \leq \frac{2\alpha_1^2}{(1+\alpha_1)}. \end{cases}$$

For a given value of c , we can solve the outer problem and determine \hat{w}_0 , and then L and c_m . A typical result is shown in Figure 4.11. The point of intersection of the two curves gives the speed of the wave that we expect to be generated in an initial value problem, either the travelling wave of minimum speed or the unique travelling wave solution.

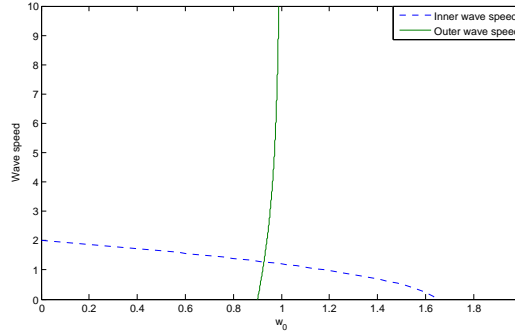


Figure 4.11: Travelling wave speeds determined from the inner and outer solutions

when $\alpha_{1,2} = 0.6404$, $\gamma_{1,2} = 0.6404$, and $D = 3$.

Figures 4.12 shows a comparison of the travelling wave speeds predicted by the asymptotic solution and the numerical solution of the initial value problem, and demonstrates that there is good agreement between the two.

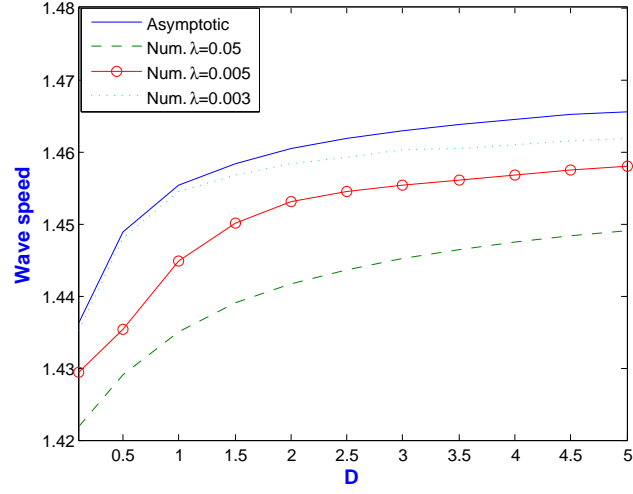


Figure 4.12: Comparison between the wave speeds of the asymptotic and numerical solutions for different values of D . $\alpha_{1,2} = 1$, $\gamma_1 = 0.5$, and $\gamma_2 = 0.9$.

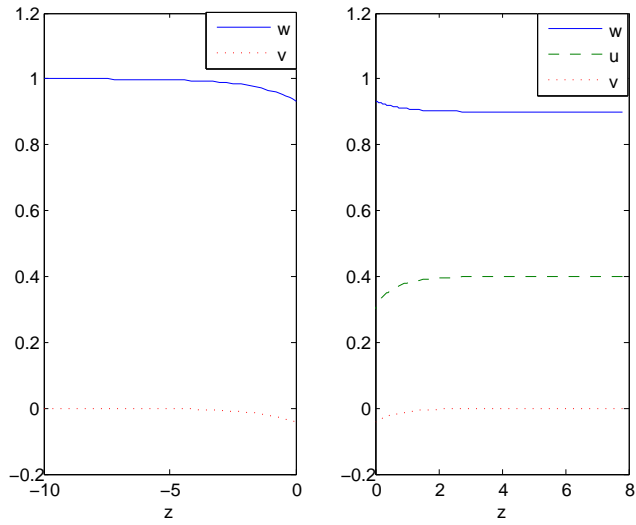


Figure 4.13: Asymptotic solutions for travelling wave of type (I_a) , the parameters are,

$$\alpha_{1,2} = 1, \gamma_1 = 1.2, \gamma_2 = 0.7 \text{ and } D = 2.8.$$

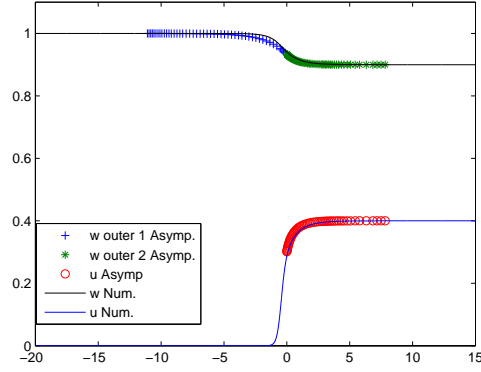


Figure 4.14: Comparison between numerical and asymptotic solutions for travelling wave of type (I_a) , the parameters are, $\alpha_{1,2} = 1$, $\gamma_1 = 1.2$, $\gamma_2 = 0.7$ and $D = 2.8$.

4.5 Solutions for type (II)

The travelling wave solutions for type (II) can be derived from the results shown in [HR75]. For type (II_a) , the asymptotic solutions can be found from (4.4.3) with $L = 1$ ($L = 1 - \gamma_1 w_0$, and $w_0 = 0$ in this case). In type (II_b) , the asymptotic solutions can be derived from (4.4.1), if we rescale $Z = D^{\frac{1}{2}}z$ then it becomes

$$\frac{d^2 W}{dz^2} + \hat{c} \frac{dW}{dz} + W(1 + \alpha_2 W - \beta_2 W^2) = 0, \quad (4.5.1)$$

where $\hat{c} = \frac{c}{D^{\frac{1}{2}}}$. This equation again is similar to (4.4.3) with $L = 1$. Thus the travelling

wave solutions exist for $\hat{c} \geq c_m(1)$, where $c_m(1)$ satisfies

$$c_m(1) = \begin{cases} 2 & 1 \geq \frac{2\alpha_1^2}{(1+\alpha_1)}, \\ \frac{3\sqrt{\alpha_1^2+4(1+\alpha_1)}-\alpha_1}{\sqrt{8(1+\alpha_1)}} & 1 \leq \frac{2\alpha_1^2}{(1+\alpha_1)}. \end{cases}$$

4.6 Asymptotic solutions for type (III)

In this subsection, we discuss the asymptotic solutions for type (III). It is equivalent to a singular perturbation problem with two outer regions and one inner region.

4.6.1 Asymptotic solutions for type (III_r)

In type (III_r), the outer solutions can be derived from (4.4.1) for $Z > 0$ and (4.2.3) for $Z < 0$ subject to the boundary conditions,

$$U \rightarrow 0, \quad W \rightarrow 1, \quad \text{as } Z \rightarrow \infty,$$

$$U \rightarrow 1, \quad W \rightarrow 0, \quad \text{as } Z \rightarrow -\infty.$$

We integrate forward from the unstable separatrix of the saddle point $(W, V) = (0, 0)$ at $Z < 0$ using ODE45 in MATLAB. Also, we integrate backward from the unstable separatrix of $(W, V) = (1, 0)$. Figure 4.15, shows the asymptotic solutions in both outer regions.

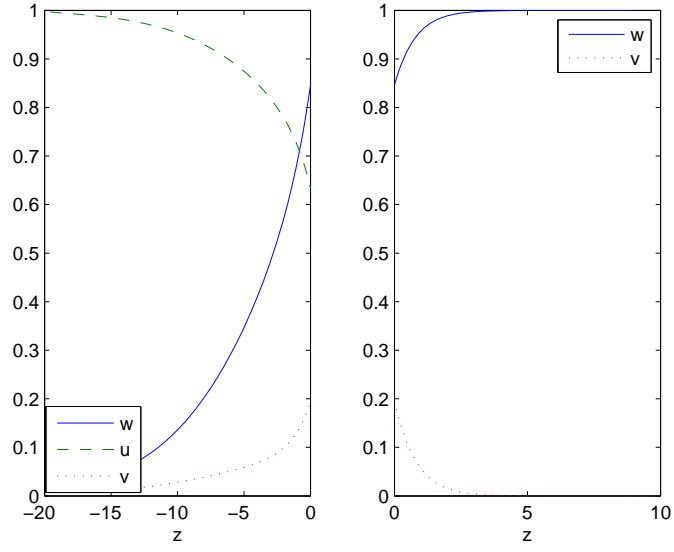


Figure 4.15: Asymptotic solutions in the outer regions in type (III_r) , the parameters are,

$$\alpha_1 = 0.7, \alpha_2 = 0.6, \gamma_1 = 0.9, \gamma_2 = 1.5, D = 2.5.$$

4.6.2 Inner solutions for type (III_r)

The inner solutions can be found in the same way as in the inner solutions of type (I_a) , and because $L > 0$ in both types. The boundary conditions are,

$$\begin{aligned} \hat{u} &\rightarrow 0 \quad \text{as} \quad z \rightarrow \infty, \\ \hat{u} &\rightarrow \frac{\alpha_1 + \sqrt{\alpha_1^2 + 4(1 + \alpha_1)L}}{2(1 + \alpha_1)} \quad \text{as} \quad z \rightarrow -\infty. \end{aligned} \tag{4.6.1}$$

We matched between the wave speed from inner and outer regions and we compare between wave speed from asymptotic and numerical solutions in Figure 4.16, which shows a good agreement between both methods.

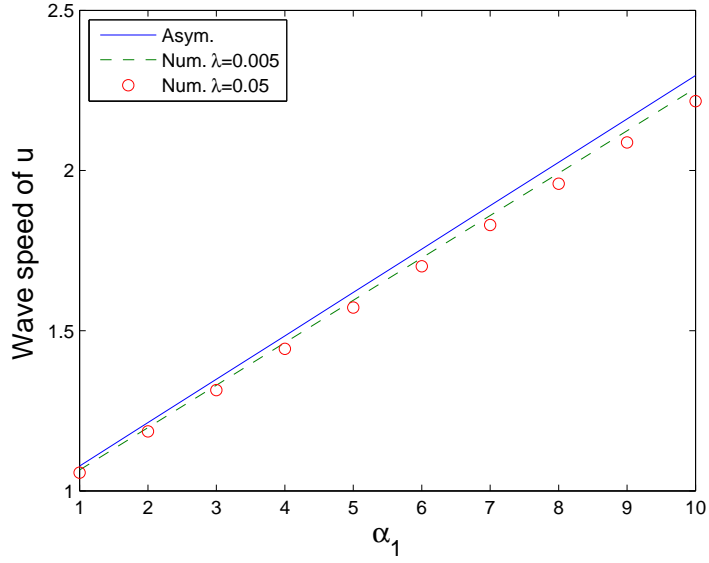


Figure 4.16: Comparison between both asymptotic and numerical solutions in type (III_r) , the parameters are, $\alpha_2 = 0.6, \gamma_1 = 0.9, \gamma_2 = 1.5$ and $D = 2.5$.

4.6.3 Asymptotic solutions for type (III_l)

In type (III_l) , the outer solutions can be derived from (4.4.1) for $Z < 0$ and (4.2.3) for $Z > 0$ subject to the boundary conditions

$$U \rightarrow 1, \quad W \rightarrow 0, \quad \text{as } Z \rightarrow \infty,$$

$$U \rightarrow 0, \quad W \rightarrow 1, \quad \text{as } Z \rightarrow -\infty.$$

We choose the saddle point $(W, V) = (1, 0)$ at $Z < 0$, so that we integrate forward from the unstable separatrix of this point using ODE45 in MATLAB. Also, we integrate backward from the unstable separatrix of $(W, V) = (0, 0)$. In Figure 4.17, we show the outer solutions for type (III_l) .

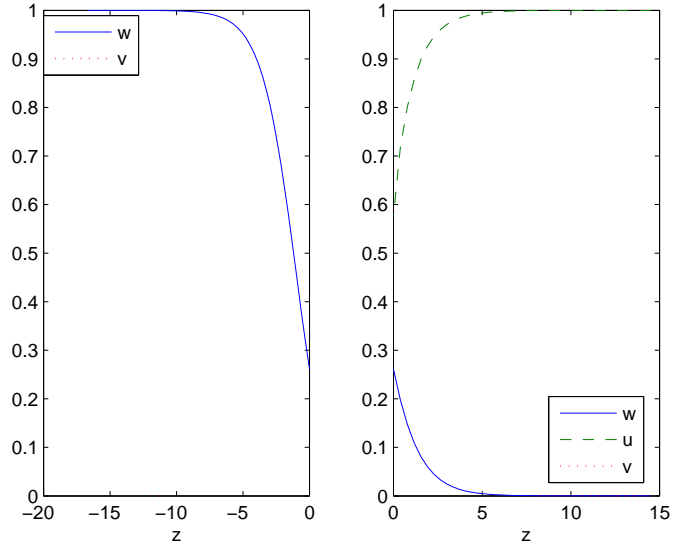


Figure 4.17: Asymptotic solutions in the outer regions in type (III_l) , the parameters are,

$$\alpha_1 = 2.8, \alpha_2 = 0.1, \gamma_1 = 6, \gamma_2 = 0.8 \text{ and } D = 2.8.$$

4.6.4 Inner solutions for type (III_l)

The inner solution for type (III_l) is not similar to the inner solutions in types (I_a) and (III_r) , since $L < 0$ in (4.4.3) for type (III_l) , whilst $L > 0$ in both (I_a) and (III_r) . The reason why in this case $L < 0$ is because we need $\gamma_1 > 1$ in order to have a stable state, $(u, w) = (0, 1)$. The boundary conditions are

$$\begin{aligned} \hat{u} &\rightarrow 0 \quad \text{as } z \rightarrow \infty, \\ \hat{u} &\rightarrow \frac{\alpha_1 + \sqrt{\alpha_1^2 + 4(1 + \alpha_1)L}}{2(1 + \alpha_1)} \quad \text{as } z \rightarrow -\infty. \end{aligned} \tag{4.6.2}$$

From [HR75] and in section (1.1.2) (case 2 number 3), we showed that the travelling wave solutions of,

$$\frac{d^2U}{dz^2} + c \frac{dU}{dz} + U(-\mu + (1 + \mu)U - U^2) = 0, \quad (4.6.3)$$

exist for all wave speeds such that

$$c \geq 2\sqrt{\mu(1 - \mu)},$$

where $0 < \mu < 1$. If we rescale (4.6.3) using

$$U = ku, \quad z = As \quad \text{and} \quad \frac{dU}{dz} = \frac{k}{A} \frac{du}{ds},$$

and then compare the parameters in this equation with (4.4.3), we deduce that the travelling wave solution for (4.4.3) satisfies

$$c \geq \frac{2\sqrt{\mu(1 - \mu)}}{A},$$

where

$$\mu = \frac{-(-\alpha_1 \pm \sqrt{\alpha_1^2 + 4(1 + \alpha_1 L)})^2}{4(1 + \alpha_1 L)}, \quad A = \pm \sqrt{\frac{-L}{\mu}}.$$

The wave speeds from outer and inner solutions are matched asymptotically, and compared with numerical solutions as shown in Figure 4.18 which are of type (III).

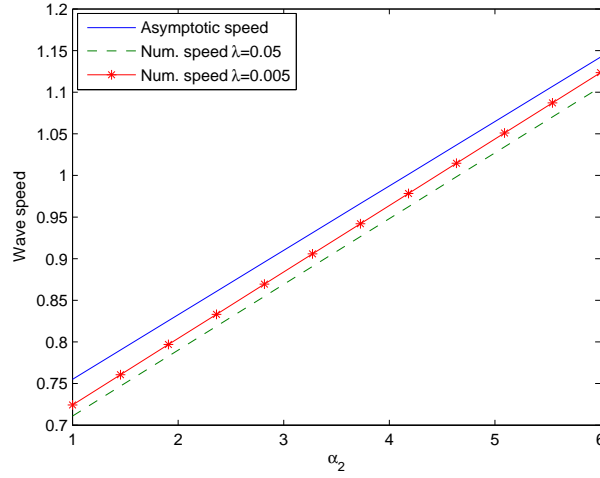


Figure 4.18: Wave speeds of asymptotic and numerical travelling wave solutions in type (III_l) , the parameters are, $\alpha_1 = 2$, $\gamma_1 = 3.5$, $\gamma_2 = 0.8$ and $D = 0.3$.

4.7 Computing the wave speed in the range of $0 < \lambda = O(1)$

In this subsection, we compute the wave speeds of travelling wave for types (I) and (III) for different values of λ . In Figure 4.19, the wave speed are computed for type (I_a) for values of λ . We see that the maximum value of the wave speed is when $\lambda \ll 1$. Also, the wave speed from numerical and asymptotic solutions are getting close when $\lambda \ll 1$. In type (III_r) the idea is similar to type (I_a) as shown in Figure 4.20. This analysis shows that the asymptotic solutions agree with numerical solutions when $\lambda \ll 1$.

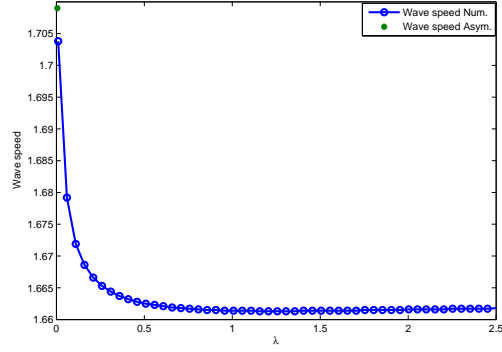


Figure 4.19: The wave speeds for type (I_a) , the parameters are, $\alpha_{1,2} = 4$, $\gamma_{1,2} = 0.6$ and $D = 1$.

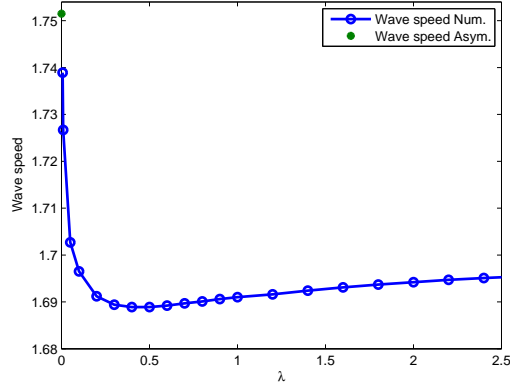


Figure 4.20: The wave speeds for type (III_r) , $\alpha_{1,2} = 4$, $\gamma_1 = 0.6$, $\gamma_2 = 2$ and $D = 1$.

4.8 The reaction-diffusion system (1.5.3) for $\lambda \gg 1$

In this subsection we study (1.5.3) with $\lambda \gg 1$ and try to find if there is any connection with the results of the case $\lambda \ll 1$. Now for $\lambda \gg 1$ we rescale

$$x = \frac{D^{\frac{1}{2}} \bar{x}}{\lambda}, \quad t = \frac{\bar{t}}{\lambda},$$

to get

$$\begin{aligned}\frac{\partial u}{\partial \bar{t}} &= \frac{\lambda}{D} \frac{\partial^2 u}{\partial \bar{x}^2} + \frac{1}{\lambda} u(1 + \alpha_1 u - (1 + \alpha_1)u^2 - \gamma_1 w), \\ \frac{\partial w}{\partial \bar{t}} &= \frac{\partial^2 w}{\partial \bar{x}^2} + w(1 + \alpha_2 w - (1 + \alpha_2)w^2 - \gamma_2 u).\end{aligned}\tag{4.8.1}$$

If we replace

$$\alpha_1 \leftrightarrow \alpha_2, \gamma_1 \leftrightarrow \gamma_2, D \rightarrow \frac{1}{D}, \lambda \rightarrow \frac{1}{\lambda},$$

we get the same system as (1.5.3) with fast diffusion and slow reaction and the same parameters. Thus, (4.8.1) with $\lambda \gg 1$ has the same results which we get for (1.5.3) with $\lambda \ll 1$.

Stability of travelling wave solutions in two dimensions

In this chapter we study the reaction-diffusion system (1.5.3) but this time in two dimensions and for $0 < \lambda \ll 1$. We use finite difference methods to study the types of travelling wave solutions in two dimensions which we have classified in one dimension. We investigate the stability of the travelling waves for different values of parameters. We also study the stability of travelling waves in two dimensions analytically using asymptotic methods.

5.1 Numerical solutions

Consider the two dimensional reaction-diffusion equations

$$\frac{\partial u}{\partial t} = \nabla^2 u + u(1 + \alpha_1 u - (1 + \alpha_1)u^2 - \gamma_1 w), \quad (5.1.1)$$

$$\frac{\partial w}{\partial t} = \frac{D}{\lambda} \nabla^2 w + \lambda w(1 + \alpha_2 w - (1 + \alpha_2)w^2 - \gamma_2 u),$$

where

$$\nabla^2 = \frac{\partial^2}{\partial x^2} + \frac{\partial^2}{\partial y^2},$$

subject to the initial conditions

$$u(x, y, 0) = u_0(x, y), \quad (x, y) \in R,$$

$$w(x, y, 0) = w_0(x, y), \quad (x, y) \in R,$$

and boundary conditions

$$\begin{aligned} \frac{\partial u(0, y, t)}{\partial x} &= 0, & \frac{\partial u(x, 0, t)}{\partial y} &= 0, & t > 0 \\ \frac{\partial w(0, y, t)}{\partial x} &= 0, & \frac{\partial w(x, 0, t)}{\partial y} &= 0, & t > 0, \end{aligned}$$

where

$$R = \{(x, y) | 0 \leq x < \infty, \quad 0 \leq y < \infty\}.$$

We solve (5.1.1) at the range of small parameter $0 < \lambda \ll 1$. We truncate the domain to a finite domain where it is possible to study the properties of a travelling wave. We rescale the variables in (5.1.1) such that, $X = \lambda x$, $Y = \lambda y$ and $\bar{t} = \lambda t$, i.e. the inner region of $O(\lambda)$ and the outer regions of $O(1)$, so that we save time and reduce the domain. Thus, (5.1.1) becomes

$$\begin{aligned} \frac{\partial u}{\partial \bar{t}} &= \lambda \nabla^2 u + u(1 + \alpha_1 u - (1 + \alpha_1)u^2 - \gamma_1 w) / \lambda \\ \frac{\partial w}{\partial \bar{t}} &= D \nabla^2 w + w(1 + \alpha_2 w - (1 + \alpha_2)w^2 - \gamma_2 u). \end{aligned} \tag{5.1.2}$$

We work in a moving frame of reference to capture the whole travelling wave as it propagates. In order to do that we use the coordinate $\bar{X} = X - S(t)$ with $S(0) = L_N/2$,

$u = u(\bar{X}, Y, t)$ and $w = w(\bar{X}, Y, t)$, where L_N is constant. So that (5.1.2) becomes

$$\begin{aligned}\frac{\partial u}{\partial t} &= \lambda \nabla^2 u + \dot{S} \frac{\partial u}{\partial \bar{X}} + u(1 + \alpha_1 u - (1 + \alpha_1)u^2 - \gamma_1 w) / \lambda \\ \frac{\partial w}{\partial t} &= D \nabla^2 w + \dot{S} \frac{\partial w}{\partial \bar{X}} + w(1 + \alpha_2 w - (1 + \alpha_2)w^2 - \gamma_2 u).\end{aligned}\quad (5.1.3)$$

We will study the same two types of travelling wave, (I) and (III) that we studied in one dimension. The initial conditions are of type A, B and C but in two dimensions (see below). The asymptotic analysis of travelling wave solutions in one dimension has shown that we could use a non uniform grid in the x-direction (for example, type (I_a) has inner region with scale $O(1)$, whilst the outer regions are of $O(\frac{1}{\lambda})$). We use a uniform grid in the Y-direction with grid size ΔY . We solve (5.1.3) in the domain Ω ,

$$\Omega = \{(\bar{X}, Y) | 0 \leq \bar{X} \leq N, \quad 0 \leq Y \leq M\},$$

where M and N are positive constants. In order to make the travelling wave stay in the domain Ω , we find the wave speed for (5.1.3) in one dimension and choose $\dot{S} = c$ in (5.1.3). We solve subject to the initial conditions

$$u(\bar{X}, Y, 0) = f(\bar{X}, Y), \quad (\bar{X}, Y) \in \Omega,$$

$$w(\bar{X}, Y, 0) = g(\bar{X}, Y), \quad (\bar{X}, Y) \in \Omega.$$

The new boundary conditions, are

$$\frac{\partial u(0, Y, t)}{\partial \bar{X}} = 0, \quad \frac{\partial u(\bar{X}, 0, t)}{\partial Y} = 0, \quad t > 0,$$

$$\frac{\partial w(0, Y, t)}{\partial \bar{X}} = 0, \quad \frac{\partial w(\bar{X}, 0, t)}{\partial Y} = 0, \quad t > 0,$$

$$\frac{\partial u(0, M, t)}{\partial \bar{X}} = 0, \quad \frac{\partial u(N, 0, t)}{\partial Y} = 0, \quad t > 0$$

$$\frac{\partial w(0, M, t)}{\partial \bar{X}} = 0, \quad \frac{\partial w(N, 0, t)}{\partial Y} = 0, \quad t > 0.$$

We use the initial conditions of type (A),

$$f(\bar{X}, Y) = \begin{cases} 1, & \text{for } 0 \leq \bar{X} \leq L_N, 0 \leq Y \leq M, \\ 0, & \text{for } \bar{X} > L_N, 0 \leq Y \leq M, \end{cases}$$

$$g(\bar{X}, Y) = 1, \quad \text{for } 0 \leq \bar{X} \leq N, \quad 0 \leq Y \leq M,$$

the initial conditions of type (B),

$$f(\bar{X}, Y) = 1, \quad \text{for } 0 \leq \bar{X} \leq N, \quad 0 \leq Y \leq M.$$

$$g(\bar{X}, Y) = \begin{cases} 1, & \text{for } 0 \leq \bar{X} \leq L_N, 0 \leq Y \leq M, \\ 0, & \text{for } \bar{X} > L_N, 0 \leq Y \leq M, \end{cases}$$

and for type (C),

$$f(\bar{X}, Y) = \begin{cases} 1, & \text{for } 0 \leq \bar{X} \leq L_N, 0 \leq Y \leq M, \\ 0, & \text{for } \bar{X} > L_N, 0 \leq Y \leq M, \end{cases}$$

$$g(\bar{X}, Y) = \begin{cases} 1, & \text{for } 0 \leq \bar{X} \leq L_N, 0 \leq Y \leq M, \\ 0, & \text{for } \bar{X} > L_N, 0 \leq Y \leq M. \end{cases}$$

Now let

$$h_i = x_{i+1} - x_i, \quad i = 0, 1, 2 \dots n,$$

$$x_i = h_0 + h_1 + \dots h_{i-1}, \quad i = 0, 1, 2 \dots n.$$

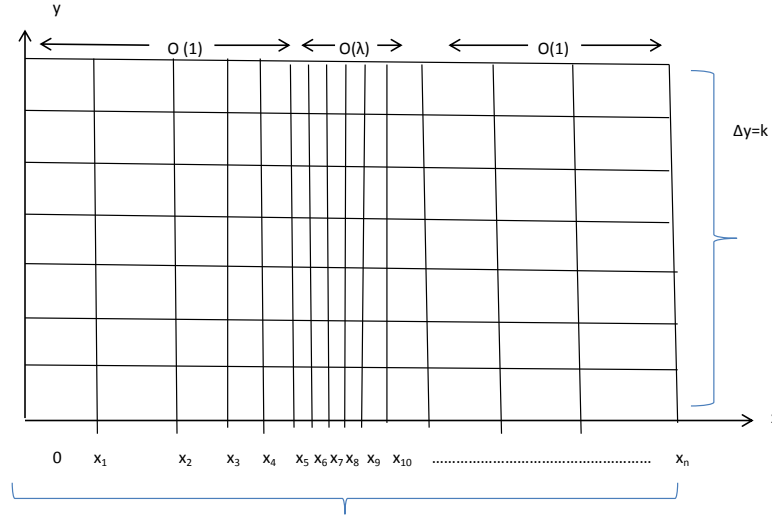


Figure 5.1: Grid points in the domain R^2 .

We choose small step sizes ($h_i = O(\lambda)$) at the position of the head of the wavefront where the inner region lies, and step sizes increases gradually behind and in front the head of the wavefront and becomes of $O(1)$. We discretise the first and second derivative for u and w with respect to x and y using the Taylor expansion. For Neumann boundary conditions, we discretize $\frac{\partial u}{\partial x}$ and $\frac{\partial u}{\partial y}$ taking into account the uniform and non uniform grid for y and x respectively. Thus

$$\frac{\partial u}{\partial x} = -\frac{2h_i + h_{i+1}}{h_i(h_i + h_{i+1})}u_{i,j}^{t+1} + \frac{h_i + h_{i+1}}{h_i h_{i+1}}u_{i+1,j}^{t+1} - \frac{h_i}{h_{i+1}(h_i + h_{i+1})}u_{i+2,j}^{t+1} = 0.$$

$$\frac{\partial u}{\partial y} = \frac{-3u_{i,j}^{t+1} + 4u_{i,j+1}^{t+1} - u_{i,j+2}^{t+1}}{2k} = 0.$$

We use an implicit method to discretise the diffusion operator. For the non linear reaction part we use an explicit method, with a forward difference formula for the derivative with respect to t

$$\begin{aligned}\frac{\partial u}{\partial t} &= \frac{u_{i,j}^{t+\Delta t} - u_{i,j}^t}{\Delta t} \\ \frac{\partial^2 u}{\partial x^2} &= \frac{2}{h_i(h_i + h_{i-1})} u_{i+1,j}^{t+\Delta t} - \frac{2}{(h_i h_{i-1})} u_{i,j}^{t+\Delta t} + \frac{2\Delta t}{h_{i-1}(h_i + h_{i-1})} u_{i-1,j}^{t+\Delta t} \\ \frac{\partial^2 u}{\partial y^2} &= \frac{(u_{i,j+1}^{t+\Delta t} - 2u_{i,j}^{t+\Delta t} + u_{i,j-1}^{t+\Delta t})}{k^2}.\end{aligned}$$

Substituting these relations in (5.1.3) we get,

$$\begin{aligned}& -(\lambda k_1 + k_4) u_{i+1,j}^{t+\Delta t} + (1 + \lambda k_2 + 2\lambda r) u_{i,j}^t - (\lambda k_3 - k_4) u_{i-1,j}^{t+\Delta t} + \lambda r u_{i,j+1}^{t+\Delta t} + \\ & \lambda r u_{i,j-1}^{t+\Delta t} = u_{i,j}^t + \frac{\Delta t}{\lambda} u_{i,j}^t (1 + \alpha_1 u_{i,j}^t - (1 + \alpha_1)(u_{i,j}^t)^2 - \gamma_1 w_{i,j}^t), \\ & -(Dk_1 + k_4) w_{i+1,j}^{t+\Delta t} + (1 + Dk_2 + 2Dr) w_{i,j}^t - (Dk_3 - k_4) w_{i-1,j}^{t+\Delta t} + Dr w_{i,j+1}^{t+\Delta t} + \\ & Dr w_{i,j-1}^{t+\Delta t} = w_{i,j}^t + \Delta t \lambda w_{i,j}^t (1 + \alpha_2 w_{i,j}^t - (1 + \alpha_2)(w_{i,j}^t)^2 - \gamma_2 u_{i,j}^t),\end{aligned}$$

where

$$\begin{aligned}k_1 &= \frac{2\Delta t}{h_i(h_i + h_{i-1})}, & k_2 &= \frac{2\Delta t}{(h_i h_{i-1})}, & k_3 &= \frac{2\Delta t}{h_{i-1}(h_i + h_{i-1})}, \\ k_4 &= \frac{\ddot{X}\Delta t}{(h_i + h_{i-1})}, & r &= \frac{\Delta t}{k^2}.\end{aligned}$$

This is a system of algebraic equations which can be written in the form

$$AU^{t+1} = bU^t, \quad BW^{t+1} = cW^t.$$

The matrices A and B contain entries from the Laplacian and the boundary equations and need to be formulated carefully. In Figure 5.2, we show how to formulate these matrices from the coefficients of the algebraic equations.

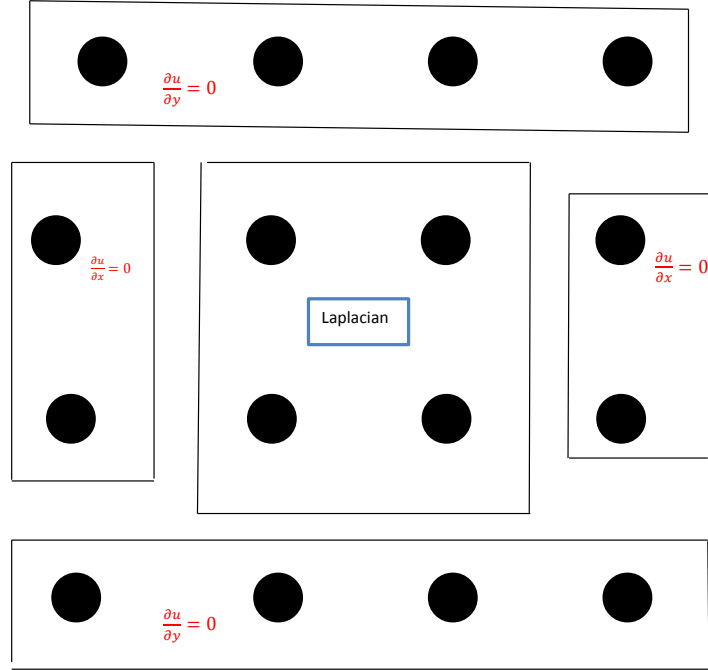


Figure 5.2: The entries of matrices A and B .

5.2 Perturbation of the planar wavefront

We discuss in this section the stability of the wavefront for travelling waves of types (I) and (III). The stability of travelling waves can be investigated by making a small perturbation to the position of the wavefront. If the wavefront returns to its original position then it is stable, otherwise, it is unstable. In type (III_r) , we use the perturbed

initial condition (A),

$$\begin{aligned} u(x, y, 0) &= \frac{1 - \tanh(\bar{X} - a \cos(kY))}{2}, \\ w(x, y, 0) &= \frac{1 + \tanh(\bar{X} - a \cos(kY))}{2}, \end{aligned}$$

which has wavelength $\frac{2\pi}{k}$ in the Y -direction and a is the amplitude. This perturbation has compact support and will not therefore generate travelling wave solutions that propagate above the minimum wave speed. We are interested only in the lateral stability of the underlying wave.

5.2.1 Example test: Gray-Scott

We applied our numerical method to the Gray-Scott system which has unstable travelling wave solutions that are subject to a two-dimensions (see for example [HPSS93] and [ZF94]). The Gray-Scott system in two dimensions, is

$$\begin{aligned} \frac{\partial u}{\partial t} &= D \nabla^2 u - uv^2 - \kappa uw \\ \frac{\partial w}{\partial t} &= \nabla^2 w + uv^2 + \kappa uw, \end{aligned} \tag{5.2.1}$$

where D is a diffusion coefficient and κ is a constant. The travelling wave solution connects the equilibrium solution $(0, 1)$ behind the wavefront to $(1, 0)$ (same as in type (III_l)). We have found the same results as [HPSS93] with $D = 5$ and $\kappa = 0$. The results are shown in Figures 5.3 and 5.4 which are for wave number $k = 0.1$. With $k = 0.05$ in Figures 5.5 and 5.6. These figures show an unstable wavefront for $D = 5$. This suggests that we may see something similar in our solutions of 5.1.3.

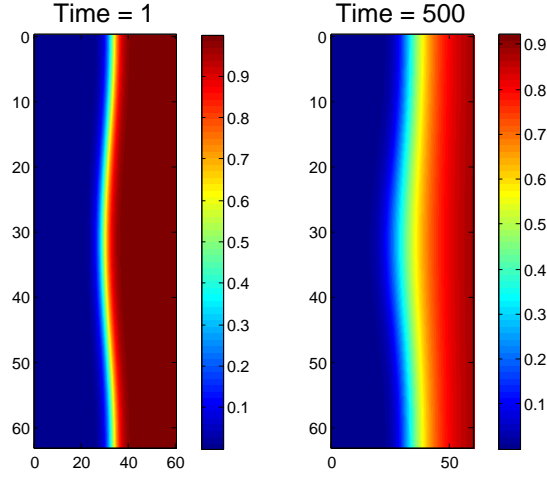


Figure 5.3: Unstable travelling wave solution for species u in (5.2.1), with $k = 0.1$, $\kappa = 0$ and $D = 5$

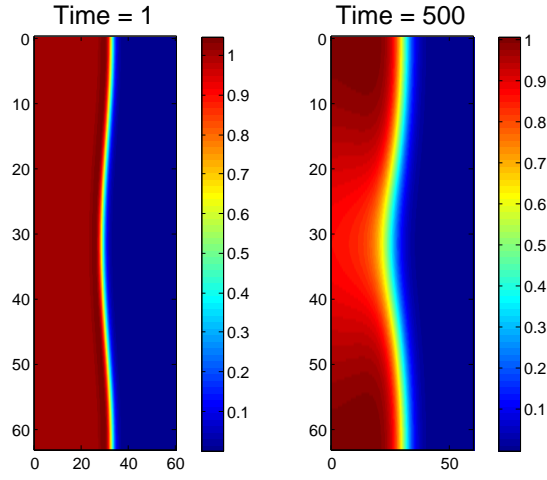


Figure 5.4: Unstable travelling wave solution for species w in (5.2.1), with $k = 0.1$, $\kappa = 0$ and $D = 5$

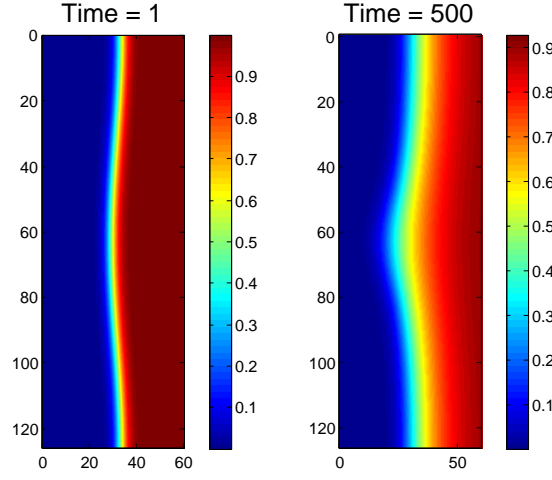


Figure 5.5: Unstable travelling wave solution for species u in (5.2.1), with $k = 0.05, \kappa = 0$ and $D = 5$

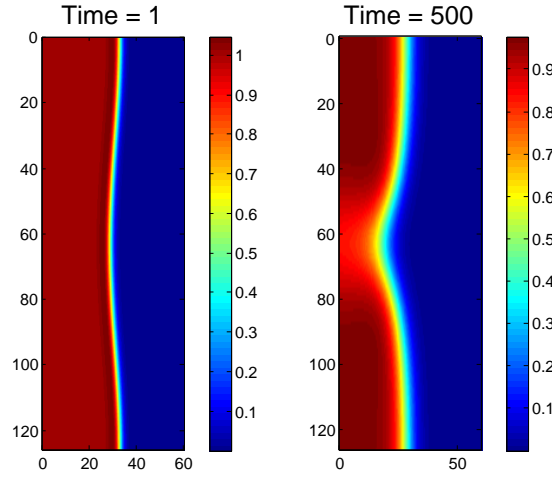


Figure 5.6: Unstable travelling wave solution for species w in (5.2.1), with $k = 0.05, \kappa = 0$ and $D = 5$

5.2.2 Numerical results

We solve (5.1.2) and look for instability of the travelling wave solutions for the types (I) and (II). Although, we have computed the instability of wavefronts for many para-

meter values, we were unable to see any evidence of unstable wavefronts. We found for all parameter values we have chosen, and for all the types of travelling waves, that the wavefront is stable for the two dimensional initial value problem (5.1.3). The following figures show that the travelling wave solutions are stable for specific values of parameters. Figure 5.7 and 5.8 are of type I_a with $k = 0.2$ and $a = 2$. Figure 5.9 and 5.10 show stable travelling waves of type (I_b) with $k = 0.1$ and $a = 2$. Figure 5.11 and 5.12 are of type III_r with $k = 0.1$ and $a = 2$. Figure 5.13 and 5.14 are of type III_l with $k = 0.1$ and $a = 2$.

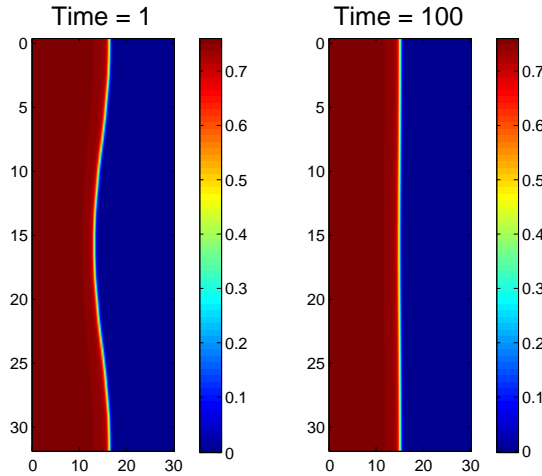


Figure 5.7: Stable travelling wave of type I_a for u in (5.1.3), when $k = 0.2$ for specific values of parameters, $\alpha_1 = 1, \alpha_2 = 1, \gamma_1 = 0.7, \gamma_2 = 0.5, D = 1$ and $\lambda = 0.05$.

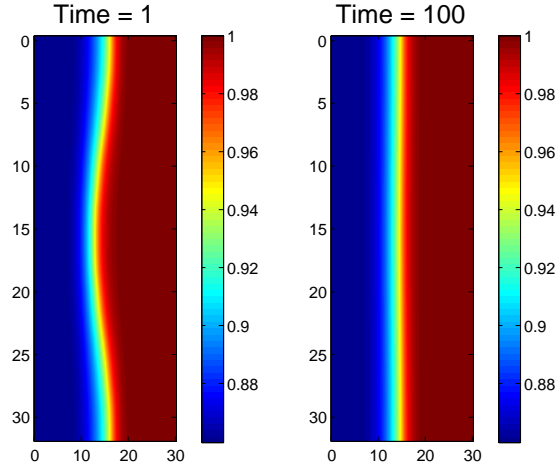


Figure 5.8: Stable travelling wave of type I_a for w in (5.1.3), when $k = 0.2$ for specific values of parameters, $\alpha_1 = 1, \alpha_2 = 1, \gamma_1 = 0.7, \gamma_2 = 0.5, D = 1$ and $\lambda = 0.05$.

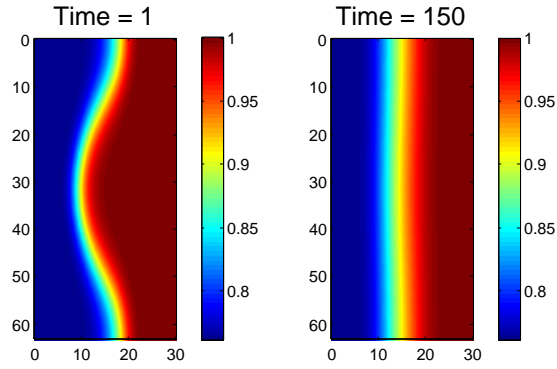


Figure 5.9: Stable travelling wave of type (I_b) for u in (5.1.3), when $\alpha_1 = 1, \alpha_2 = 1, \gamma_1 = 0.7, \gamma_2 = 0.5, D = 1$ and $\lambda = 0.05$.

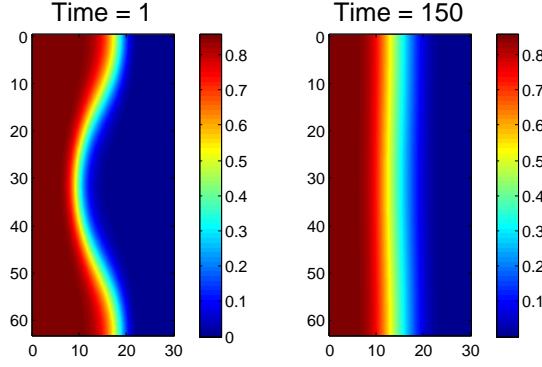


Figure 5.10: Stable travelling wave of type (I_b) for w in (5.1.3), when $\alpha_1 = 1, \alpha_2 = 1, \gamma_1 = 0.7, \gamma_2 = 0.5, D = 1$ and $\lambda = 0.05$.

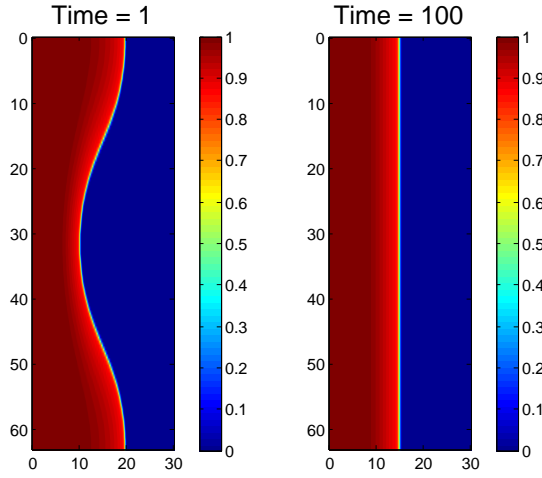


Figure 5.11: Stable travelling wave of type (III_r) for u in (5.1.3), when $\alpha_1 = 1, \alpha_2 = 1, \gamma_1 = 0.5, \gamma_2 = 2, D = 1$ and $\lambda = 0.05$.

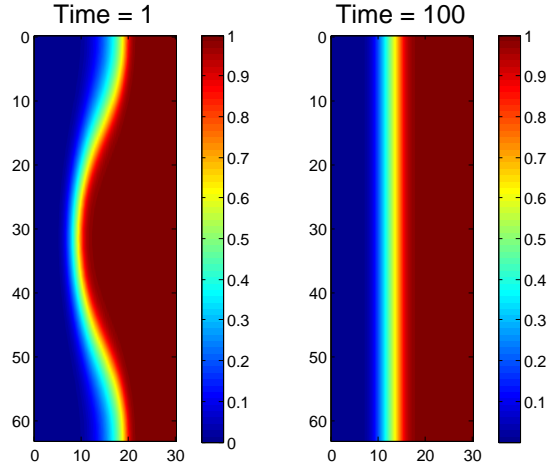


Figure 5.12: Stable travelling wave of type (III_r) for w in (5.1.3), when $\alpha_1 = 1, \alpha_2 = 1, \gamma_1 = 0.5, \gamma_2 = 2, D = 1$ and $\lambda = 0.05$.

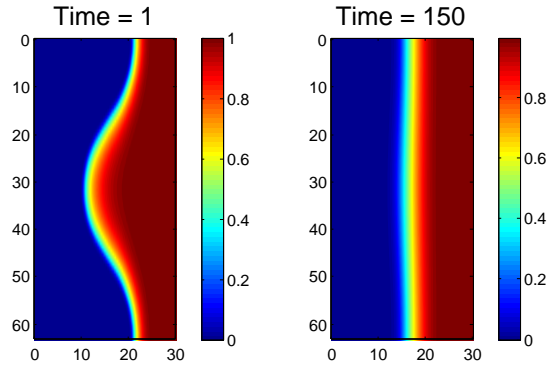


Figure 5.13: Stable travelling wave of type (III_l) for u in (5.1.3), when $\alpha_1 = 1, \alpha_2 = 1, \gamma_1 = 2, \gamma_2 = 0.5, D = 1$ and $\lambda = 0.05$.

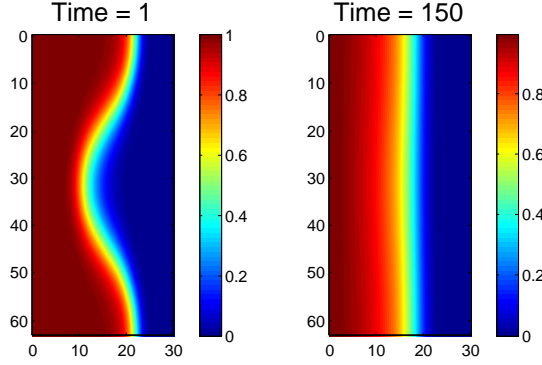


Figure 5.14: Stable travelling wave of type (III_l) for w in (5.1.3), when $\alpha_1 = 1, \alpha_2 = 1, \gamma_1 = 2, \gamma_2 = 0.5, D = 1$ and $\lambda = 0.05$.

5.3 Stability analysis of travelling waves of (5.1.1)

In this section, we study the stability of travelling waves in two dimensions analytically using asymptotic methods. We linearise (5.1.1) around a travelling wave, and determine whether the solutions of the new linear system grow or decay. We study the linear system which is produced from (5.1.1) in the limit of $0 < \lambda \ll 1$ using asymptotic methods.

5.4 Linearisation of (5.1.3)

The first step in studying the stability of a travelling wave is to linearise (5.1.1) around the travelling wave solution. We linearise (5.1.1) using,

$$u(x, y, t) = U(z) + \psi_1(z, y, t), \quad w(x, y, t) = W(z) + \psi_2(z, y, t),$$

where U and W are travelling wave, ψ_1 and ψ_2 are small perturbation terms, and $z = x - ct$. Two coupled evolution equations for the linear perturbations, ψ_1 and ψ_2 are

$$\begin{aligned}\frac{\partial \psi_1}{\partial t} &= \frac{\partial^2 \psi_1}{\partial z^2} + \frac{\partial^2 \psi_1}{\partial y^2} + c \frac{\partial \psi_1}{\partial z} + M_1 \psi_1 + M_2 \psi_2 \\ \frac{\partial \psi_2}{\partial t} &= \frac{D}{\lambda} \left(\frac{\partial^2 \psi_2}{\partial z^2} + \frac{\partial^2 \psi_2}{\partial y^2} \right) + c \frac{\partial \psi_2}{\partial z} + \lambda N_1 \psi_1 + \lambda N_2 \psi_2,\end{aligned}\tag{5.4.1}$$

where

$$\begin{aligned}M_1 &= 1 + 2\alpha_1 U - 3(1 + \alpha_1)U^2 - \gamma_1 W, \quad M_2 = -\gamma_1 U, \\ N_1 &= -\gamma_2 W, \quad N_2 = 1 + 2\alpha_2 W - 3(1 + \alpha_2)W^2 - \gamma_2 U.\end{aligned}$$

Next, we look for a solution with wave number k in the y -direction,

$$\psi(z, y, t) = \bar{\psi}(z, t) \exp(iky).\tag{5.4.2}$$

This leads to

$$\begin{aligned}\frac{\partial \bar{\psi}_1}{\partial t} &= \frac{\partial^2 \bar{\psi}_1}{\partial z^2} + c \frac{\partial \bar{\psi}_1}{\partial z} + (M_1 - k^2) \bar{\psi}_1 + M_2 \bar{\psi}_2 \\ \frac{\partial \bar{\psi}_2}{\partial t} &= \frac{D}{\lambda} \left(\frac{\partial^2 \bar{\psi}_2}{\partial z^2} - k^2 \bar{\psi}_2 \right) + c \frac{\partial \bar{\psi}_2}{\partial z} + \lambda N_1 \bar{\psi}_1 + \lambda N_2 \bar{\psi}_2.\end{aligned}\tag{5.4.3}$$

This is a system of linear second order parabolic partial differential equations which is difficult to solve analytically. We will work in the limit $\lambda \ll 1$ and try to find the asymptotic solution.

5.5 Asymptotic solutions for (5.4.3)

We use the same scale as we applied to the asymptotic analysis for types of travelling solutions in one dimension when $\lambda \ll 1$ (see Chapter 5). When $z = O(1)$, we rewrite

$$\bar{\psi}_1 = \bar{\psi}_{10} + \lambda \bar{\psi}_{11},$$

$$\bar{\psi}_2 = \bar{\psi}_{20} + \lambda \bar{\psi}_{21}.$$

At leading order,

$$\frac{\partial \bar{\psi}_{10}}{\partial t} = \frac{\partial^2 \bar{\psi}_{10}}{\partial z^2} + c \frac{\partial \bar{\psi}_{10}}{\partial z} + (M_1 - k^2) \bar{\psi}_{10} + M_2 \bar{\psi}_{20},$$

$$\frac{\partial^2 \bar{\psi}_{20}}{\partial z^2} - k^2 \bar{\psi}_{20} = 0.$$

(5.5.1)

From the second equation in (5.5.1),

$$\bar{\psi}_{20} = f_1(t) \exp(-kz) + f_2(t) \exp(kz). \quad (5.5.2)$$

This means $f_{1,2}(t) = 0$ when $z \rightarrow \pm\infty$, and it suggests $t = O(\lambda)$ and that we need to use multiple scales method.

Next we scale (5.4.3), such that

$$Z = \lambda z,$$

then (5.4.3) becomes,

$$\begin{aligned}\frac{\partial \bar{\psi}_1}{\partial t} &= \lambda^2 \frac{\partial^2 \bar{\psi}_1}{\partial Z^2} + c\lambda \frac{\partial \bar{\psi}_1}{\partial Z} + (M_1 - k^2)\bar{\psi}_1 + M_2\bar{\psi}_2, \\ \frac{\partial \bar{\psi}_2}{\partial t} &= \lambda \left\{ D \frac{\partial^2 \bar{\psi}_2}{\partial Z^2} + c \frac{\partial \bar{\psi}_2}{\partial Z} + N_1\bar{\psi}_1 + N_2\bar{\psi}_2 \right\} - \frac{D}{\lambda} k^2 \bar{\psi}_2.\end{aligned}\tag{5.5.3}$$

From the equation of $\bar{\psi}_2$ in (5.5.3), we see that only one term is of order $O(\frac{1}{\lambda})$, and all the other terms are of $O(\lambda)$. In order to make a balance between terms we scale k to be,

$$k = \lambda \bar{k}, \quad \bar{k} = O(\lambda) \quad \text{as } \lambda \rightarrow 0,$$

then we get,

$$\begin{aligned}\frac{\partial \bar{\psi}_1}{\partial t} &= \lambda^2 \frac{\partial^2 \bar{\psi}_1}{\partial Z^2} + c\lambda \frac{\partial \bar{\psi}_1}{\partial Z} + (M_1 - \lambda^2 \bar{k}^2)\bar{\psi}_1 + M_2\bar{\psi}_2, \\ \frac{\partial \bar{\psi}_2}{\partial t} &= \lambda \left\{ D \frac{\partial^2 \bar{\psi}_2}{\partial Z^2} - \bar{k}^2 \bar{\psi}_2 + c \frac{\partial \bar{\psi}_2}{\partial Z} + N_1\bar{\psi}_1 + N_2\bar{\psi}_2 \right\}.\end{aligned}\tag{5.5.4}$$

At leading order,

$$\frac{\partial \bar{\psi}_{10}}{\partial t} = M_1 \bar{\psi}_{10} + M_2 \bar{\psi}_{20},\tag{5.5.5}$$

$$\frac{\partial \bar{\psi}_{20}}{\partial t} = \lambda \left\{ D \frac{\partial^2 \bar{\psi}_{20}}{\partial Z^2} - \bar{k}^2 \bar{\psi}_{20} + c \frac{\partial \bar{\psi}_{20}}{\partial Z} + N_1 \bar{\psi}_{10} + N_2 \bar{\psi}_{10} \right\} = 0,\tag{5.5.6}$$

or

$$\frac{\partial \bar{\psi}_{10}}{\partial t} = O(1), \quad \frac{\partial \bar{\psi}_{20}}{\partial t} = O(\lambda),$$

this means that the solution of $\bar{\psi}_{10}$ has a faster scale with respect to t than to the solution of $\bar{\psi}_{20}$. The multiple scale method is a suitable method for solving this problem.

5.5.1 Multiple scale method

In this section we use the method of multiple scales to solve (5.5.4). In this method we need to scale

$$T = \lambda t, \quad \bar{\psi}_1(Z, t) = q_1(Z, T, t), \quad \bar{\psi}_2(Z, t) = q_2(Z, T, t), \quad (5.5.7)$$

$$q_1(Z, T, t) = q_{10}(Z, T, t) + \lambda q_{11}(Z, T, t) + o(\lambda^2),$$

$$q_2(Z, T, t) = q_{20}(Z, T, t) + \lambda q_{21}(Z, T, t) + o(\lambda^2),$$

and from the relations,

$$\begin{aligned} \frac{\partial \bar{\psi}_1}{\partial t} &= \frac{\partial q_1}{\partial t} + \lambda \frac{\partial q_1}{\partial T}, \\ \frac{\partial \bar{\psi}_2}{\partial t} &= \frac{\partial q_2}{\partial t} + \lambda \frac{\partial q_2}{\partial T}, \end{aligned} \quad (5.5.8)$$

by substituting (5.5.7) and (5.5.8) in (5.5.4), we get at leading order,

$$\begin{aligned} \frac{\partial q_{20}}{\partial t} &= 0, \\ \frac{\partial q_{10}}{\partial t} &= M_1 q_{10} + M_2 q_{20}, \\ \frac{\partial q_{21}}{\partial t} + \frac{\partial q_{20}}{\partial T} &= D \frac{\partial^2 q_{20}}{\partial Z^2} - D \bar{k}^2 q_{20} + c \frac{\partial q_{20}}{\partial Z} + N_1 q_{10} + N_2 q_{20}. \end{aligned}$$

(5.5.9)

The analytical solution of q_{10} in (5.5.9) is

$$q_{10} = \frac{-M_2}{M_1} q_{20} + F(T, Z) \exp(M_1 t), \quad M_1(Z) \neq 0,$$

where

$$F(0, Z) = Q_1(Z) + \frac{M_2}{M_1} Q_2(Z),$$

$Q_1(Z)$ and $Q_2(Z)$ are continuous functions of Z , comes from integration at $T = 0$. By substituting q_{10} in (5.5.9) we get,

$$q_{21} = \left(-\frac{\partial q_{20}}{\partial T} + D \frac{\partial^2 q_{20}}{\partial Z^2} - D \bar{k}^2 q_{20} + c \frac{\partial q_{20}}{\partial Z} + N_1 \frac{-M_2}{M_1} q_{20} + N_2 q_{20} \right) t + \frac{N_1}{M_1} F(T, Z) \exp(M_1 t). \quad (5.5.10)$$

The term proportional to t in (5.5.10) is known as the secular term, and to keep the asymptotic expansion uniform, we must eliminate it, therefore we get,

$$\frac{\partial q_{20}}{\partial T} = D \frac{\partial^2 q_{20}}{\partial Z^2} - D \bar{k}^2 q_{20} + c \frac{\partial q_{20}}{\partial Z} + \frac{(N_2 M_1 - N_1 M_2)}{M_1} q_{20}. \quad (5.5.11)$$

In conclusion, from (5.5.10), the solution of (5.4.3) grows exponentially when $M_1(Z) > 0$. In other words, a sufficient condition for instability is $M_1(Z) > 0$. In the next subsection, we will investigate if the condition $M_1(Z) > 0$ can be satisfied for any of the types of travelling waves solutions. Also we need to solve (5.5.11) and find the stability of the travelling wave using Evans function (see for example [GMSW03], [HZ06]). We will use Evans function to study the instability of travelling wave for the wavefront in the inner region, whilst we study the instability at the outer region for (5.5.11).

5.5.2 Calculating M_1

The aim of this subsection is to compute whether $M_1 > 0$ for any of the types of travelling wave solutions. As we have shown in Chapter 4, in the singular perturbation problem, there is always an equilibrium state has $u = 0$ connected by a travelling wave. Thus, in one of the outer regions (in the singular perturbation problem we have two outer regions split by inner region) where $u = 0$, it can be easily perturbed when we disturb u . This is because a small perturbation in u where $u = 0$ leads to an exponentially growth of solutions but this can not be considered as an instability case. Also, when $u = 0$

$$M_1 = 1 - \gamma_1 w,$$

and when $\gamma_1 < 1$, we should get $M_1 > 0$. The numerical computations show $M_1 > 0$ when $u = 0$, and this can be seen in Figure 5.15 for type (I_a) , and Figure 5.16 for type (III_r) . We will avoid this case and will focus on the case where $u \neq 0$ and investigate whether $M_1 > 0$ for any values of the parameters. The numerical calculations show no evidence of $M_1 > 0$ in the range of parameters we have calculated, which agrees with the numerical solutions in the two dimensional problem in the previous sections. The following figures show that $M_1 < 0$ always in the region $u \neq 0$, in Figure 5.17, with values of α_1 and this is type (I_a) . Figure 5.18 is for type (III_r) and similar thing happen in type (III_l) . In type (I_b) , we have a similar case as shown in Figure 5.19.

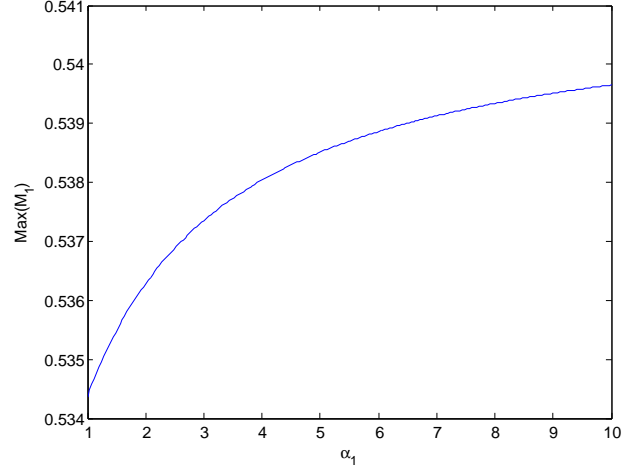


Figure 5.15: The maximum values of M_1 for type I_a when $u = 0$, specific values of parameters, $\alpha_2 = 4, \gamma_1 = 0.5, \gamma_2 = 0.5$ and $D = 5$.

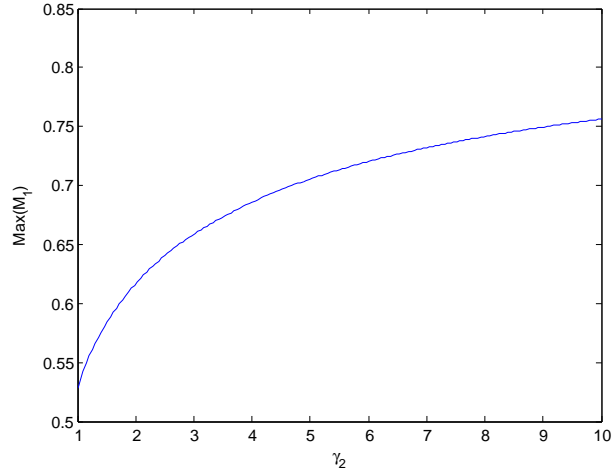


Figure 5.16: The maximum values of M_1 for type III_r when $u = 0$, values of parameters, $\alpha_2 = 1, \gamma_1 = 0.6, \gamma_2 = 1.3$ and $D = 1.2$.

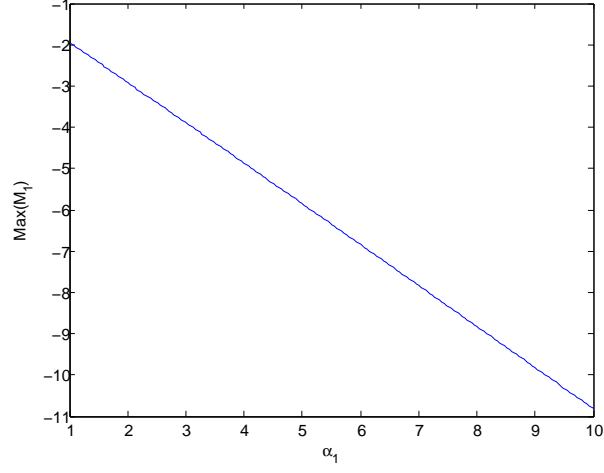


Figure 5.17: The values of M_1 for type I_a when $u \neq 0$, specific values of parameters, $\alpha_2 = 4, \gamma_1 = 0.5, \gamma_2 = 0.5$ and $D = 5$.

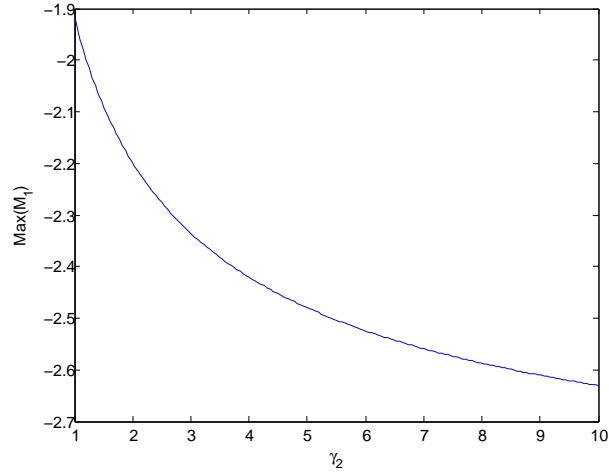


Figure 5.18: The maximum values of M_1 for type III_r when $u \neq 0$, value of parameters, $\alpha_1 = 1, \alpha_2 = 1, \gamma_1 = 0.6$ and $D = 1.2$.

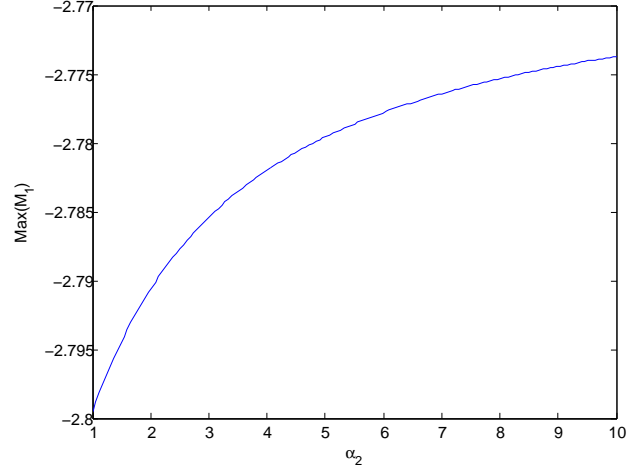


Figure 5.19: The maximum values of M_1 for type (I_b) , specific values of parameters,

$$\alpha_1 = 1, \gamma_1 = 0.5, \gamma_2 = 0.7 \text{ and } D = 1.$$

5.5.3 Calculating the Evans function for (5.5.11) and the travelling wave of type (I_a)

We discussed in Chapter 1 the role of the Evans function in finding the stability of travelling wave solutions. In this section, we compute the Evans function for (5.5.11) when the travelling wave solutions are of type (I_a) . First, we rewrite (5.5.11) as a first order system,

$$\frac{dq}{dz} = A(\sigma, \bar{k}, Z)q, \quad (5.5.12)$$

where,

$$A = \begin{pmatrix} 0 & 1 \\ \frac{\sigma}{D} + \bar{k}^2 - \frac{(N_2 M_1 - N_1 M_2)}{M_1 D} & \frac{-c}{D} \end{pmatrix}.$$

The limit matrices $A_{\pm}(\sigma, \bar{k}^2)$ can be found from the boundary conditions,

$$U \rightarrow u_0, \quad W \rightarrow w_0, \quad \text{as} \quad Z \rightarrow -\infty$$

$$U \rightarrow 0, \quad W \rightarrow 1, \quad \text{as} \quad Z \rightarrow \infty.$$

The limit matrix $A_{-\infty}$ is,

$$A_{-\infty} = \begin{pmatrix} 0 & 1 \\ \frac{\sigma}{D} + \bar{k}^2 - f(-\infty) & \frac{-c}{D} \end{pmatrix},$$

where $f(-\infty)$ depends on the values of u_0 and w_0 , and the eigenvalues are,

$$\mu_1^- = -\frac{c}{2D} + \frac{\sqrt{\frac{c^2}{D^2} + \frac{4(\sigma + \bar{k}^2 D - f(-\infty))}{D}}}{2},$$

$$\mu_2^- = -\frac{c}{2D} - \frac{\sqrt{\frac{c^2}{D^2} + \frac{4(\sigma + \bar{k}^2 D - f(-\infty))}{D}}}{2},$$

and the eigenvectors are,

$$v_{1,2}^- = \begin{pmatrix} 1 \\ \mu_{1,2}^- \end{pmatrix}.$$

The limit matrix A_{∞} is

$$A_{\infty} = \begin{pmatrix} 0 & 1 \\ \frac{\sigma}{D} + \bar{k}^2 - \frac{(1-\gamma_2)}{D} & \frac{-c}{D} \end{pmatrix},$$

the eigenvalues are

$$\mu_1^+ = -\frac{c}{2D} + \frac{\sqrt{\frac{c^2}{D^2} + \frac{4(\sigma + \bar{k}^2 D - (1-\gamma_2))}{D}}}{2},$$

$$\mu_2^+ = -\frac{c}{2D} - \frac{\sqrt{\frac{c^2}{D^2} + \frac{4(\sigma + \bar{k}^2 D - (1-\gamma_2))}{D}}}{2},$$

and the eigenvectors are

$$v_{1,2}^+ = \begin{pmatrix} 1 \\ \mu_{1,2}^+ \end{pmatrix}.$$

We integrate the system,

$$\frac{dq}{dZ} = [A(\sigma, \bar{k}, Z) - \mu_1^- I]q, \quad (5.5.13)$$

forward from $Z \rightarrow -\infty$ to $Z \rightarrow 0$, and we integrate the system,

$$\frac{dq}{dz} = [A(\sigma, \bar{k}, Z) - \mu_2^+ I]q, \quad (5.5.14)$$

backward from $Z \rightarrow \infty$ to $Z \rightarrow 0$. Our numerical results show there are no zeros for $E(\sigma + \bar{k}^2)$ in the region $\sigma + k^2 > 0$ which means there is no indication of instability of travelling waves in the outer region for type (I_a) . We found in Figure (5.20), that $E(\sigma + \bar{k}^2)$ has a zero for $\sigma + k^2 > 0$, specifically for the parameter values $\alpha_1 = 1, \alpha_2 = 10, \gamma_1 = 0.5, \gamma_2 = 0.9, D = 3$, but this occurs in the outer region where $u = 0$, which we have excluded as we explained in section (6.2.2). Figure 5.21, shows the Evans function for $0 < \alpha_1 < 10$.

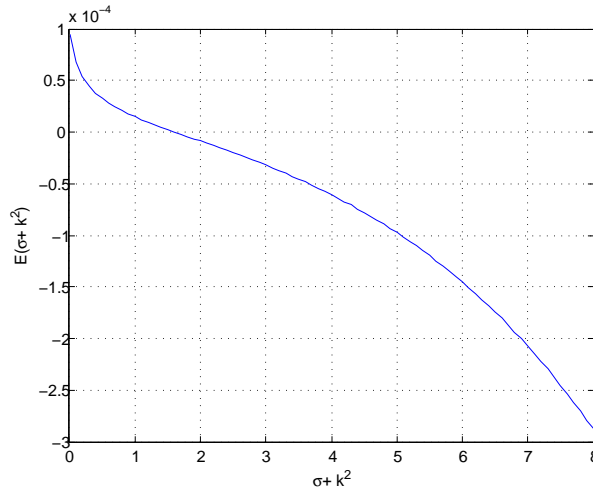


Figure 5.20: Evans function values for type (I_a) , specific values of parameters, $\alpha_2 = 1, \gamma_1 = 0.5, \gamma_2 = 0.9$ and $D = 3$.

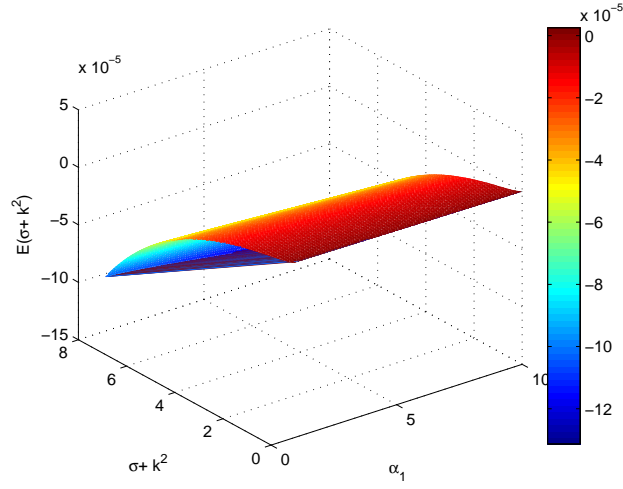


Figure 5.21: Evans function values for type (I_a) , specific values of parameters, $\alpha_2 = 1$, $\gamma_1 = 0.5$, $\gamma_2 = 0.9$ and $D = 3$.

5.5.4 Computing the Evans function for (5.5.11) with type (III_r)

In this case, the boundary conditions are,

$$U \rightarrow 1, \quad W \rightarrow 0, \quad \text{as} \quad Z \rightarrow -\infty$$

$$U \rightarrow 0, \quad W \rightarrow 1, \quad \text{as} \quad Z \rightarrow \infty,$$

and the limit matrix $A_{+\infty}$ is similar to the one in the previous section, whilst,

$$A_{-\infty} = \begin{pmatrix} 0 & 1 \\ \frac{\sigma}{D} + \bar{k}^2 - \frac{(2+\alpha_2)}{D} & -\frac{c}{D} \end{pmatrix}.$$

The eigenvalues of $A_{-\infty}$ are

$$\mu_1^- = -\frac{c}{2D} + \frac{\sqrt{\frac{c^2}{D^2} + \frac{4(2+\alpha_2)}{D}}}{2},$$

$$\mu_2^- = -\frac{c}{2D} - \frac{\sqrt{\frac{c^2}{D^2} + \frac{4(2+\alpha_2)}{D}}}{2},$$

and the eigenvectors are

$$v_{1,2}^- = \begin{pmatrix} 1 \\ \mu_{1,2}^- \end{pmatrix}.$$

In the same way as in the previous section we integrate (5.5.14) and we compute the Evans function for different values of parameters. Figure (5.22) shows no zero for $E(\sigma + \bar{k}^2)$ for $\sigma + \bar{k}^2 > 0$.

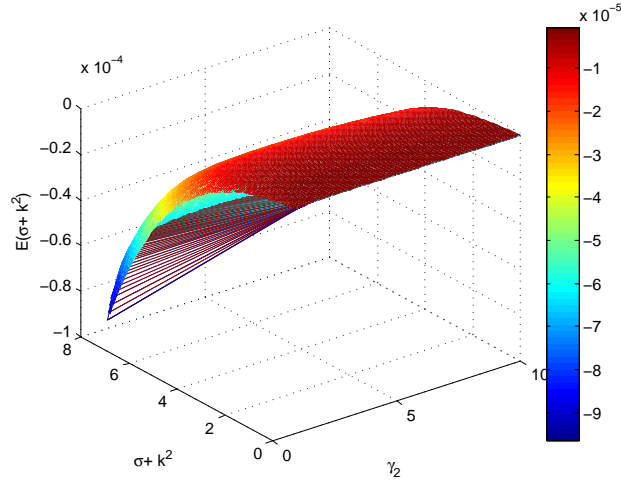


Figure 5.22: Evans function values for type III_r , specific values of parameters, $\alpha_1 = 0.7, \alpha_2 = 0.6, \gamma_1 = 0.9$ and $D = 2.5$.

5.5.5 Computing the Evans function for (5.5.11) for type (I_b)

In this case, the boundary conditions are,

$$U \rightarrow u_0, \quad W \rightarrow w_0, \quad \text{as} \quad Z \rightarrow -\infty$$

$$U \rightarrow 1, \quad W \rightarrow 0, \quad \text{as} \quad Z \rightarrow \infty,$$

and the limit matrices are

$$A_{-\infty} = \begin{pmatrix} 0 & 1 \\ \frac{\sigma}{D} + \bar{k}^2 - g(-\infty) & -\frac{c}{D} \end{pmatrix},$$

where $g(-\infty)$ depends on the values of u_0 and w_0 , the eigenvalues are

$$\begin{aligned} \mu_1^- &= -\frac{c}{2D} + \frac{\sqrt{\frac{c^2}{D^2} + \frac{4(\sigma + \bar{k}^2 D - g(-\infty))}{D}}}{2}, \\ \mu_2^- &= -\frac{c}{2D} - \frac{\sqrt{\frac{c^2}{D^2} + \frac{4(\sigma + \bar{k}^2 D - g(-\infty))}{D}}}{2}. \end{aligned}$$

The limit matrix A_∞ is,

$$A_\infty = \begin{pmatrix} 0 & 1 \\ \frac{\sigma}{D} + \bar{k}^2 - \frac{(1-\gamma_2)}{D} & -\frac{c}{D} \end{pmatrix},$$

and the eigenvalues are

$$\begin{aligned} \mu_1^+ &= -\frac{c}{2D} + \frac{\sqrt{\frac{c^2}{D^2} + \frac{4(\sigma + \bar{k}^2 D - (1-\gamma_2))}{D}}}{2}, \\ \mu_2^+ &= -\frac{c}{2D} - \frac{\sqrt{\frac{c^2}{D^2} + \frac{4(\sigma + \bar{k}^2 D - (1-\gamma_2))}{D}}}{2}. \end{aligned}$$

The Evans function has been computed for type (I_b) for the whole profile. However, numerical results for this cases show again no evidence of unstable travelling wave solutions. Figure 5.23, shows no zeroes for $E(\sigma + \bar{k}^2)$ at $\sigma + \bar{k}^2 > 0$ in type (I_b) .

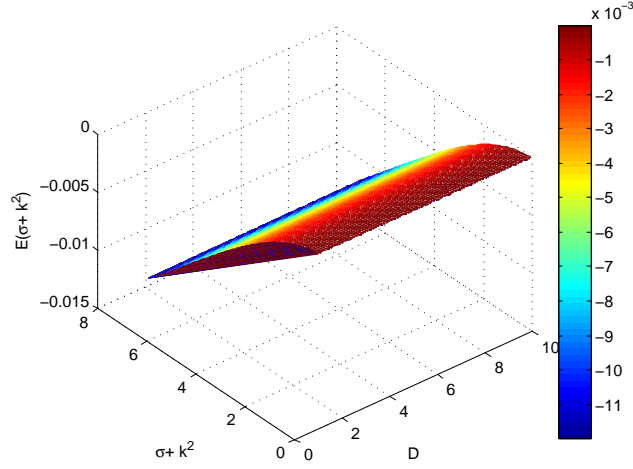


Figure 5.23: Evans function values for type (I_b), specific values of parameters, $\alpha_1 = 4$, $\alpha_2 = 1$, $\gamma_1 = 0.5$ and $\gamma_2 = 0.5$.

In conclusion, computing the Evans function for all types of travelling waves in the outer regions for the singular perturbation problem and for the parameter ranges we considered, consistent with all numerical solutions of the full system, suggests that all the types of travelling waves are stable.

5.6 Calculating the Evans function for inner problem

In this subsection we compute the Evans function for the inner problem where the wave-front lies, and find if there is instability in travelling waves. The equation in the inner region as shown in Chapter 4 but in two dimensions is

$$\frac{\partial U}{\partial t} = \frac{\partial^2 U}{\partial Z^2} + \frac{\partial^2 U}{\partial y^2} + U(L + \alpha_1 U - (1 + \alpha_1)U^2). \quad (5.6.1)$$

By linearising (5.6.1) around the wave front and substituting the Fourier transform formula, we get the one dimensional linear problem

$$\frac{\partial \psi}{\partial t} = \frac{\partial^2 \psi}{\partial Z^2} + c \frac{\partial \psi}{\partial Z} - k^2 \psi + (L + 2\alpha_1 u - 3(1 + \alpha_1)u^2)\psi, \quad (5.6.2)$$

where ψ is the perturbation term and u is the travelling wave solution. Now substitute,

$$\psi(Z, t) = \exp(\sigma t)q(Z),$$

into (5.6.2) and rewrite it in the first order form,

$$\frac{dq}{dz} = B(\sigma, k, Z)q, \quad (5.6.3)$$

where,

$$B = \begin{pmatrix} 0 & 1 \\ \sigma + k^2 - (L + 2\alpha_1 u - 3(1 + \alpha_1)u^2) & -c \end{pmatrix}.$$

We study the travelling waves of type (I_a) and (III_r) . The boundary conditions for type (I_a) are,

$$u \rightarrow \frac{\alpha_1 + \sqrt{\alpha_1^2 + 4(1 + \alpha_1)L}}{2(1 + \alpha_1)}, \quad \text{as } Z \rightarrow -\infty$$

$$u \rightarrow 0, \quad \text{as } Z \rightarrow \infty.$$

The limit matrices are

$$B_{-\infty} = \begin{pmatrix} 0 & 1 \\ \sigma + k^2 - M & -c \end{pmatrix},$$

where,

$$M = 2L + \frac{\alpha_1^2}{2(1 + \alpha_1)} + \frac{\alpha_1 \sqrt{\alpha_1^2 + 4(1 + \alpha_1)L}}{2(1 + \alpha_1)},$$

the eigenvalues are

$$\mu_1^- = -\frac{c}{2} + \frac{\sqrt{c^2 + 4(\sigma + k^2 + M)}}{2},$$

$$\mu_2^- = -\frac{c}{2} - \frac{\sqrt{c^2 + 4(\sigma + k^2 + M)}}{2},$$

and the eigenvectors are

$$v_{1,2}^- = \begin{pmatrix} 1 \\ \mu_{1,2}^+ \end{pmatrix}.$$

The limit matrix B_∞ is

$$B_\infty = \begin{pmatrix} 0 & 1 \\ \sigma + k^2 - L & -c \end{pmatrix},$$

the eigenvalues are

$$\begin{aligned} \mu_1^+ &= -\frac{c}{2} + \frac{\sqrt{c^2 + 4(\sigma + k^2 - L)}}{2}, \\ \mu_2^+ &= -\frac{c}{2} - \frac{\sqrt{c^2 + 4(\sigma + k^2 - L)}}{2}, \end{aligned}$$

and the eigenvectors are

$$v_{1,2}^- = \begin{pmatrix} 1 \\ \mu_{1,2}^+ \end{pmatrix}.$$

The computation of the Evans function show that the wavefront in the inner region is stable and agrees with the result of the numerical solution of the two dimensions problem. Figure 5.24 is an example of the stability of wavefront in type (I_a) . The stability of the wavefront in type (III_r) was not different from that of type (I_a) and the computation are showing that the inner problem (5.6.1) has stable travelling waves . Figure 5.25 is an example on type (III_r) .

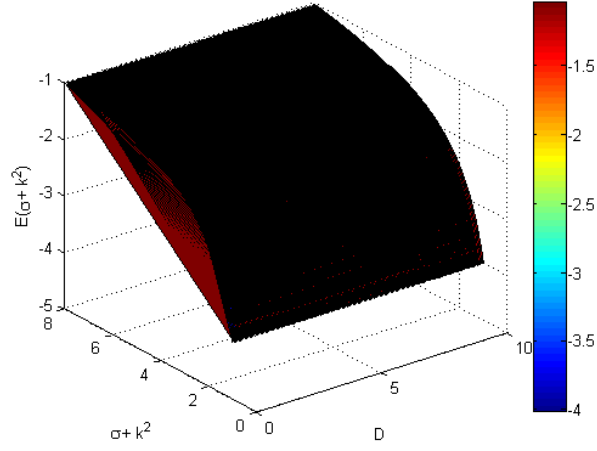


Figure 5.24: Evans function values for type (I_a) , specific values of parameters, $\alpha_1 = 1, \alpha_2 = 4, \gamma_1 = 0.5$ and $D = 3$.

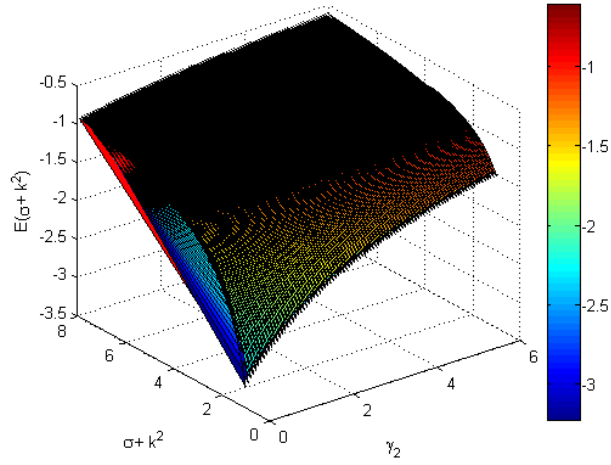


Figure 5.25: Evans function values for type (III_r) , specific values of parameters, $\alpha_1 = 1, \alpha_2 = 1, \gamma_1 = 0.6$ and $D = 1.2$.

Conclusions and future work

6.1 Conclusions

In this thesis, we have studied (1.5.3) a reaction-diffusion system for inter-species competition and intra-species cooperation. The system consist of two non linear reaction-diffusion equations, and can be considered as a natural extension of the Lotka-Volterra competition diffusion system. The Lotka-Volterra system in (1.3.1) has four topologically different regions, RL_1 , RL_2 , RL_3 and RL_4 which are shown in Chapter 1 (see Figure 1.4). In Chapter 2, we studied the spatial uniform solution for (1.5.3), and showed that our system is richer than the Lotka-Volterra diffusion competition system in terms of the equilibrium solutions. There are always two single species equilibrium solutions and an extinction equilibrium solution. The extra equilibrium solutions are either one or three in maximum, which are the coexistence equilibrium solutions. When there is just one coexistence state, we get the same cases as in the Lotka-Volterra system. The key fact about the coexistence equilibrium solutions in (1.5.3) is that only one state is stable. The two systems have four common topologically different regions namely R_1 , R_3 , R_6 and R_7 (see Figure 2.3). In two of the four regions, there are two stable single species equilibrium

solution and no coexistence equilibrium solution. The other two regions have either one stable coexistence equilibrium and two unstable single species equilibrium solution, or an unstable coexistence equilibrium state and two stable single species equilibrium solution. What makes (1.5.3) an extension to the Lotka-Volterra system is, besides the similar four topologically different regions in both systems, the three extra regions that contain either two or three coexistence equilibrium solutions. Some of these regions are separated by the transcritical bifurcation boundaries $\gamma_{1,2} = 1$, which are the same in both systems. The rest of the regions are separated by a saddle-node bifurcation boundary. We have examined (1.5.3) as a competition system only, by making the cooperative coefficients $\alpha_{1,2} = 0$, and we tried to find whether that will affect the existence of the seven regions. We have found that it does not change the number of topologically different regions, but it affects the size of R_2 , R_4 and R_5 .

We have also considered the case of fast diffusion and slow reaction in one of the species, by considering the dynamics when $\lambda \ll 1$ in (1.5.3). We have examined the types of travelling wave solutions that connect any two of the equilibrium solutions in the regions $R_1 - R_7$, when the equilibrium state behind the wavefront is stable. We have classified the possible travelling waves into three types, type (I), (II) and (III). In type (I_a), the travelling wave connects a coexistence equilibrium state say (\hat{u}, \hat{w}) to $(1, 0)$. In type (I_b), the equilibrium points are (\hat{u}, \hat{w}) and $(0, 1)$. The two equilibrium points in type (II_a) are $(1, 0)$ and $(0, 0)$, whilst, they are $(0, 1)$ and $(0, 0)$ in type (II_b). Type (III) connects $(1, 0)$ to $(0, 1)$, and we denote it by (III_r) when the travelling wave moves to the right and (III_l) when it moves to the left. This shows that (1.5.3) is rich in the number of types of travelling waves when compared to the Lotka-Volterra system. Although, a travelling wave connects (\hat{u}, \hat{w}) to $(0, 0)$ is possible in principle, we were not able to find a travelling wave

of this type in the limit of $\lambda \ll 1$. We found that when there is a symmetry in (1.5.3), the above type of travelling waves can exist but then we need $\lambda = 1$ which is out of the range of what we assumed it to be so far.

In Chapter 3, for the initial value problem (1.5.3), we computed the travelling wave solutions of the three types using numerical methods. We used a semi-implicit method (an implicit method for diffusion and an explicit method for reaction) to discretise (1.5.3), with three types of initial conditions. The initial conditions are of types, *A* (u is a step function and $w = 1$), type *B* ($u = 1$ and w is a step function), type *C* (u and w are step functions), which are ecologically interesting cases. We showed that travelling waves of type (*I*) exist in regions R_1, R_2, R_4 and R_5 , whilst, types (*II*) and (*III*) can be found in regions R_3, R_6 and R_7 .

For initial conditions *C*, we found that two or three travelling waves developed with different wave speeds, one of these waves is always of type (*II*). The diffusion coefficient D has a significant role in determining the types of the travelling wave solutions. Also, with initial conditions *C* (with small initial value of w), we studied the dynamics of the process shown in Figure 3.33. Initially, w becomes small and u propagates into the domain as a travelling wave. However, after a long induction period, w begins to grow at the wavefront. The spike in w expands and finally forms a new wavefront that allows w to propagate into $x > 0$, followed by a slower wavefront. The asymptotic solution is found for this typical case with the help of Laplace transforms. Although, the resulting equation is complicated, the presence of the term e^{st} , in the integrand means that the solution will decay exponentially if the ranges of integration do not extend into $s > 0$, which will occur if $1 - c^2/4D < 0$, and hence $c > 2\sqrt{D}$. Since $2\sqrt{D}$ is the linearized wave speed of the wavefront in w , this suggests that if the wavefront in u moves faster than that in w , w

will decay to zero, otherwise, w will grow and (once nonlinear terms become important) will form a wavefront.

We used asymptotic methods in Chapter 4 to find the travelling wave solutions for the three types of travelling waves in the limit of $(\lambda \ll 1)$. We solved a regular perturbation problem in the case of type (I_b) , The phase plane analysis and the existence of trajectories for the cases, saddle-node connection and saddle-saddle connection were studied. We found a good agreement between the wave speed for both numerical and asymptotic solutions. For type (I_a) , (II) and (III) , we had a singular perturbation problem to solve, with one inner solution of $O(1)$ and two outer solutions of $O(\frac{1}{\lambda})$. The equation of the inner region is,

$$\frac{d^2\hat{u}}{dz^2} + c\frac{d\hat{u}}{dz} + \hat{u}(L + \alpha_1\hat{u} - (1 + \alpha_1)\hat{u}^2) = 0, \quad (6.1.1)$$

where $L = 1 - \gamma_1\hat{w}_0$. In [HR75], the travelling wave solution for (6.1.1) is studied and the minimum wave speed is found. We studied the outer and inner solutions of types, (I_a) , (II) and (III) and we matched the wave speed for both solutions, and then compared it to the numerical solutions. Good agreement between the wave speeds in both methods for small λ is shown.

In [Bil04], it was shown for a similar system that, if the local wavespeed, determined by an asymptotic analysis, is smaller than a lower bound on the wavespeed determined by the solution far ahead of the wavefront, then several different types of unsteady behaviour can emerge on an $O(\lambda^{-1})$ timescale in the initial value problem. In our system, far ahead of the wavefront, when $u \ll 1$ and $w \sim w_\infty$, (??) becomes

$$\frac{\partial u}{\partial t} \sim \frac{\partial^2 u}{\partial x^2} + u(1 - \gamma_1 w_\infty),$$

which shows that the wavespeed must be greater than $2\sqrt{1 - \gamma_1 w_\infty}$. If w_∞ is greater than the value of w at the wavefront, this lower bound is less restrictive than that which exists at the wavefront. It is only if w decreases ahead of the wavefront, which is the case for the system studied in [Bil04], that the local wavespeed can be below the global lower bound. Although, as we discussed above, there is no obvious *a priori* reason why a travelling wave that connects (u_0, w_0) to $(0, 0)$ cannot exist, we have been unable to find one, either numerically or asymptotically. This type of wave is the only candidate to display unsteady behaviour. We conclude that unsteady behaviour is unlikely to exist in our system. Finally, we have shown that a similar reaction-diffusion system to 1.5.3 can be derived for $\lambda \gg 1$ and has a same results as we discussed above.

The second part of our thesis is about the stability of travelling wave solutions in two dimensions. We used the same system as in one dimension and we extend it to two dimensions. We solved the initial value problem numerically in two dimensions for the three types of travelling wave solutions and initial conditions. We scaled the domain with different grid sizes (for example, type I_a has inner region with scale $O(1)$, whilst the outer regions are of $O(\frac{1}{\lambda})$). We used a non uniform grid size in the x-direction and a uniform grid in the y-direction. We are interested in travelling waves that move to the right in the x-direction. Our aim is to make a small perturbation in the wavefront and find whether the travelling waves are stable or not.

One system shown to have an unstable wavefront is the Gray-Scott system (see for example [HPSS93] and [ZF94]). We have shown similar results as in [HPSS93] for specific value of parameters using numerical methods. We examined the three type of travelling waves for the stability of travelling waves. We did not find any evidence of unstable wavefront for the parameter values we tested in the limit of $\lambda \ll 1$. We performed

an asymptotic analysis for the stability of the travelling wave in two dimensions. We have linearised (5.1.1) around the wavefront solutions with the decomposition Fourier formula. We obtained a one dimension system of linear partial differential equations (5.4.3). The method of multiple scales is used to make an analysis of (5.4.3) when $\lambda \ll 1$. The Evans function is used to study the stability of travelling wave solutions. We found a stable solution for all the parameter values we examined, which agrees with the result we obtained from numerical methods. The Evans function method was more efficient than the numerical method we used, and we tested a large range of parameter values for instability.

Although, we did not check all the parameter values which are possible with the numerical and asymptotic analysis, all the evidence shows that our system has stable travelling waves. We can conclude that it is hard to study the stability of travelling waves for the non-linear competition reaction-diffusion system with many parameters. If we compare our system to the Gray-Scott system, we find that there are only two parameters in the Gray-Scott system, whilst there are six parameters in our system. Finally, we can conclude that the single species state $(1, 0)$ excludes $(0, 1)$ and wins in R_3 , whilst $(0, 1)$ wins in R_7 . The winner in R_6 depends on the initial conditions. Coexistence happens in R_1 , R_2 , R_4 and R_5 . There is always an invasion of one of the species, and sometimes two invasions especially with initial conditions type C.

6.2 Future work

In the future, we aim to study similar system of reaction-diffusion equations in any of the three cases, fast reaction and slow diffusion, fast reaction and diffusion, and slow reaction

and diffusion. We want to find the numerical and asymptotic solutions for the travelling waves in any of the three cases. We will study the existence of unsteady travelling waves in systems similar to that in [Bil04]. For the two dimensional reaction-diffusion equations, we will study the stability of travelling wave solutions and find unstable wavefronts. A similar system to Gray-Scott which produces unstable wavefront is most likely to be studied in the future, since it does not contains many parameters which make the search of stability of travelling waves more complicated. In 1952, A. Turing studied pattern formation in reaction-diffusion equations for ecological and chemical models [Tur52]. He showed that in the chemical problems, a stable uniform state in a kinetic system can become unstable when you add diffusion. This phenomena is called pattern formation or Turing instability. We will study the pattern formation for reaction-diffusion equation in (1.5.3) in a finite domain, and find the condition of diffusion driven instability.

Appendix

Sylvester's Method of Elimination

An eliminant, sometimes called a resultant, is the result obtained by eliminating a variable x from two equations in the form,

$$p(x) = a_mx^m + a_{m-1}x^{m-1} + \dots + a_1x + a_0, \quad (6.2.1)$$

$$q(x) = b_nx^n + b_{n-1}x^{n-1} + \dots + b_1x + b_0. \quad (6.2.2)$$

Sylvester algorithm (see for example [[Afo95](#)]) is useful to compute the eliminant of the two equations (6.2.1) and (6.2.2). The resultant is a determinant has the form,

$$\begin{vmatrix} a_m & a_{m-1} & a_{m-2} & \dots & a_0 & 0 & \dots & 0 \\ 0 & a_m & a_{m-1} & a_{m-2} & \dots & a_0 & \ddots & 0 \\ 0 & \ddots & \ddots & \ddots & \ddots & \dots & \ddots & \\ 0 & \dots & 0 & a_m & a_{m-1} & a_{m-2} & \dots & a_0 \\ b_n & b_{n-1} & b_{n-2} & \dots & b_0 & 0 & \dots & 0 \\ 0 & b_n & b_{n-1} & b_{n-2} & \dots & b_0 & \ddots & 0 \\ 0 & \ddots & \ddots & \ddots & \ddots & \dots & \ddots & \\ 0 & \dots & 0 & b_n & b_{n-1} & b_{n-2} & \dots & b_0 \end{vmatrix} = 0. \quad (6.2.3)$$

The entries of the determinant are distributed as follows: first row is the coefficients of p , padded with zeros at the end. Then in the following rows we construct subsequent rows shifting one column to the right each time, and we stop when no zeros are left at the end. We apply the same procedure to q . The resultant can be useful to solve a system of equations by eliminating a variable from the equations and solve it for the other variable.

In Chapter 2 we solve the system of equations

$$a_3u^3 + a_2u^2 + a_1u + a_0 = 0, \quad (6.2.4)$$

$$b_3u^3 + b_2u^2 + b_1u + b_0 = 0,$$

where

$$\begin{aligned} a_3 &= \frac{-2}{(1 + \alpha_2)}(4\alpha_1 + \alpha_2 + \alpha_2^2 + 4\alpha_2\alpha_1 + \alpha_2\alpha_1^2 + 1), \\ a_2 &= \frac{3}{(1 + \alpha_2)}(\alpha_1 + \alpha_1^2 + \alpha_2\alpha_1 + \alpha_2\alpha_1^2), \\ a_1 &= \frac{-1}{(1 + \alpha_2)}(-2\alpha_1 - 2\alpha_2 + \alpha_1^2 - 2 + \gamma_1\alpha_2\alpha_1 - 2\alpha_2\alpha_1 + \alpha_2\alpha_1^2 + \gamma_1\alpha_2), \\ a_0 &= \frac{-1}{2(1 + \alpha_2)}(\gamma_2\gamma_1^2 + 2\alpha_2\alpha_1 + 2\alpha_1 - \gamma_1\alpha_2\alpha_1), \\ b_3 &= (4\gamma_2 + 8\gamma_2\alpha_2\alpha_1 + 4\gamma_2\alpha_2\alpha_1^2 + 4\gamma_2\alpha_1^2 + 4\gamma_2\alpha_2 + 8\gamma_2\alpha_1), \\ b_2 &= (-8\alpha_1 - 4\alpha_1^2 - 4\alpha_2 - \alpha_2^2 - 4\gamma_2\alpha_2\alpha_1 - 4\gamma_2\alpha_2\alpha_1^2 - 8\alpha_2\alpha_1 - \\ &\quad 4\alpha_2\alpha_1^2 - 4\gamma_2\alpha_1 - 4\gamma_2\alpha_1^2 - 2\alpha_2^2\alpha_1 - 2\alpha_2^2\alpha_1^2 - 4), \\ b_1 &= (4\alpha_1 + 4\alpha_1^2 + \gamma_2\alpha_2\alpha_1^2 + 4\alpha_2 - \alpha_1 + 4\alpha_2 - \alpha_1^2 + \gamma_2\alpha_1^2 + \alpha_2^2\alpha_1 + \alpha_2^2 + \alpha_1^2), \\ b_0 &= (-\alpha_1^2 + \frac{\gamma_2^2\gamma_1^2}{4} - \alpha_2\alpha_1^2 - \frac{-\alpha_2^2\alpha_1^2}{4}). \end{aligned}$$

We solve (6.2.4) using the Sylvester matrix, and note that a solution of (6.2.4) exists when its determinant is equal to zero, so that

$$\begin{vmatrix} a_3 & a_2 & a_1 & a_0 & 0 & 0 \\ 0 & a_3 & a_2 & a_1 & a_0 & 0 \\ 0 & 0 & a_3 & a_2 & a_1 & a_0 \\ b_3 & b_2 & b_1 & b_0 & 0 & 0 \\ 0 & b_3 & b_2 & b_1 & b_0 & 0 \\ 0 & 0 & b_3 & b_2 & b_1 & b_0 \end{vmatrix} = 0, \quad (6.2.5)$$

which gives,

$$\begin{aligned} & \frac{1}{8} \frac{1}{1+\alpha_2} \gamma_2^2 \gamma_1^2 (256 + 6144\alpha_2\alpha_1 + 7296\alpha_1^2 + 21888\alpha_2\alpha_1^2 + 25536\alpha_2^2\alpha_1^2 + \\ & 288\gamma_2^2\gamma_1^2 - 256\gamma_1^2 - 1792\gamma_2\alpha_1^2 - 256\gamma_2\alpha_1 + 7168\alpha_2^2\alpha_1 - 256\gamma_1\alpha_2 + 15232\alpha_1^3 \\ & + 512\alpha_2^3 + 45696\alpha_2\alpha_1^3 + 53312\alpha_2^2\alpha_1^3 - 5504\gamma_2\alpha_1^3 + 4096\alpha_2^3\alpha_1 + 14592\alpha_2^3\alpha_1^2 + \\ & 30464\alpha_2^3\alpha_1^3 - 7232\gamma_1\alpha_2\alpha_1^2 + 384\gamma_2\gamma_1^2\alpha_1 - 16512\gamma_2\alpha_2\alpha_1^3 - 5824\gamma_2\alpha_2^2\alpha_1^2 - \\ & 17888\gamma_2\alpha_2^2\alpha_1^3 + 576\gamma_2^2\gamma_1^2\alpha_2 + 2016\gamma_2^2\gamma_1^2\alpha_1 - 832\gamma_2\alpha_2^2\alpha_1 - 5376\gamma_2\alpha_2\alpha_1^2 - \\ & 768\gamma_2\alpha_2\alpha_1 - 2048\gamma_1\alpha_2\alpha_1 + 768\alpha_2 + 2048\alpha_1 + 16560\alpha_1^4\gamma_2^2\alpha_2\gamma_1^2 + 19840\alpha_1^5\gamma_2\alpha_2^2\gamma_1 + \\ & 9920\alpha_1^5\gamma_2\gamma_1\alpha_2 - 1008\gamma_1^3\alpha_2^2\alpha_1\gamma_2^2 + 1176\gamma_2^2\gamma_1^2\alpha_2^2\alpha_1 + 3150\alpha_2^2\alpha_1^4\gamma_2^2\gamma_1^2 + \\ & 12400\alpha_2^3\alpha_1^5\gamma_2\gamma_1 + 768\alpha_2\alpha_1\gamma_2\gamma_1^2 + 10752\alpha_2^2\alpha_1^3\gamma_2\gamma_1^2 + 16128\alpha_2\alpha_1^3\gamma_2\gamma_1^2 \\ & + 2688\alpha_2^3\alpha_1^3\gamma_2\gamma_1^2 + 18720\gamma_2^2\alpha_1^3\alpha_2\gamma_1^2 + 18688\gamma_2\alpha_1^4\alpha_2^2\gamma_1 - 5040\gamma_2^2\alpha_1^3\gamma_1^3\alpha_2 \\ & + 9344\gamma_2\alpha_1^4\gamma_1\alpha_2 + 17920\gamma_2\alpha_1^4\gamma_1^2\alpha_2^2 + 5376\alpha_2\alpha_1^2\gamma_2\gamma_1^2 + 128\alpha_2^3\alpha_1\gamma_2\gamma_1^2 \\ & + 512\alpha_2^2\gamma_2\gamma_1^2\alpha_1 + 3584\alpha_2^2\alpha_1^2\gamma_2\gamma_1^2 + 4788\gamma_2^2\alpha_2^2\alpha_1^3\gamma_1^2 + 11680\gamma_2\alpha_2^3\alpha_1^4\gamma_1 \\ & - 5040\gamma_2^2\alpha_2^2\alpha_1^3\gamma_1^3 + 4480\gamma_2\alpha_2^3\alpha_1^4\gamma_1^2 + 3346\gamma_2^2\alpha_2^2\alpha_1^2\gamma_1^2 + 6800\gamma_2\alpha_2^3 \\ & \alpha_1^3\gamma_1 + 11856\gamma_2^2\alpha_2\alpha_1^2\gamma_1^2 - 3024\gamma_2^2\alpha_2^2\alpha_1^2\gamma_1^3 + 10880\gamma_2\alpha_2^2\alpha_1^3\gamma_1 \\ & - 3024\gamma_2^2\alpha_1^2\gamma_1^3\alpha_2 + 5440\gamma_2\alpha_1^3\gamma_1\alpha_2 + 896\alpha_2^3\alpha_1^2\gamma_2\gamma_1^2 - 1008\gamma_1^3\alpha_2\alpha_1\gamma_2^2 \end{aligned}$$

$$\begin{aligned}
& + 26880\alpha_1^4\alpha_2\gamma_2\gamma_1^2 + 4032\gamma_2^2\gamma_1^2\alpha_2\alpha_1 + 256\alpha_2\gamma_2\gamma_1\alpha_1 - 256\gamma_2^2 + 896\alpha_2^2 - 3872 \\
& \gamma_2^2\alpha_1^6 - 1184\gamma_2^2\alpha_1^7 - 1184\gamma_2\alpha_1^8 - 10896\gamma_2^2\alpha_1^4 - 27\gamma_2^4\gamma_1^4 - 8016\gamma_2^2\alpha_1^5 + 952 \\
& \alpha_2^5\alpha_1^3 + 87\alpha_2^5\alpha_1^8 - 8016\alpha_1^6\gamma_2 + 10112\alpha_1^7\alpha_2^3 + 17696\alpha_1^7\alpha_2^2 + 15168\alpha_1^7\alpha_2 + 2844\alpha_2^4 \\
& \alpha_1^7 - 3872\alpha_1^7\gamma_2 + 2784\alpha_1^8\alpha_2^3 + 4872\alpha_1^8\alpha_2^2 + 4176\alpha_1^8\alpha_2 + 783\alpha_1^8\alpha_2^4 + 1289\alpha_2^5\alpha_1^4 + \\
& 1182\alpha_2^5\alpha_1^5 + 743\alpha_2^5\alpha_1^6 + 316\alpha_2^5\alpha_1^7 + 41248\alpha_2^3\alpha_1^4 + 72184\alpha_2^2\alpha_1^4 + 61872\alpha_2\alpha_1^4 + \\
& 11601\alpha_2^4\alpha_1^4 - 9728\gamma_2\alpha_1^4 + 4104\alpha_2^4\alpha_1^2 + 8568\alpha_2^4\alpha_1^3 + 37824\alpha_2^3\alpha_1^5 + 66192\alpha_2^2\alpha_1^5 + \\
& 56736\alpha_2\alpha_1^5 - 10896\alpha_1^5\gamma_2 + 23776\alpha_1^6\alpha_2^3 + 41608\alpha_1^6\alpha_2^2 + 35664\alpha_1^6\alpha_2 + 10638\alpha_2^4\alpha_1^5 + \\
& 6687\alpha_2^4\alpha_1^6 - 128\alpha_1\alpha_2^4\gamma_1^2 - 384\gamma_2\alpha_2^3\alpha_1 + 320\gamma_2\alpha_2^3\alpha_1\gamma_1 - 1024\alpha_2^4\gamma_1\alpha_1 + 1152 \\
& \alpha_2^4\alpha_1 - 1024\gamma_1^2\alpha_2^3\alpha_1 - 28672\alpha_2^3\alpha_1^3\gamma_1^2 - 35840\alpha_1^4\alpha_2\gamma_1^2 - 14336\alpha_2\alpha_1^6\gamma_1^2 + 128 \\
& \alpha_2^5\alpha_1 - 128\alpha_2^5\alpha_1\gamma_1 - 452\alpha_2^5\alpha_1^2\gamma_1 + 456\alpha_2^5\alpha_1^2 - 28672\alpha_1^5\alpha_2\gamma_1^2 + 64\gamma_2\alpha_2^4 \\
& \gamma_1\alpha_1 - 64\gamma_2\alpha_2^4\alpha_1 - 448\gamma_2\alpha_2^4\alpha_1^2 + 448\gamma_2\alpha_2^4\alpha_1^2\gamma_1 + 8192\alpha_1^2\alpha_2^3\gamma_1\gamma_2^2 - \\
& 16512\alpha_1^2\alpha_2\gamma_2^2 - 29184\alpha_1^3\alpha_2^2\gamma_2^2 + 14208\alpha_1^3\alpha_2\gamma_1\gamma_2^2 - 5504\alpha_1^2\alpha_2^3\gamma_2^2 + 16384 \\
& \alpha_1^2\alpha_2^2\gamma_1\gamma_2^2 - 29184\alpha_1^3\alpha_2\gamma_2^2 - 16512\alpha_1^2\alpha_2^2\gamma_2^2 + 8192\alpha_1^2\alpha_2\gamma_1\gamma_2^2 + 14208 \\
& \alpha_1^3\alpha_2^3\gamma_1\gamma_2^2 - 9728\alpha_1^3\alpha_2^3\gamma_2^2 + 28416\alpha_1^3\alpha_2^2\gamma_1\gamma_2^2 + 2688\alpha_1\alpha_2\gamma_1\gamma_2^2 - \\
& 5376\alpha_1\alpha_2\gamma_2^2 + 2688\alpha_1\alpha_2^3\gamma_1\gamma_2^2 - 1792\alpha_1\alpha_2^3\gamma_2^2 + 5376\alpha_1\alpha_2^2\gamma_1\gamma_2^2 - 5376 \\
& \alpha_1\alpha_2^2\gamma_2^2 - 14336\alpha_2\alpha_1^2\gamma_1^2 - 4096\alpha_2\alpha_1\gamma_1^2 - 4096\alpha_1^7\alpha_2\gamma_1^2 - 512\alpha_1^8\alpha_2\gamma_1^2 \\
& - 3072\alpha_1^7\alpha_2^2\gamma_1^2 - 128\alpha_1^7\alpha_2^4\gamma_1^2 - 384\alpha_1^8\alpha_2^2\gamma_1^2 - 1024\alpha_1^7\alpha_2^3\gamma_1^2 - 16\alpha_1^8 \\
& \alpha_2^4\gamma_1^2 - 128\alpha_1^8\alpha_2^3\gamma_1^2 + 8\alpha_2^4\gamma_2\gamma_1^2\alpha_1 - 2048\alpha_1^7\gamma_1^2 - 256\alpha_1^8\gamma_1^2 + 384 \\
& \alpha_2^3\gamma_1\gamma_2^2 - 256\alpha_2^3\gamma_2^2 + 768\alpha_2^2\gamma_1\gamma_2^2 - 768\alpha_2^2\gamma_2^2 + 384\alpha_2\gamma_1\gamma_2^2 - 1792\alpha_1\gamma_2^2 \\
& - 768\alpha_2\gamma_2^2 - 5504\alpha_1^2\gamma_2^2 - 16\alpha_2^5\gamma_1 - 16\alpha_2^4\gamma_1^2 - 9728\alpha_1^3\gamma_2^2 + 16\alpha_2^5 - 7168\alpha_1 \\
& ^6\gamma_1^2 - 14336\alpha_1^5\gamma_1^2 + 144\alpha_2^4 - 128\alpha_2^4\gamma_1 - 128\gamma_1^2\alpha_2^3 - 14336\alpha_1^3\gamma_1^2 - 17920\alpha_1^4\gamma_1^2 \\
& - 384\gamma_1\alpha_2^3 - 512\gamma_1\alpha_2^2 - 2048\alpha_1\gamma_1^2 - 384\alpha_2^2\gamma_1^2 - 7168\alpha_1^2\gamma_1^2 - 512\alpha_2\gamma_1^2 + 512\gamma_2 \\
& \alpha_2^2\gamma_1\alpha_1 + 768\alpha_2\alpha_1^8\gamma_2\gamma_1^2 + 5376\alpha_1^7\alpha_2\gamma_2\gamma_1^2 - 328\gamma_2^3\alpha_1^7\alpha_2\gamma_1^2 + 336 \\
& \gamma_2^2\alpha_1^8\alpha_2^2\gamma_1 + 168\gamma_2^2\alpha_1^8\gamma_1\alpha_2 - 164\gamma_2^3\alpha_1^7\alpha_2^2\gamma_1^2 + 168\gamma_2^2\alpha_1^8\alpha_2^3
\end{aligned}$$

CHAPTER 6: CONCLUSIONS AND FUTURE WORK

$$\begin{aligned}
& \gamma_1 - 864\gamma_2^2\alpha_1^7\alpha_2\gamma_1^2 - 8\gamma_2^3\alpha_1^8\alpha_2\gamma_1^2 + 16\gamma_2^2\alpha_1^9\alpha_2^2\gamma_1 + 8\gamma_2^2\alpha_1^9 \\
& \gamma_1\alpha_2 - 4\gamma_2^3\alpha_1^8\alpha_2^2\gamma_1^2 + 8\gamma_2^2\alpha_1^9\alpha_2^3\gamma_1 + 72\gamma_2^3\alpha_1^7\gamma_1^3\alpha_2 - 182\gamma_2^2 \\
& \alpha_1^8\gamma_1^2\alpha_2^2 - 27\gamma_2^4\alpha_1^6\alpha_2\gamma_1^4 + 72\gamma_2^3\alpha_1^7\alpha_2^2\gamma_1^3 - 62\gamma_2^2\alpha_1^8\alpha_2^3\gamma_1^2 - 240\gamma_2^2\alpha_1^8\alpha_2\gamma_1^2 + 432\gamma_2^3\alpha_1^6\gamma_1^3\alpha_2 \\
& - 162\gamma_2^4\alpha_1^5\alpha_2\gamma_1^4 + 432\gamma_2^3\alpha_1^6\alpha_2^2\gamma_1^3 - 4\gamma_2^2\alpha_1^7\gamma_1^3\alpha_2^3 - 924\gamma_2^2\alpha_1^7\gamma_1 \\
& ^2\alpha_2^2 - 492\gamma_2^2\alpha_1^7\alpha_2^3\gamma_1^2 - 28\gamma_2^2\alpha_1^6\gamma_1^3\alpha_2^3 + 128\gamma_2\alpha_1^9\alpha_2^2\gamma_1 + 64\gamma_2 \\
& \alpha_1^9\gamma_1\alpha_2 + 80\gamma_2\alpha_1^9\alpha_2^3\gamma_1 + 16\gamma_2\alpha_1^9\gamma_1\alpha_2^4 + 128\gamma_2\alpha_1^8\gamma_1^2\alpha_2^3 + 512\gamma_2 \\
& \alpha_1^8\gamma_1^2\alpha_2^2 + 8\gamma_2\alpha_1^8\gamma_1^2\alpha_2^4 + 56\gamma_2\alpha_1^7\gamma_1^2\alpha_2^4 + 896\gamma_2\alpha_1^7\gamma_1^2\alpha_2^3 + \\
& 3584\gamma_2\alpha_1^7\gamma_1^2\alpha_2^2 + 1280\gamma_2\alpha_1^8\alpha_2^2\gamma_1 + 640\gamma_2\alpha_1^8\gamma_1\alpha_2 + 800\gamma_2\alpha_1^8\alpha_2^3 \\
& \gamma_1 + 160\gamma_2\alpha_1^8\gamma_1\alpha_2^4 - 1008\gamma_2^2\alpha_1^6\gamma_1^3\alpha_2^2 - 144\gamma_2^2\alpha_1^7\gamma_1^3\alpha_2^2 - 144\gamma_2^2 \\
& \alpha_1^7\gamma_1^3\alpha_2 - 1008\gamma_2^2\alpha_1^6\gamma_1^3\alpha_2 - 96\alpha_2^3\alpha_1^9\gamma_1 - 128\alpha_2^2\alpha_1^9\gamma_1 - 32\alpha_2^4\alpha_1^9 \\
& \gamma_1 - 4\alpha_2^5\alpha_1^9\gamma_1 + 384\alpha_1^8\gamma_2\gamma_1^2 - 64\alpha_1^9\gamma_1\alpha_2 - 1408\alpha_1^8\alpha_2^2\gamma_1 + 2688\alpha_1^7\gamma_2 \\
& \gamma_1^2 - 704\alpha_1^8\gamma_1\alpha_2 - 1056\alpha_1^8\alpha_2^3\gamma_1 - 352\alpha_1^8\gamma_1\alpha_2^4 - 44\gamma_1\alpha_2^5\alpha_1^8 - 312\gamma_2\alpha_1^9 \\
& \alpha_2^3 - 676\gamma_2\alpha_1^9\alpha_2^2 - 624\gamma_2\alpha_1^9\alpha_2 - 52\gamma_2\alpha_1^9\alpha_2^4 - 24\gamma_2\alpha_1^10\alpha_2^3 - 52\gamma_2\alpha_1^10 \\
& \alpha_2^2 - 48\gamma_2\alpha_1^10\alpha_2 - 4\gamma_2\alpha_1^10\alpha_2^4 - 16\gamma_2^2\alpha_1^9\alpha_2^3 - 48\gamma_2^2\alpha_1^9\alpha_2 - 48\gamma_2^2 \\
& \alpha_1^9\alpha_2^2 - 4\gamma_2^3\alpha_1^8\gamma_1^2 - 120\gamma_2^2\alpha_1^8\gamma_1^2 - 27\gamma_2^4\alpha_1^6\gamma_1^4 - 162\gamma_2^4\alpha_1^5\gamma_1^4 \\
& - 208\gamma_2^2\alpha_1^8\alpha_2^3 - 624\gamma_2^2\alpha_1^8\alpha_2 - 624\gamma_2^2\alpha_1^8\alpha_2^2 - 164\gamma_2^3\alpha_1^7\gamma_1^2 - 432\gamma_2^2 \\
& \alpha_1^7\gamma_1^2 - 2688\gamma_2\alpha_2^3\alpha_1^2 + 14\alpha_2^5\alpha_1^9 + 448\alpha_1^9\alpha_2^3 + 784\alpha_1^9\alpha_2^2 + 672\alpha_1^9\alpha_2 + 126 \\
& \alpha_1^9\alpha_2^4 + 9\alpha_2^4\alpha_1^10 + 32\alpha_2^3\alpha_1^10 + 56\alpha_2^2\alpha_1^10 + \alpha_2^5\alpha_1^10 + 48\alpha_2\alpha_1^10 - 208\gamma_2^2 \\
& \alpha_1^8 - 16\gamma_2^2\alpha_1^9 - 16\gamma_2\alpha_1^10 - 208\gamma_2\alpha_1^9 + 2240\gamma_2\alpha_2^3\alpha_1^2\gamma_1 + 15368\gamma_2^2\alpha_1^4\gamma_1 \\
& \alpha_2 + 72\gamma_2^3\alpha_1\gamma_1^3\alpha_2 - 288\gamma_2^3\alpha_2\alpha_1\gamma_1^2 - 144\gamma_2^3\alpha_2^2\alpha_1\gamma_1^2 + 15368\gamma_2^2\alpha_2^3 \\
& \alpha_1^4\gamma_1 + 30736\gamma_2^2\alpha_2^2\alpha_1^4\gamma_1 + 72\gamma_2^3\alpha_2^2\alpha_1\gamma_1^3 - 1808\gamma_2^3\alpha_1^6\alpha_2\gamma_1^2 + 2464\gamma_2 \\
& ^2\alpha_1^7\alpha_2^2\gamma_1 + 1232\gamma_2^2\alpha_1^7\gamma_1\alpha_2 - 904\gamma_2^3\alpha_1^6\alpha_2^2\gamma_1^2 + 1232\gamma_2^2\alpha_1^7\alpha_2^3 \\
& \gamma_1 - 4400\gamma_2^3\alpha_1^5\alpha_2\gamma_1^2 + 9376\gamma_2^2\alpha_1^6\alpha_2^2\gamma_1 + 1080\gamma_2^3\alpha_1^5\gamma_1^3\alpha_2 + 4688\gamma_2^2\alpha_1^6 \\
& \gamma_1\alpha_2 - 2200\gamma_2^3\alpha_1^5\alpha_2^2\gamma_1^2 + 4688\gamma_2^2\alpha_1^6\alpha_2^3\gamma_1 - 405\gamma_2^4\alpha_1^4\alpha_2\gamma_1^4 + 1080
\end{aligned}$$

CHAPTER 6: CONCLUSIONS AND FUTURE WORK

$$\begin{aligned}
& \gamma_2^3 \alpha_1^5 \alpha_2^2 \gamma_1^3 - 540 \gamma_2^4 \alpha_1^3 \alpha_2 \gamma_1^4 + 1440 \gamma_2^3 \alpha_1^4 \alpha_2^2 \gamma_1^3 + 1440 \gamma_2^3 \alpha_1^4 \\
& \gamma_1^3 \alpha_2 - 162 \gamma_2^4 \gamma_1^4 \alpha_2 \alpha_1 - 864 \gamma_2^3 \alpha_2^2 \alpha_1^2 \gamma_1^2 - 2900 \gamma_2^3 \alpha_2^2 \alpha_1^4 \gamma_1^2 + 10664 \\
& \gamma_2^2 \alpha_2^3 \alpha_1^5 \gamma_1 + 1080 \gamma_2^3 \alpha_2^2 \alpha_1^3 \gamma_1^3 - 2164 \gamma_2^3 \alpha_2^2 \alpha_1^3 \gamma_1^2 + 432 \gamma_2^3 \alpha_2^2 \\
& \alpha_1^2 \gamma_1^3 + 3584 \gamma_2 \alpha_2^2 \alpha_1^2 \gamma_1 + 1792 \gamma_2 \alpha_1^2 \gamma_1 \alpha_2 - 405 \gamma_2^4 \alpha_2 \alpha_1^2 \gamma_1^4 - 1728 \gamma_2^3 \\
& \alpha_1^2 \gamma_1^2 \alpha_2 - 5800 \gamma_2^3 \alpha_1^4 \alpha_2 \gamma_1^2 + 21328 \gamma_2^2 \alpha_1^5 \alpha_2^2 \gamma_1 + 10664 \gamma_2^2 \alpha_1^5 \gamma_1 \alpha_2 + 1080 \\
& \gamma_2^3 \alpha_1^3 \gamma_1^3 \alpha_2 - 4328 \gamma_2^3 \alpha_1^3 \gamma_1^2 \alpha_2 + 432 \gamma_2^3 \alpha_1^2 \gamma_1^3 \alpha_2 + 56 \alpha_2^4 \alpha_1^2 \gamma_2 \\
& \gamma_1^2 - 1770 \alpha_2^3 \alpha_1^6 \gamma_2^2 \gamma_1^2 + 688 \alpha_2^4 \alpha_1^7 \gamma_2 \gamma_1 - 3760 \alpha_2^3 \alpha_1^5 \gamma_2^2 \gamma_1^2 - 84 \gamma_1^3 \\
& \alpha_2^3 \alpha_1^5 \gamma_2^2 + 168 \gamma_1^2 \alpha_2^4 \alpha_1^6 \gamma_2 + 1664 \gamma_1 \alpha_2^4 \alpha_1^6 \gamma_2 + 2336 \gamma_2 \alpha_2^4 \alpha_1^4 \gamma_1 + 280 \\
& \gamma_2 \alpha_2^4 \alpha_1^4 \gamma_1^2 - 5130 \gamma_2^2 \alpha_2^3 \alpha_1^4 \gamma_1^2 - 140 \gamma_2^2 \alpha_2^3 \alpha_1^4 \gamma_1^3 + 2480 \gamma_2 \alpha_2^4 \\
& \alpha_1^5 \gamma_1 + 280 \gamma_2 \alpha_2^4 \alpha_1^5 \gamma_1^2 + 7296 \alpha_1^5 \gamma_2^2 \alpha_2 \gamma_1^2 + 13312 \alpha_1^6 \gamma_2 \alpha_2^2 \gamma_1 + 6656 \alpha_1 \\
& ^6 \gamma_2 \gamma_1 \alpha_2 - 112 \alpha_2^2 \alpha_1^5 \gamma_2^2 \gamma_1^2 + 8320 \alpha_2^3 \alpha_1^6 \gamma_2 \gamma_1 + 26880 \alpha_1^5 \alpha_2 \gamma_2 \gamma_1^2 + 432 \\
& \alpha_1^6 \gamma_2^2 \alpha_2 \gamma_1^2 + 5504 \alpha_1^7 \gamma_2 \alpha_2^2 \gamma_1 + 2752 \alpha_1^7 \gamma_2 \gamma_1 \alpha_2 - 1554 \alpha_1^6 \alpha_2^2 \gamma_2^2 \\
& \gamma_1^2 + 3440 \alpha_1^7 \alpha_2^3 \gamma_2 \gamma_1 - 3024 \alpha_1^5 \gamma_2^2 \gamma_1^3 \alpha_2 + 10752 \alpha_1^6 \gamma_2 \gamma_1^2 \alpha_2^2 - 3024 \alpha_1^5 \\
& \gamma_2^2 \alpha_2^2 \gamma_1^3 + 2688 \alpha_1^6 \gamma_2 \alpha_2^3 \gamma_1^2 + 16128 \alpha_1^6 \alpha_2 \gamma_2 \gamma_1^2 - 28 \gamma_1^3 \alpha_2^3 \alpha_1 \gamma_2^2 - \\
& 840 \gamma_2^2 \gamma_1^2 \alpha_2^3 \alpha_1 - 2582 \gamma_2^2 \alpha_2^3 \alpha_1^2 \gamma_1^2 - 84 \gamma_2^2 \alpha_2^3 \alpha_1^2 \gamma_1^3 + 1360 \gamma_2 \alpha_2^4 \\
& \alpha_1^3 \gamma_1 + 168 \gamma_2 \alpha_2^4 \alpha_1^3 \gamma_1^2 - 5040 \gamma_2^2 \alpha_1^4 \gamma_1^3 \alpha_2 - 5040 \gamma_2^2 \alpha_1^4 \alpha_2^2 \gamma_1^3 + 17920 \\
& \gamma_2 \alpha_1^5 \gamma_1^2 \alpha_2^2 + 4480 \gamma_2 \alpha_1^5 \alpha_2^3 \gamma_1^2 - 4572 \gamma_2^2 \alpha_2^3 \alpha_1^3 \gamma_1^2 - 140 \gamma_2^2 \alpha_2^3 \\
& \alpha_1^3 \gamma_1^3 - 32688 \gamma_2^2 \alpha_2 \alpha_1^4 - 32688 \gamma_2^2 \alpha_2^2 \alpha_1^4 - 10896 \gamma_2^2 \alpha_2^3 \alpha_1^4 - 144 \gamma_2^3 \alpha_1 \gamma_1^2 \\
& - 1776 \gamma_2 \alpha_1^8 \alpha_2^3 - 3848 \gamma_2 \alpha_1^8 \alpha_2^2 - 3552 \gamma_2 \alpha_1^8 \alpha_2 - 296 \gamma_2 \alpha_1^8 \alpha_2^4 - 1184 \gamma_2^2 \alpha_1^7 \\
& \alpha_2^3 - 3872 \gamma_2^2 \alpha_1^6 \alpha_2^3 - 540 \gamma_2^4 \alpha_1^3 \gamma_1^4 - 3552 \gamma_2^2 \alpha_1^7 \alpha_2 - 3552 \gamma_2^2 \alpha_1^7 \alpha_2^2 - \\
& 904 \gamma_2^3 \alpha_1^6 \gamma_1^2 - 11616 \gamma_2^2 \alpha_1^6 \alpha_2^2 - 11616 \gamma_2^2 \alpha_1^6 \alpha_2 - 405 \gamma_2^4 \alpha_1^4 \gamma_1^4 - 2200 \gamma_2^3 \\
& \alpha_1^5 \gamma_1^2 - 162 \gamma_2^4 \gamma_1^4 \alpha_1 - 405 \gamma_2^4 \alpha_1^2 \gamma_1^4 - 27 \alpha_2 \gamma_2^4 \gamma_1^4 - 24048 \gamma_2^2 \alpha_1^5 \alpha_2 - \\
& 24048 \gamma_2^2 \alpha_1^5 \alpha_2^2 - 2164 \gamma_2^3 \alpha_1^3 \gamma_1^2 - 2900 \gamma_2^3 \alpha_1^4 \gamma_1^2 - 924 \alpha_2^5 \alpha_1^3 \gamma_1 - 8016 \gamma_2^2 \\
& \alpha_2^3 \alpha_1^5 - 3072 \alpha_2^3 \gamma_1 \alpha_1 - 4096 \gamma_1 \alpha_2^2 \alpha_1 - 3072 \gamma_1^2 \alpha_2^2 \alpha_1 - 864 \gamma_2^3 \alpha_1^2 \gamma_1^2 - 968
\end{aligned}$$

CHAPTER 6: CONCLUSIONS AND FUTURE WORK

$$\begin{aligned}
& \alpha_2^4 \alpha_1^7 \gamma_2 - 5808 \alpha_1^7 \alpha_2^3 \gamma_2 - 11616 \alpha_1^7 \gamma_2 \alpha_2 - 12584 \alpha_1^7 \gamma_2 \alpha_2^2 + 216 \alpha_1^6 \gamma_2^2 \gamma_1^2 \\
& - 6784 \alpha_1^7 \alpha_2^2 \gamma_1 + 8064 \alpha_1^6 \gamma_2 \gamma_1^2 - 3392 \alpha_1^7 \gamma_1 \alpha_2 - 5088 \alpha_1^7 \alpha_2^3 \gamma_1 - 1696 \alpha_1^7 \gamma_1 \\
& \alpha_2^4 - 120 \gamma_2^2 \gamma_1^2 \alpha_2^3 - 4 \gamma_1^3 \alpha_2^3 \gamma_2^2 - 1036 \gamma_1 \alpha_2^5 \alpha_1^5 - 1204 \alpha_2^5 \alpha_1^4 \gamma_1 - 588 \gamma_1 \\
& \alpha_2^5 \alpha_1^6 - 212 \gamma_1 \alpha_2^5 \alpha_1^7 - 3584 \gamma_1^2 \alpha_2^3 \alpha_1^6 - 10752 \gamma_1^2 \alpha_2^2 \alpha_1^6 - 448 \gamma_1^2 \alpha_2^4 \\
& \alpha_1^6 - 896 \gamma_1^2 \alpha_2^4 \alpha_1^5 - 7168 \gamma_1^2 \alpha_2^3 \alpha_1^5 - 21504 \gamma_1^2 \alpha_2^2 \alpha_1^5 - 2004 \alpha_2^4 \alpha_1^6 \gamma_2 - 16344 \\
& \alpha_2^3 \alpha_1^5 \gamma_2 - 1376 \gamma_2 \alpha_2^4 \alpha_1^3 - 2432 \gamma_2 \alpha_2^4 \alpha_1^4 - 2724 \gamma_2 \alpha_2^4 \alpha_1^5 - 12024 \alpha_2^3 \alpha_1^6 \\
& \gamma_2 - 24048 \alpha_1^6 \gamma_2 \alpha_2 - 26052 \alpha_1^6 \gamma_2 \alpha_2^2 + 3648 \alpha_1^5 \gamma_2^2 \gamma_1^2 - 18816 \alpha_1^6 \alpha_2^2 \gamma_1 + 13440 \alpha_1^5 \\
& \gamma_2 \gamma_1^2 - 9408 \alpha_1^6 \gamma_1 \alpha_2 - 14112 \alpha_1^6 \alpha_2^3 \gamma_1 - 4704 \gamma_1 \alpha_2^4 \alpha_1^6 - 14592 \gamma_2 \alpha_2^3 \alpha_1^4 \\
& - 8256 \gamma_2 \alpha_2^3 \alpha_1^3 + 5928 \gamma_2^2 \alpha_1^2 \gamma_1^2 - 7392 \alpha_2^4 \alpha_1^3 \gamma_1 - 896 \alpha_2^4 \alpha_1^3 \gamma_1^2 - \\
& 144 \gamma_1^3 \alpha_2 \gamma_2^2 - 32688 \alpha_1^5 \gamma_2 \alpha_2 - 35412 \alpha_1^5 \gamma_2 \alpha_2^2 + 8280 \alpha_1^4 \gamma_2^2 \gamma_1^2 \\
& - 33152 \alpha_1^5 \alpha_2^2 \gamma_1 + 13440 \alpha_1^4 \gamma_2 \gamma_1^2 - 16576 \alpha_1^5 \gamma_1 \alpha_2 - 24864 \alpha_1^5 \alpha_2^3 \gamma_1 + 168 \gamma_2^2 \gamma_1^2 \\
& \alpha_2^2 - 144 \gamma_1^3 \alpha_2^2 \gamma_2^2 - 8288 \gamma_1 \alpha_2^4 \alpha_1^5 - 14464 \alpha_2^2 \alpha_1^2 \gamma_1 - 10752 \gamma_1^2 \alpha_2^2 \alpha_1^2 - 28896 \\
& \alpha_2^3 \alpha_1^4 \gamma_1 - 38528 \alpha_2^2 \alpha_1^4 \gamma_1 - 8960 \alpha_2^3 \alpha_1^4 \gamma_1^2 - 9632 \alpha_2^4 \alpha_1^4 \gamma_1 - 1120 \alpha_2^4 \alpha_1^4 \\
& \gamma_1^2 - 31616 \gamma_2 \alpha_1^4 \alpha_2^2 - 29184 \gamma_2 \alpha_1^4 \alpha_2 + 9360 \gamma_2^2 \alpha_1^3 \gamma_1^2 - 29568 \alpha_2^2 \alpha_1^3 \gamma_1 + 2688 \gamma_2 \\
& \gamma_1^2 \alpha_1^2 - 14784 \gamma_1 \alpha_2 \alpha_1^3 - 21504 \gamma_1^2 \alpha_2^2 \alpha_1^3 - 3616 \alpha_2^4 \alpha_1^2 \gamma_1 - 10848 \alpha_2^3 \gamma_1 \alpha_1^2 \\
& - 448 \alpha_2^4 \gamma_1^2 \alpha_1^2 + 8064 \alpha_1^3 \gamma_2 \gamma_1^2 - 19264 \alpha_1^4 \gamma_1 \alpha_2 - 26880 \alpha_1^4 \gamma_1^2 \alpha_2^2 - 3584 \gamma_1^2 \\
& \alpha_2^3 \alpha_1^2 - 22176 \alpha_2^3 \alpha_1^3 \gamma_1 - 7168 \alpha_2^3 \alpha_1^3 \gamma_1^2 + 224 \alpha_1^9 + 16 \alpha_1^1 0 + 1392 \alpha_1^8 + 20624 \alpha_1^4 + \\
& 18912 \alpha_1^5 + 11888 \alpha_1^6 + 5056 \alpha_1^7) = 0.
\end{aligned}$$

Bibliography

- [AB01] A. L. Afendikov and T. J. Bridges. Instability of the Hocking-Stewartson Pulse and Its Implications for Three-Dimensional Poiseuille Flow. *Proceedings of the Royal Society of London A*, 457:257–272, 2001.
- [Afo95] D. Afolabi. Sylvester Eliminant and Stability Criteria for Gyroscopic Systems. *Journal of Sound and Vibration*, 2:229–244, 1995.
- [AGJ90] J. Alexander, R. Gardner, and C. T. Jones. A Topological Invariant Arising in the Stability of Travelling Waves. *Journal fur Reine and Angewandte Mathematik*, 410:167–212, 1990.
- [AZ79] M.J. Ablowitz and A. Zeppetella. Explicit Solutions of Fisher’s Equation for a Special Wave Speed. *Bulletin of Mathematical Biology*, 41:835–840, 1979.
- [BCM99] N. J. Balmforth, R. V. Craster, and S. J. A. Malham. Unsteady Fronts in an Autocatalytic System. *Proceedings of the Royal Society of London. Series A: Mathematical, Physical and Engineering sciences*, 455(1984):1401–1433, 1999.
- [BDG02] T. J. Bridges, G. Derks, and G. Gottwald. Stability and Instability of Solitary Waves of the Fifth-Order KdV Equation: A Numerical Framework. *Physica D*, 172:190–216, 2002.

BIBLIOGRAPHY

- [Bil04] J. Billingham. Dynamics of a Strongly Nonlocal Reaction-Diffusion Population Model. *Nonlinearity*, 17:313–346, 2004.
- [BK06] J. Billingham and A.C. King. *Wave Motion*. Cambridge University Press, 2006.
- [BN91] J. Billingham and D.J. Needham. A Note on The Properties of a Family of Travelling-Wave Solutions Arising in Cubic Autocatalysis. *Dynamics and Stability of Systems*, 6:33–49, 1991.
- [Bri90] N. F. Britton. Spatial Structures and Periodic Travelling Waves in an Integro-Differential Reaction-Diffusion Population Model. *SIAM Journal on Applied Mathematics*, 50:1663–1688, 1990.
- [Bri01] L. Q. Brin. Numerical Testing of the Stability of Viscous Shock Waves. *Mathematics of Computation*, 70(235):1071–1088, 2001.
- [Bri05] N. Britton. *Essential Mathematical Biology*. Springer-Verlag London limited, 2005.
- [DG05] G. Derks and G. Gottwald. A Robust Numerical Method to Study Oscillatory Instability of Solitary Waves . *SIAM Journal on Applied Dynamical Systems*, 4:140–158, 2005.
- [Eva75] J. W. Evans. Nerve Axon Equations: IV The Stable and Unstable Pulse. *Indiana University of Mathematical Journal*, 24(12):1169–1190, 1975.
- [FaP03] M. Facão and D. F. Parker. Stability of Screening Solitons in Photorefractive Media. *Physical Review E*, 68:016610, 2003.

BIBLIOGRAPHY

- [FC03] N. Fei and J. Carr. Existence of Travelling Waves with Their Minimum Speed for a Diffusing Lotka - Volterra System. *Nonlinear Analysis: Real World Applications*, 4(3):503 – 524, 2003.
- [Fis37] R.A. Fisher. The Wave of Advance of Advantageous Genes. *Annals of Eugenics*, 7:353–369, 1937.
- [GC74] J. Gazdag and J. Canosa. Numerical Solution of Fisher’s Equation. *Journal of Applied Probability*, 11(3):445–457, 1974.
- [GC91] B. Guo and Z. Chen. Analytical Solutions of the Fisher Equation. *Journal of Physics A: Mathematical and General*, 24:645–650, 1991.
- [GJ91] R. Gardner and C. K. R. T. Jones. Stability of Travelling Wave Solutions of Diffusive Predator-Prey Systems. *Transactions of the American Mathematical Society*, 327(2):465–524, 1991.
- [GMSW03] V. Gubernov, G. Mercer, H. Sidhu, and R. Weber. Evans Function Stability of Combustion Waves. *SIAM Journal on Applied Mathematics*, 36:1259–1275, 2003.
- [Gop82] K. Gopalsamy. Exchange of Equilibria in Two Species Lotka-Volterra Competition Models. *The Journal of the Australian Mathematical Society*, 24:160–170, 1982.
- [Gou00] S.A. Gourley. Travelling Front Solutions of a Nonlocal Fisher Equation. *Journal of Mathematical Biology*, 41:272–284, 2000.
- [Guo12] Y. Guo. Existence and Stability of Traveling Fronts in a Lateral Inhibition

BIBLIOGRAPHY

- Neural Network. *SIAM Journal on Applied Dynamical Systems*, 11(4):1543–1582, 2012.
- [HJW11] S. Hsu, J. Jiang, and F. Wang. Reaction-Diffusion Equations of Two Species Competing for Two Complementary Resources with Internal Storage. *Journal of Differential Equations*, 25:918–940, 2011.
- [Hos03] Y. Hosono. Travelling Waves for a Diffusive Lotka-Volterra Competition Model I: Singular Perturbations. *Discrete and Continuous Dynamical Systems-Series B*, 3:79–95, 2003.
- [HPSS93] D. Horvath, V. Petrov, S. K. Scott, and K. Showalter. Instabilities in Propagating Reaction-Diffusion Fronts. *Journal of Chemical Physics*, 98:6332–6342, 1993.
- [HR75] K. Hardler and F. Rothe. Travelling Fronts in Nonlinear Diffusion Equations. *Mathematical Biology*, 2:251–263, 1975.
- [HZ06] J. Humpherys and K. Zumbrun. An Efficient Shooting Algorithm for Evans Function Calculations in Large Systems. *Physica D: Nonlinear Phenomena*, 220(2):116–126, 2006.
- [Jon84] C. K. R. T. Jones. Stability of the Travelling Wave Solution of the Fitzhugh-Nagumo System. *Transactions of the American Mathematical society*, 286(2):431–469, 1984.
- [Ked01] P. A. Keddy. *Competition*. John Wiley and Sons, Ltd, UK, 2001.
- [Kot01] M. Kot. *Elements of Mathematical Ecology*. Cambridge university press, UK, 2001.

BIBLIOGRAPHY

- [LLM11] S. Lafortune, J. Lega, and S. Madrid. Instability of Local Deformations of an Elastic Rod: Numerical Evaluation of the Evans Function. *SIAM Journal of Applied Mathematics*, 71:1653–1672, 2011.
- [LN01] J.A. Leach and D.J. Needham. The Evolution of Travelling Waves in Generalized Fisher Equations Via Matched Asymptotic Expansions: Algebraic Corrections. *The Quarterly Journal of Mechanics and Applied Mathematics*, 54:157–175, 2001.
- [LN04] J.A. Leach and D.J. Needham. *Matched Asymptotic Expansions in Reaction-Diffusion Theory*. Springer-Verlag London limited, 2004.
- [MN08] S. Malham and J. Niesen. Evaluating the Evans Function: Order Reduction in Numerical Methods. *Mathematics of Computation*, 77:159–179, 2008.
- [MT09] Y. Morita and K. Tachibana. An Entire Solution to the Lotka-Volterra Competition-Diffusion Equations. *SIAM Journal on Mathematical Analysis*, 40(6):2217–2240, 2009.
- [Mur02] J.D. Murray. *Mathematical Biology I: An Introduction*. Springer-Verlag, New York, third edition, 2002.
- [Neu98] C. Neuhauser. Mathematical Challenges in Spatial Ecology. *Notices American Mathematical Society*, 48:1304–1314, 1998.
- [Owe01] M. Owen. How Predation Can Slow, Stop or Reverse a Prey Invasion. *Bulletin of Mathematical Biology*, 63:655–684, 2001.
- [Pas08] J. Pastor. *Mathematical Ecology of Populations and Ecosystems*. A John Wiley and Sons, Ltd, Wiley-Blackwell, UK, 2008.

BIBLIOGRAPHY

- [PB94] S. Puri and A. J. Bray. Asymptotic Linearization of the Fisher Equation for a Class of Initial Conditions. *Journal of Physics A: Mathematical and General*, 27:453–460, 1994.
- [PSW93] R. Pego, P. Smereka, and M. Weinstein. Oscillatory Instability of Travelling Waves for a KdV- Burgers Equation. *Physica D*, 67:45–65, 1993.
- [PW92] R. L. Pego and M. I. Weinstein. Eigenvalues, and Instabilities of Solitary Waves. *Philosophical Transactions of the Royal Society A: Mathematical, physical and Engineering Sciences*, 340:47–94, 1992.
- [RB13] S. M. Rasheed and J. Billingham. A Reaction Diffusion Model for Inter-Species Competition and Intra-Species Cooperation. *Mathematical Modelling of Natural Phenomena*, 8:154–181, 1 2013.
- [RM00] M. Rodrigo and M. Mimura. Exact Solutions of a Competition-Diffusion System. *Hiroshima Mathematical Journal*, 30:257–270, 2000.
- [San98] B. Sandstede. Stability of Multiple-Pulse Solutions. *Transactions of the American Mathematical Society*, 350(2):429–472, 1998.
- [San02] Björn Sandstede. Stability of Travelling Waves. *Handbook of dynamical systems*, 2:983–1055, 2002.
- [SE90] J. Swington and J. Elgin. Stability of Travelling Pulse Solutions to a Laser Equation. *Physics Letters A*, 145:428–433, 1990.
- [SEs11] K. M. Saad and A. M. El-shrae. Numerical Methods for Computing the Evans Function. *ANZIAM Journal*, 52(E):E76–E99, 2011.

BIBLIOGRAPHY

- [SM96a] J. Sherratt and B. Marchant. Algebraic Decay and Variable Speeds in Wave-front Solutions of a Scalar Reaction-Diffusion Equation. *IMA Journal of Applied Mathematics*, 56(3):289–302, 1996.
- [SM96b] J. Sherratt and B. Marchant. Nonsharp Travelling Wave Fronts in the Fisher Equation With Degenerate Nonlinear Diffusion. *Applied Mathematics Letters*, 9:33–38, 1996.
- [SS01] B. Sandstede and A. Scheel. Essential Instabilities of Fronts: Bifurcation and Bifurcation Failure. *Dynamical Systems*, 16(1):1–28, 2001.
- [Ter90] D. Terman. Stability of Planar Wave Solutions to Combustion Model. *SIAM Journal on Mathematical Analysis*, 21:1139–1171, 1990.
- [Tur52] A. M. Turing. The Chemical Basis of Morphogenesis. *Philosophical Transactions of the Royal Society of London*, 237(641):37–72, 1952.
- [VG03] H. Vandermeer and D. Globerg. *Population Ecology*. Princeton University Press, UK., 2003.
- [VP09] V. Volpert and S. Petrovskii. Reaction-Diffusion Waves in Biology. *Physics of Life Reviews*, 6:267–310, 2009.
- [VV94] V.A. Volpert, A.I. Volpert and V.A. Volpert. *Traveling Waves Solutions of Parabolic Systems*. American Mathematical Society, 1994.
- [Wan78] PJ Wangersky. Lotka-Volterra Population Models. *Annual Review of Ecology and Systematics*, 9(1):189–218, 1978.

BIBLIOGRAPHY

- [Wit94] T. P. Witelski. An Asymptotic Solution for Travelling Waves of a Nonlinear-Diffusion Fisher's Equation. *Journal of Mathematical Biology*, 33:1–16, 1994.
- [Xin00] J. Xin. Front Propagation in Heterogeneous Media. *SIAM Review*, 42(2):161–230, 2000.
- [ZF94] Z. Zhang and S. Falle. Stability of Reaction-Diffusion Fronts. *Proceeding of the Royal Society London A*, 446:517–528, 1994.